MONASH University

DOES THE NOVEL GC ACTIVITY OF IRAK3 AFFECT ITS SIGNALLING?

Lubna A. Freihat

B.SC. (PHARM.), B.PHARM.SCI. (HONS.)

A thesis submitted to

Monash Institute of Pharmaceutical Sciences

Monash University

For the Degree of

- DOCTOR OF PHILOSOPHY –

DRUG DISCOVERY BIOLOGY

MONASH INSTITUTE OF PHARMACEUTICAL SCIENCES

FACULTY OF PHARMACY AND PHARMACEUTICAL SCIENCES

MONASH UNIVERSITY, VICTORIA, AUSTRALIA

MAY 12, 2017

Table of Contents

LIST OF FIGURES AND TABLES

CHAPTER 5

CHAPTER 6

GENERAL DECLARATION

I hereby declare that this thesis contains no material which has been accepted for the award of any other degree or diploma at any university or equivalent institution and that, to the best of my knowledge and belief, this thesis contains no material previously published or written by another person, except where due reference is made in the text of the thesis.

This thesis includes sections of two original papers published in peer reviewed journals. The core theme of the thesis is biochemistry. The ideas, development and writing up of all the papers in the thesis were the principal responsibility of myself, the candidate, working within the Drug Discovery Biology under the supervision of Associate Professor Helen R. Irving.

The inclusion of co-authors reflects the fact that the work came from active collaboration between researchers and acknowledges input into team-based research. In the case of Chapter 3 and 4, my contribution to the work involved the following:

Thesis chapter	Publication title	Publication status	Nature and extent (%) of students contribution	Co-author (s) Nature and % of Co-author contribution	Co-author Monash student Y/N*
Chapter 3	A cyclic nucleotide sensitive promoter reporter system suitable for bacteria and plant cells	Published	Approximately 40% contribution to the total paper, of that 25% is experimental work and 15% is contribution to draft preparation and revision of paper. Paper is redrafted, discussed and referenced in chapter 3. Chapter 3 also has further discussion, added experiments and data not published.	Janet I. Wheeler *40% input.* Helen R. Irving *20% input.*	N N

Chapter 4	Comparison of moonlighting guanylate cyclases: roles in signal direction?	Published	Approximately 50% contribution to total paper, of that 30% is experimental and 20% is draft preparation and review of paper. Paper is also referenced in text. Extra data and discussion not published in the paper is added to chapter 4.	Victor Muleya *5% input.* David T. Manallack *15% input.* Janet I. Wheeler *5% input.* Helen R. Irving *25% input.*	Y N N N

I have redrafted sections of submitted or published papers in order to generate a consistent presentation within the thesis.

Student signature: *(Lubna Freiha* [redacted] **Date:** 17/05/17

The undersigned hereby certify that the above declaration correctly reflects the nature and extent of the student's and co-authors' contributions to this work. In instances where I am not the responsible author I have consulted with the responsible author to agree on the respective contributions of the authors.

Main Supervisor signature: *(* [redacted] **Date:** 17/05/2017

ABSTRACT

Interleukin-1 receptor associated kinase 3 (IRAK3) acts as a negative regulator of inflammation by inhibiting downstream signalling in the innate immune response. IRAK3 is proposed to be useful as a diagnostic and prognostic marker in inflammation, and possibly a target for intervention in cancer and sepsis. IRAK3 was unearthed as a potential novel guanylate cyclase (GC) using a homology-guided bioinformatics data mining tool. GCs are enzymes that catalyse the formation of cyclic guanosine monophosphate (cGMP) from guanosine triphosphate (GTP), cGMP is a second messenger important in mediating physiological processes in eukaryotes.

IRAK3 is predicted to be a representative of a new class of GCs containing a unique architecture, in which the GC centre is encapsulated within the kinase domain, thereby exhibiting a dual kinase-GC functionality. The unusual IRAK3 GC architecture is similar to that seen in some plant leucine-rich repeat receptors like kinases where GC activity is partially characterised. The exact mechanism of action and the selectivity of IRAK3 is however still largely unclear and further evaluation is needed.

Currently, cellular cyclic nucleotide levels have been assessed using antibody kits (ELISA) or mass spectrometry analyses, both of which have drawbacks. To address this need we have designed a cGMP sensitive luciferase reporter system screening tool to determine guanylate cyclase activity in cells. A promoter system containing the oligopeptide transporter X (OPTX) promoter was fused to a luciferase gene. OPTX responds to cGMP in plant cells, and surprisingly the OPTX promoter fragment contains the mammalian cGMP response element. To enhance the promoter response to cGMP, we inserted three additional cGMP response elements into the OPTX promoter. Another construct was designed containing five gibberellic acid response elements (GARE) that was postulated to be upregulated by cGMP. The constructs were tested for response to cGMP and cAMP in BL21-AI as a

representative of bacterial cells and HEK 293T cells representing mammalian cells. Significantly increased luciferase activity occurred in bacterial cells transformed with the OPTX promoter system in response to both cAMP and cGMP. Bacteria co-transformed with the OPTX promoter system and the soluble cytoplasmic domain of phytosulfokine receptor 1 (PSKR1; a novel guanylate cyclase) had enhanced luciferase activity, signifying the presence of increased cGMP production following induction of PSKR1 expression. The OPTX promoter system presents an effective screening tool that can be used in bacteria to screen recombinant proteins for guanylate cyclase activity. This tool can be used to measure changes in GC activity in proteins like IRAK3.

The unusual position of the GC centre omitted within the kinase domain presents several conceptual problems. Therefore, the structural conformations of this novel class of GCs were considered. An IRAK3 homology model was designed based on the only available crystal structure in the IRAK family, IRAK4. In addition, alignment of the homology models of the kinase domains of IRAK3 and PSKR1 reveal structural similarities between these two proteins. The uniformity in the structural topology of PSKR1 and IRAK3 may explain the observed GC activity in IRAK3. The homology model of IRAK3 is a useful tool to assist in designing the mutagenesis experiments. We were able to use the models to show that mutating specific residues in the GC centre affected either the general structure in the GC vicinity or possible interactions in the GC centre upon docking of the nucleotide triphosphate, GTP.

The next approach was to look at the actual IRAK3 GC activity, initially using the available cGMP detection techniques including ELISA and mass spectrometry. Recombinant IRAK3 protein is capable of producing cGMP at levels comparable to those produced by our positive control, PSKR1. In separate experiments, HEK 293T cells transfected with IRAK3 produced significantly higher levels of cGMP when compared to control cells transfected with empty vector or IRAK4. Mutating specific

residues in the GC centre caused alterations in cGMP production where cGMP was reduced or in other cases not significantly altered. These findings were in agreement with homology modelling.

The final approach looks at how the cGMP generated by the IRAK3 protein selectivity modulates IRAK3 regulated innate immune signalling. Overexpression of IRAK3 in HEK BLUE hTLR4 cells significantly reduces NFκB activation observed using a SEAP reporter system. IRAK3 mutants with reduced cGMP-generating capacity, failed to inhibit NFκB induced SEAP activity. Whereas mutants with reduced cGMP-generating capacity affected LPS-induced NFκB pathway in the presence of added cell-permeable cGMP. These findings are providing insight into the hidden functions of IRAK3 and may assist in explaining the selectivity and functionality of IRAK3 in the inflammatory signalling cascade.

COMMUNICATIONS

JOURNAL ARTICLES

Wheeler J I, Wong A, Marondedze C, Groen A, Kwezi L, **Freihat L,** Vyas J, Raji M, Irving H R and Gehring C. (2017) **The brassinosteroid receptor BRI1 can generate cGMP enabling cGMP-dependent downstream signalling.** (Plant Journal 2017, Accepted 21/04/17 TPJ-00071-2017)

Freihat L, Muleya V, Manallack D T, Wheeler J I and Irving H R. (2014) **Comparison of moonlighting guanylate cyclases: roles in signal direction?** (Biochemical Society Transactions (2014) 42, (1773–1779) doi:10.1042/BST20140223)

Muleya V, Wheeler J I, Ruzvidzo O, **Freihat L**, Manallack D T, Gehring C and Irving H R. (2014) **Calcium is the switch in the moonlighting dual function of the ligand-activated receptor kinase phytosulfokine receptor 1.** (Cell Communication and Signalling 2014, 12:60 doi:10.1186/s12964-014-0060-z)

Wheeler J I*, **Freihat L*** and Irving H R. (2013) **A cyclic nucleotide sensitive promoter reporter system suitable for bacteria and plant cells.** (BMC Biotechnology 2013, 13:97 doi:10.1186/1472-6750-13-97)

*Equal first authors

CONFERENCE PROCEEDINGS

Freihat L.A., Manallack D., Wheeler J.I. and Irving H.R. IRAK3 modulates NFκB through its GC activity. Oral/Abstract *Proceedings of the Australian Society for Biochemistry and Molecular Biology:* Cancer cell biology and signalling COL-04-06, 2016.

Freihat L.A., Manallack D., Wheeler J.I. and Irving H.R. New points of modulation of IRAK3 function. Poster/Abstract *Proceedings of the Australian Society for Biochemistry and Molecular Biology:* POS-TUE-054, 2015.

Freihat L.A., Manallack D., Wheeler J.I. and Irving H.R. The hidden guanylate cyclase function of IRAK3: a new trick from an immune protein. Oral/Abstract *Proceedings of the Australian Society for Biochemistry and Molecular Biology:* Immune cell signalling SYM- 26- 04, 2014.

Freihat L.A., Wheeler J.I., Manallack D. and Irving H.R. Characterisation of the guanylate cyclase catalytic activity in IRAK3. Poster/Abstract The 16th EMBL PhD Symposium: Inspired by Biology - Exploring Nature's Toolbox (October 2014).

Freihat L.A., Wheeler J.I., Manallack D. and Irving H.R. Characterisation of the guanylate cyclase catalytic activity in IRAK3. Poster/Abstract *Pharmaceutical Sciences World Congress 2014:* PC-018.

Freihat L.A., Wheeler J.I., Manallack D. and Irving H.R. Moonlighting catalytic functions of IRAK3. Poster/Abstract *Proceedings of the Australian Society for Biochemistry and Molecular Biology:* POS-MON-061, 2013.

Wheeler J.I., **Freihat L.A.,** and Irving H.R. OPTX:LUC based cyclic nucleotide sensitive promoter reporter systems. Poster/Abstract *Proceedings of the Australian Society for Biochemistry and Molecular Biology:* POS-MON-010, 2012.

ABBREVIATIONS

A20 (TNFAIP3)	The tumour necrosis factor alpha-induced protein 3
BMT	Bone marrow transplantation
BRI1	Brassinosteroid insensitive 1
BSA	Bovine serum albumin
CD14	Cluster of differentiation 14
cGMP	Cyclic guanosine monophosphate
ELISA	Enzyme-linked immunosorbent assay
GC	Guanylate cyclase
IL-1	Interleukin 1
IL-13	Interleukin 13
IRAK	Interleukin-1 receptor-associated kinase
JNK	c-Jun NH2-terminal kinase
LBP	LPS binding protein
LPS	Lipopolysaccharide
Mal/TIRAP	Toll-interleukin-1 receptor domain containing adaptor protein
MAP3K7	Mitogen-activated protein kinase kinase kinase 7
MD-2	Lymphocyte antigen 96
MEKK3	Mitogen-activated protein kinase kinase kinase 3

MyD88	Myeloid differentiation primary response (88)
NFκB	Nuclear factor kappa-light-chain-enhancer of activated B cells
NTRK1	Neurotrophic receptor tyrosine kinase 1
PAMPs	Pathogen-associated molecular patterns
PBMCs	Peripheral blood monocytes
PGE2	Prostaglandin E2
PI3K	Phosphoinositide 3-kinase
PSKR1	Phytosulfokine receptor 1
SEAP	Secreted embryonic alkaline phosphatase
SHIP-1	SH-2 containing inositol 5'-polyphosphatase 1
SOCS1	Suppressor of cytokine signalling 1
TAB2	TGF-Beta activated kinase 1/MAP3K7 binding protein 2
TAB3	TGF-Beta activated kinase 1/MAP3K7 binding protein 3
TAK1	Transforming growth factor beta activated kinase 1
TAMS	Tumour-associated macrophages
TGF-β	Transforming growth factor beta
TLR	Toll-like receptor
TRAF-6	Tumour necrosis factor receptor associated factors 6

ACKNOWLEDGMENTS

I would like to start by thanking my supervisor Associate Professor Helen R. Irving for all the unconditional support I have received throughout the years, thank you for taking me on and guiding me throughout the years. I appreciate all that I have gained as a PhD student to continue as a passionate scientist with no boundaries. I would also like to thank my associate supervisor Dr. Janet I Wheeler for all the early much-needed help in the lab, the continuous great advice and the moral support through the final years. Thank you to all my panel members, my external panel member Professor Roger Parish for taking the time to come all the way to Monash to guide me through my candidature, I highly appreciate your time, corrections and advice from the beginning to the end. Thank you, Professor Colin Pouton for creating a stress-free and welcoming environment at our meetings, and for all your guidance throughout. Thank you, Dr. David Manallack for all the help I have received throughout the years, from the necessary homology modelling to the help in writing, corrections and much need guidance throughout the years. Thank you, Dr. Stewart Fabb, I highly appreciate all your indispensable experimental advice in the panel meetings and the continuous help in and out of the lab.

I am grateful to Monash University for the opportunity to complete my PhD and be part of such a remarkable university, I would like to thank the Monash, Faculty of Pharmacy and Pharmaceutical Sciences for the PhD scholarship and countless training, facilities and opportunities. I am grateful to the DDB theme for all the support, equipment, training and experience received throughout the years.

Thank you to all my Monash colleagues and friends, I am extremely grateful for all the help, guidance and continuous support throughout the years, I never feared or doubted to ask for help as it was always available and beyond anticipation. I am forever grateful to all the amazing people that made MIPS such an amazing place to

work and belong. Words cannot express my gratitude to all the lifelong friends gained throughout my years as a student, your help personally, academically and socially has helped me further than expected to face the most impossible tasks.

I would finally like to thank my big amazing family, all I have done and continue to do is thanks to all the support I continue to receive throughout. However difficult it has been at times for us all, I am extremely grateful to have such a close, loving and caring family. All the challenges and blessings have only taught me to become a stronger, more optimistic, wiser and more independent being capable of achieving anything I set my mind to.

CHAPTER 1

GENERAL INTRODUCTION

CHAPTER 1

GENERAL INTRODUCTION

1.1 GUANYLATE CYCLASE IN LIVING ORGANISMS

1.1.1 Guanylate cyclase and cGMP function

The enzyme guanylate cyclase (GC) catalyses the conversion of guanosine-5'-triphosphate (GTP) to cyclic guanosine monophosphate (cGMP). cGMP is an important second messenger that mediates countless physiological processes in eukaryotic cells. In mammalian cells, cGMP is a transitory expressed molecule that directly regulates cyclic nucleotide gated ion channels, protein kinases and activates specific phosphodiesterases that degrade cGMP (Lucas et al., 2000). The physiological roles of cGMP are well characterised, in vascular smooth muscle, for example, it mediates intestinal fluid electrolyte homeostasis and relaxation (Lucas et al., 2000).

cGMP levels are an important drug target for the treatment of a number of functional isorders and disease states. Several drugs have been developed which are currently in use while others are in clinical phase studies for cardiovascular, respiratory and gastrointestinal disorders (Gheorghiade et al., 2013; Potter, 2011b; Schlossmann and Schinner, 2012). Increasing intracellular cGMP through inhibition of phosphodiesterases or the stimulation of guanylate cyclases or both have been a valid therapeutic strategy in drug development for pulmonary arterial hypertension (Chen et al., 2013). Phosphodiesterases are also excellent drug targets; the inhibition of specific phosphodiesterases is successful in treating common erectile dysfunction, using drugs such as sildenafil (Viagra), tadalafil (Cialis), and vardenafil (Levitra). Due

to its vasodilatory effect, sildenafil is also used in the treatment of pulmonary hypertension. (Barnett and Machado, 2006; Bender and Beavo, 2006). Increasing the GC activity is shown to be important in heart failure patients, where cGMP recovery can offer organ-protective effects. Other therapeutic options considered act through the selective induction of specific subtypes of GCs. (Gheorghiade et al., 2013; Schlossmann and Schinner, 2012).

There are two well-known types of GCs, classical transmembrane GCs and soluble GCs which are documented below. A novel class of GCs has been partially characterised, more recently this class of GCs differs from the classical GCs in that they possess a GC catalytic centre encapsulated within the kinase domain. (Kwezi et al., 2007; Kwezi et al., 2011; Ludidi and Gehring, 2003; Meier et al., 2010; Qi et al., 2010; Szmidt-Jaworska et al., 2009). Kinases are proteins that phosphorylate either themselves or other protein substrates, which can have profound effects on eukaryotic cellular processes and signalling pathways (Endicott et al., 2012).

1.1.2 Classical transmembrane guanylate cyclases

The structural organisation, biological function and regulation of classical transmembrane GCs are well documented (Misono, 2011; Potter, 2011b). Classical transmembrane GCs consist of an extracellular ligand binding domain and an inactive kinase homology domain that is linked to a guanylyl cyclase domain. The GC catalytic domain and the kinase homology domain are localised on the cytoplasmic side of the membrane. A single transmembrane chain separates the cytoplasmic portion of the receptor from the extracellular ligand-binding domain (Figure 1.1). The linker domain that links the kinase homology domain and the GC centre is a 50-70 amino acid stretch that is implicated in receptor dimerization (Chinkers and Wilson, 1992). There are seven transmembrane GC forms (GC A to G) which are predominantly found as homodimers (Potter, 2011b).

The kinase homology domain in classical transmembrane GCs share some sequence similarities to typical protein kinase domains. However, the kinase homology domain often lack the aspartic acid (D) in the HRD motif which is critical for phosphotransferase activity. The catalytic aspartic acid residue, however, is commonly replaced by serine, arginine, or asparagine in transmembrane GCs, therefore transmembrane GCs do not possess kinase activity (Hammarén et al., 2016). Despite the lack of kinase activity in classical transmembrane GCs, the kinase homology domain is shown to regulate the activity of the GC centre by allosteric modulation through an adenosine-5'-triphosphate (ATP) binding module. The presence of the core ATP-binding motif in the kinase homology domains of almost all of the proteins indicates the importance of ATP interaction as a means of regulating the catalytic activity of the associated GC centre (Biswas et al., 2009; Duda et al., 2011; Saha et al., 2009).

Dimerization of the GC centre is believed to be a structural requirement for its nucleotide cyclase activity, as dimer formation results in the formation of an active site cleft required for nucleotide binding (Potter et al., 2006; Potter and Hunter, 2001). The extracellular ligand-binding domain has been shown to potentiate receptor activation upon ligand binding (Qiu et al., 2004). In the absence of the ligand, the GC catalytic activity of the receptor is suppressed by the kinase homology domain. This is verified by several independent experiments which used truncated receptors lacking the kinase homology domain (Chinkers and Garbers, 1989; Deshmane et al., 1997; Koller et al., 1992). The kinase homology domain deficient receptors were shown to exhibit maximal GC activities that are unresponsive to ligand binding, thereby demonstrating that the kinase homology domain is essential for suppressing the nucleotide cyclase activity in classical transmembrane GCs (Biswas et al., 2009; Potter, 2011b).

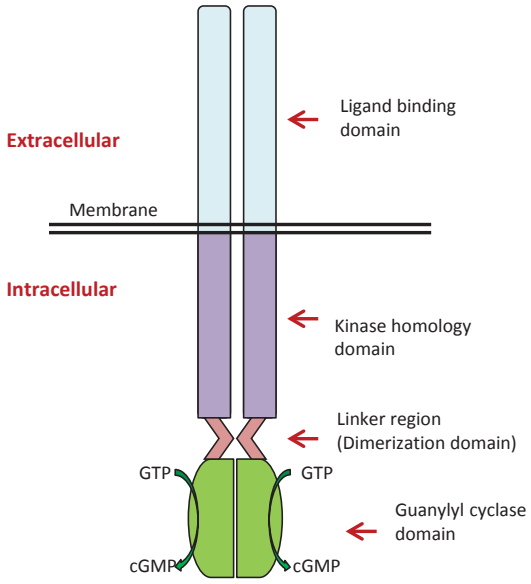

Figure 1.1 Classical transmembrane guanylate cyclase

Schematic diagram of a classical transmembrane guanylate cyclase showing the different domains, adapted from (Potter, 2011b).

1.1.3 Soluble guanylate cyclases

Soluble guanylyl cyclases (sGCs) are dimeric enzymes that in animals transduce signals downstream of nitric oxide (NO). The investigation of the effects of organic nitrates, used for over a century to help in pain associated with angina pectoris, led to the discovery of the sGCs (Waldman and Murad, 1988), and this, in turn, led to the discovery of NO. sGCs sense NO by a heme moiety bound to the N-terminal extensions (Derbyshire and Marletta, 2012; Iyer et al., 2003). This pathway includes a Ca^{2+}/calmodulin (CaM) complex that binds nitric oxide synthase (NOS), NOS catalyses the oxidation of L-arginine (L-Arg) to L-citrulline (L-Cit) and NO. NO is a gas and can diffuse to adjacent cells. NO binds to the Fe^{II} heme of the α1β1 soluble sGC, causing a significant increase in cGMP levels (Figure 1.2 A). Heterodimeric sGC consists of two homologous subunits, α and β, yet the most commonly studied isoform is the α1β1 protein; although, α2 and β2 isoforms also exist. GCs are found in most tissues; though its distribution amongst cell types is isoform specific (Derbyshire and Marletta, 2012).

Each sGC subunit consists of four distinct domains, a N-terminal heme-binding domain, a Per/Arnt/Sim (PAS) domain, a coiled-coil domain and a C-terminal catalytic domain. Both GTP and ATP can influence NO binding, dissociation and activation (Figure 1.2 B). In cells, it is likely that NO, GTP and ATP modulate cGMP production (Derbyshire and Marletta, 2012).

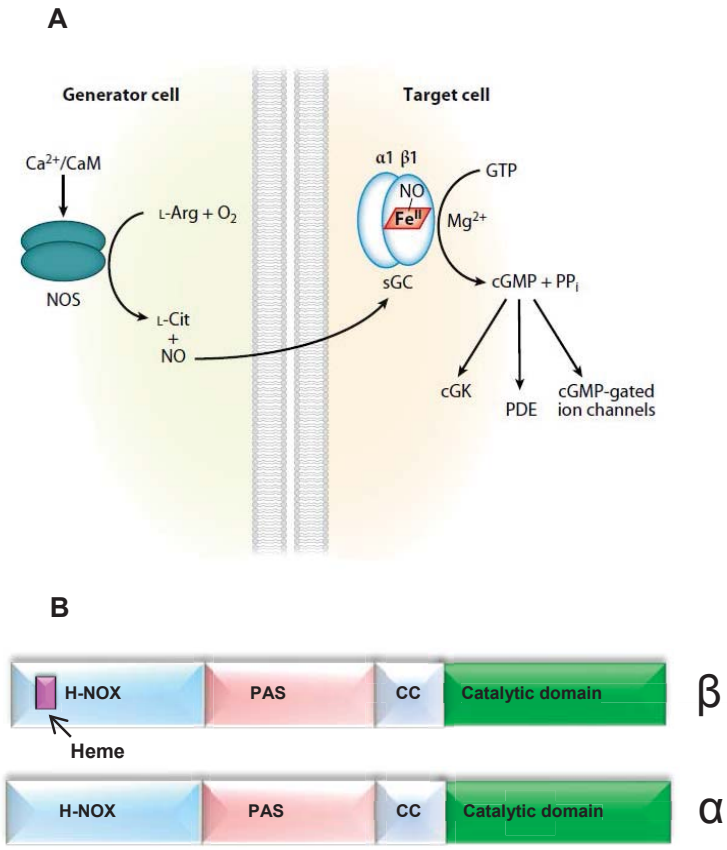

Figure 1.2 Soluble guanylate cyclase signalling and domain architecture

(a) The nitric oxide/cyclic GMP (NO/cGMP)-signalling pathway. NO is generated by NOS in response to activation by Ca/CaM. The NO can diffuse through cells to activate sGC which leads to a significant increase in cGMP which goes on to activate cGMP-dependent protein kinases (cGK), phosphodiesterases (PDE) and ion gated channels. (B) Schematic domain organisation of soluble guanylate cyclases showing the heterodimeric α and β subunits, consisting of four distinct domains, an N-terminal heme-binding domain (H-NOX), a Per/Arnt/Sim (PAS) domain, a coiled-coil domain (CC) and a C-terminal catalytic domain (Derbyshire and Marletta, 2012; Lucas et al., 2000).

1.1.4 Non-classical novel transmembrane guanylate cyclases

This new family of GC-linked receptor kinases was unearthed using sequence homology-guided bioinformatics data mining tools composed of amino acid sequence motifs that are homologous to GC catalytic centres found in lower eukaryotes (Figure 1.3 C) (Irving et al., 2012). These pattern-matching database searches yielded over 400 putative GC molecules, with more than 200 of these occurring in eukaryotes including humans. Many of the identified candidate GC molecules perform different biological functions. Several proteins in this subfamily have been genetically characterised, however, none of them have been previously suspected of possessing GC catalytic centres.

The non-classical novel class of transmembrane GCs have an atypical domain organisation that is different from the classical transmembrane GCs. Members of the non-classical novel transmembrane GCs have a GC catalytic centre that is encapsulated within the kinase domain, unlike the classical transmembrane GCs that encompass two separate domains separated by a linker region (Figure 1.3 A and B) (Irving et al., 2012)

Many of the novel non-classical transmembrane GCs belong to a superfamily of proteins known as the leucine rich repeat receptor-like kinases (LRR RLK). There are currently only four members of this new family of receptor kinases that have been experimentally demonstrated to possess both kinase and GC activity (Kwezi et al., 2007; Kwezi et al., 2011; Meier et al., 2010; Qi et al., 2010), however the various mechanisms modulating the two catalytic functions, namely the kinase and GC remain unknown. The Phytosulfokine receptor 1 (PSKR1) is an active kinase involved in regulating growth responses in plants and was also shown to be a novel GC (Kwezi et al., 2011). It was determined that the recombinant protein of the cytoplasmic domain of PSKR undergoes dramatic changes in its kinase and GC function upon

variations in calcium concentrations, indicating that a previously unrecognised molecular switch is in operation (Muleya et al., 2014).

A mammalian representative member of this subfamily which remains to be further investigated as a novel GC is the neurotrophic tyrosine kinase receptor type 1 (NTRK1), which has a similar kinase domain with a GC centre embedded within to PSKR1 and BRI1 (Figure 1.3 B).. NTRK1 is a human protein that is known to be involved in cell differentiation and in specifying sensory neuron subtypes (Indo, 2012)

The discovery of these GC catalytic centres within these receptor kinases defines a new paradigm in the classification of transmembrane GCs. Although the GC catalytic centre of the novel GCs is encapsulated in the kinase domain, it is not within the kinase active site and so the novel GC molecules are examples of dual functional enzymes rather than promiscuous enzymes that can catalyse additional reactions or use non-specific substrates (Irving et al., 2012; Muleya et al., 2016). Another mammalian protein was identified where the GC centre was embedded in the kinase domain, however it is a cytoplasmic protein unlike PSKR1 and BRI1 which are transmembrane proteins. Interleukin-1 receptor associated kinase 3 (IRAK3) holds the potential to be a soluble guanylate cyclase. IRAK3 and its distinctive GC centre will be the focus of this study (Figure 1.3 B) (Freihat et al., 2014).

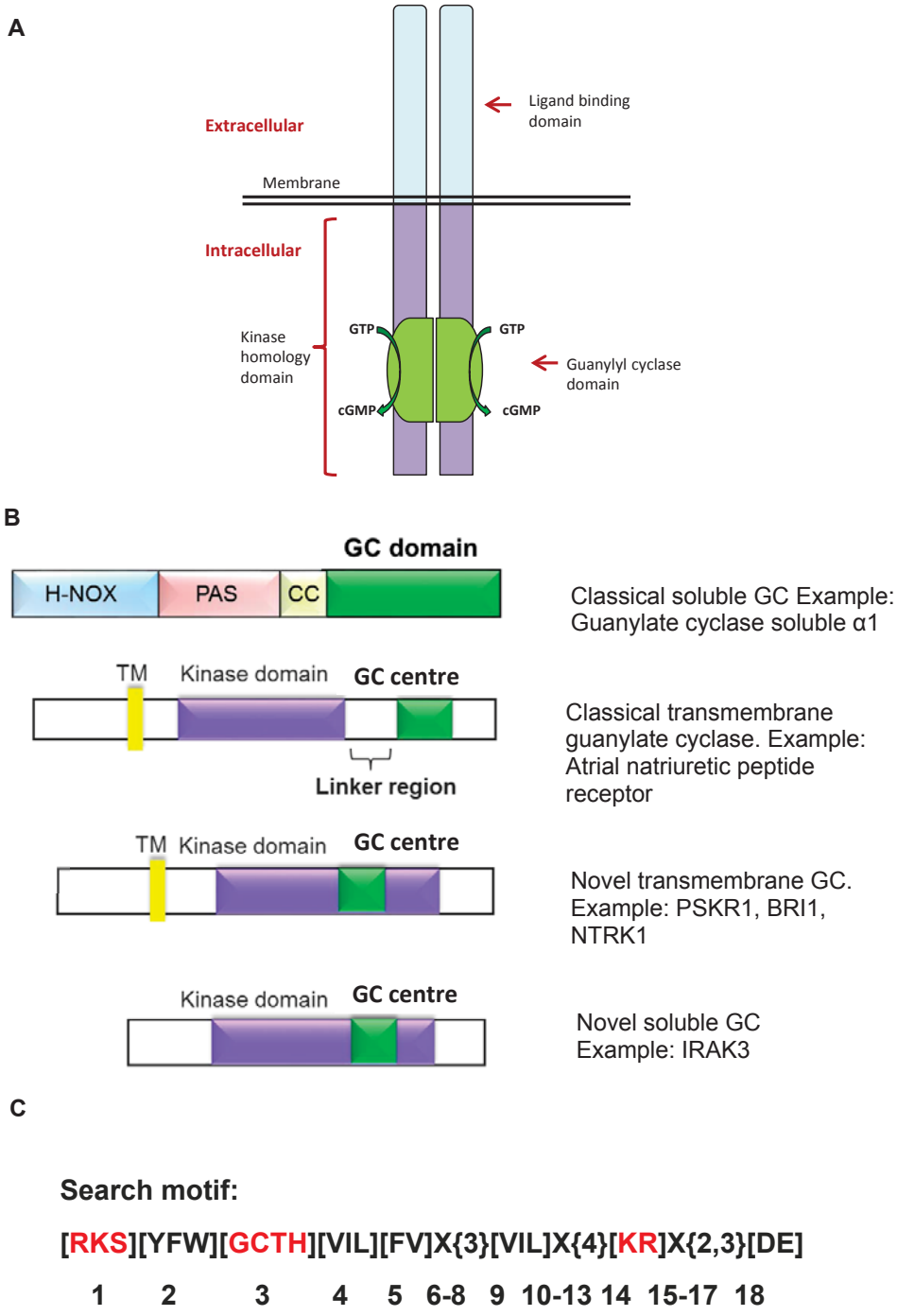

Figure 1.3 Domain architectures of GCs and the GC search motif

(A) Schematic diagram of a novel transmembrane GC showing the GC centre encapsulated within the intracellular kinase homology domain (B) Domain organisation of classical and novel transmembrane and soluble GCs (C) The search motif used to identify the new class of GCs (Irving et al., 2012).

1.2 IRAK PROTEINS IN INNATE IMMUNITY

1.2.1 The IRAK family

The interleukin-1 receptor associated kinase (IRAK) family are critical signalling mediators of the toll like receptor (TLR) and interleukin-1 receptor (IL-1R) signalling pathways in innate immunity. The IRAKs are serine/threonine kinases and are part of the downstream signalling molecules within the TLR/IL-1R pathway (Kobayashi et al., 2002).

This family consists of IRAK 1, 2, 3, and 4, each with their own specific functions (Gosu et al., 2012). Activation of TLRs stimulates IRAK1 and IRAK4 to activate the signalling cascade, finally resulting in transcription factors induced expression of cytokine and chemokines. Each IRAK protein contains a death domain and a kinase domain or kinase homology domain, IRAK1,2 and 3 also have a C-terminal domain (Figure 1.4 A). IRAK1 and IRAK4 are catalytically active kinases linked with inflammation stimulatory responses downstream of TLR (Hubbard and Moore, 2010). IRAK1 was the first member of the family to be identified (Cao et al., 1996). IRAK4 was the last member of the family to be identified however it has been extensively studied since its discovery in 2002 (Li et al., 2002). In different disease states, cytokine induction was shown to be activated by IRAK4 in a cell type specific manner and so IRAK4 is considered the master IRAK protein. IRAK4 is required for all the myeloid differentiation primary response 88 (MyD88) dependent, nuclear factor kappa-light-chain-enhancer of activated B cells (NFκB) activation. NFκB is a ubiquitous transcription factor mediating DNA transcription. Activation of NFκB is involved in regulating the inflammatory response by inducing transcription of proinflammatory genes (Cushing et al., 2014; Jain et al., 2014).

IRAK2 was originally thought to be a pseudokinase, as negligible autophosphorylation activity was detected in recombinant IRAK2 protein preparations

(Wesche et al., 1999). However, IRAK2 showed some kinase activity in macrophages also expressing IRAK4. The kinase activity of IRAK2 was demonstrated to be essential for cytokine production in response to TLR stimulation in macrophages (Kawagoe et al., 2008). The exact function of the kinase activity of IRAK2 is still under investigation and remains unclear (Hammarén et al., 2016; Pauls et al., 2013). IRAK2 has an asparagine residue at the catalytic site instead of the conserved aspartic acid in the kinase HRD motif, which is known to be essential for kinase activity (Kawagoe et al., 2008).

IRAK3 is a cytoplasmic protein which was found to contain a GC centre embedded in its kinase homology domain, this phenomenon is unique to IRAK3 in the family (Figure 1.4 B and C). In humans, IRAK3 is a pseudokinase that lacks the conserved aspartic acid in the kinase HRD motif, it is replaced by a serine 293 (Wesche et al., 1999) (Figure 1.4 B). Rodent species containing the IRAK3 gene have an asparagine residue in the catalytic site like IRAK2. Hence, sequence analysis indicates that IRAK3 may act as a possible kinase like IRAK2 in rodent species. Further investigation is necessary however to clarify the evolution of the IRAK3 gene (Gosu et al., 2012). IRAK3 is found mainly in mammalians, however, IRAK3 was also found in two fish species. Phylogenetic analysis suggested that IRAK4-like kinase is the ancestral gene of all IRAKs which has diverged from an ancestral gene in the metazoan lineage (Gosu et al., 2012).

A significant amount of our knowledge of innate immune signalling pathways have come from mouse and mouse knockout studies, however, this may not be the best model for the IRAK proteins. A study on humans deficient in specific TLR pathway components adapted a similar cellular response phenotype supporting the pathway structure established in mouse studies. However; the wider immune phenotypes often show significant differences in the human patients when compared to the corresponding knockout mouse models, this suggests a potential divergence in the

regulation of TLR dependent immune outputs at the physiological level between mice and humans (Sun et al., 2016). Considerable differences were identified in how human and mouse macrophages signal through IRAK proteins in response to different TLR ligands. Mouse cells were shown to require IRAK4 and IRAK2 for TLR signalling, however, IRAK1 was not as important. In human macrophages, IRAK1 was important, however, the phenotype in human macrophages did not change when either IRAK2 or IRAK4 was knocked down (Sun et al., 2016).

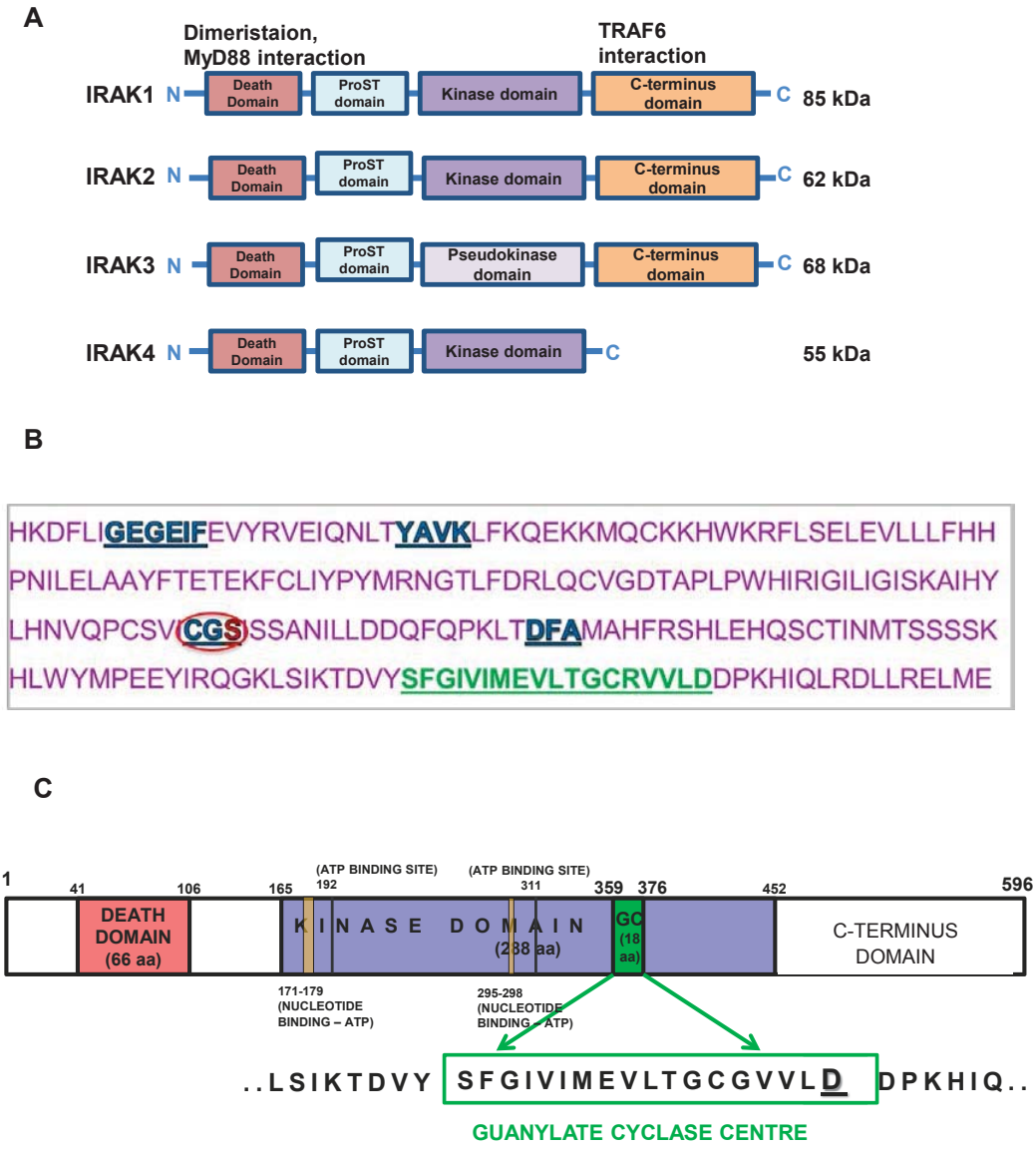

Figure 1.4 The IRAK family domain architecture

Domain organisation and size of the IRAK family proteins adapted from (Rhyasen and Starczynowski, 2015) (B) Part of the IRAK3 amino acid sequence with the conserved kinase motifs highlighted in blue. The CGS (specifically serine 293) domain circled in red is in place of the conserved HRD motif in active kinases, the guanylate cyclase motif is highlighted in green. (C) IRAK3 domain architecture adapted from UNIPROT – Q9Y616 information. The guanylate cyclase centre is in green, the kinase domain is in purple, death domain is in red and a C-terminus domain. http://www.uniprot.org/uniprot/Q9Y616 24/04/17.

1.2.2 IRAK3 function in innate immunity

TLRs are pattern recognition receptors implicated in the initiation of the innate immune response. TLRs belong to the TLR/Interleukin-1 receptor (IL-1R) superfamily, humans are known to have ten different subtypes TLR (1-10). TLR/IL-1R induction of pro-inflammatory mediators must be regulated to prevent excessive inflammation and tissue damage (Hubbard and Moore, 2010). Unlike the other IRAK family members, IRAK3 is a negative regulator of this pathway, thought to act via a negative feedback loop (Kobayashi et al., 2002; Li et al., 2011; Wesche et al., 1999). In humans IRAK3 is mainly confined to monocytes and macrophages hence it is also known as IRAKM (Xie et al., 2007) however IRAK3 has also been found in human airway epithelial cells, especially in asthmatic patients (Wu et al., 2012). Comparatively, the other IRAK members are expressed abundantly (Hubbard and Moore, 2010; Wesche et al., 1999).

Initially, Wesche et al. (1999) proposed that IRAK3 was a positive regulator of TLR signalling due to research suggesting that IRAK3 expression in IRAK1 deficient cells was able to restore NFκB activation (Wesche et al., 1999). Yet, in a study done by Kobayashi et al. (2002), IRAK3 knockout mice showed increased inflammation in response to *Salmonella typhimurium (Kobayashi et al., 2002)*. Additionally, IRAK3 was shown to play a significant part in the immunosuppressive action of glucocorticoids, where IRAK3 mRNA and protein expression was upregulated upon glucocorticoid receptor activation (Miyata et al., 2015). These results indicated that IRAK3 might, in fact, have a negative feedback role in the TLR-NFκB pathway, and acts to inhibit the release of excess pro-inflammatory mediators. The role of IRAK3 is critical to maintaining homeostasis in the innate immune response and in preventing the development of autoimmune diseases (Flannery and Bowie, 2010).

1.2.3 Signalling of IRAK3

Upon activation, TLRs transduce their signals through a complex signalling network. All the TLR except for TLR3 involves the adaptor molecule MyD88. Subsequent interaction with the IRAK family members allows for the formation of a myddosome complex. A myddosome complex is the arrangement of the protein adapters and signalling components binding through their death domain into a MyD88–IRAK4–IRAK2/1 complex. The death domain (DD) myddosome complex is crystallised, this structure demonstrates a sequential assembly of the adapter proteins. The complex forms as MyD88 recruits IRAK4, the MyD88–IRAK4 complex then goes on to recruit IRAK2 or the related IRAK1 (Lin et al., 2010). IRAK1/2 forms a complex with another adapter protein, tumour necrosis factor receptor associated factors 6 (TRAF6) and dissociates from the receptor complex (Figure 1.5). IRAK3 was shown to specifically interact with IRAK2, but not with IRAK1 in TLR subtype 7 (TLR7) activation (Figure 1.5). This cascade is known to cause TLR7-induced transforming growth factor beta activated kinase 1 (TAK1)-dependent NFκB activation. This complex goes on to activate a cascade of downstream signals. IRAK3 is believed to function as a negative regulator that prevents this dissociation, thereby inhibiting downstream signalling (Kobayashi et al., 2002; Zhou et al., 2013).

An alternative regulatory pathway demonstrates that IRAK3 is also able to interact with MyD88–IRAK4 to form an IRAK3 myddosome. This interaction mediates a TLR7-induced mitogen-activated protein kinase kinase kinase 3 (MEKK3)-dependent second wave NFκB activation, which is uncoupled from post-transcriptional regulation (Figure 1.5). The IRAK3-dependent pathway only induced expression of genes that are not regulated at the post-transcriptional level, which include the inhibitory molecules: suppressor of cytokine signalling 1 (SOCS1), SH-2 containing inositol 5'-polyphosphatase 1 (SHIP1), the tumour necrosis factor alpha-induced protein 3 (A20) and nuclear factor of kappa light polypeptide gene enhancer in B-cells inhibitor, alpha

(IκBα), causing an overall inhibitory effect on the inflammatory response (Figure 1.5) (Zhou et al., 2013).

A study looking at the IRAK family death domain interactions, showed that there is a possibility that IRAK2, IRAK1 and IRAK3 may assemble into the third layer of the myddosome interchangeably. IRAK3 may also form a fourth layer of the IRAK2 myddosome, where it is thought to inhibit downstream IRAK2 phosphorylation and consequently suppress the inflammatory response, this also agrees with Zhou et al (2013), (Figure 1.5); (Dossang et al., 2016; Zhou et al., 2013).

Interestingly, in their ongoing study, Zhou et al (2016) demonstrated that in bone marrow derived macrophages (BMDM), the myddosome complex formation and pathway selection may depend on the concentration of the TLR activating agent, in this case, lipopolysaccharide (LPS). IRAK3 but not IRAK1 was recruited to the IRAK4-MyD88 complex upon low-dose LPS stimulation (100 pg/mL), therefore this activated the MEKK3-dependent second wave pathway. However, upon high-dose LPS stimulation (1 μg/mL), both IRAK1 and IRAK3 interacted with IRAK4 activating both pathways (Zhou et al., 2016). Therefore the function of IRAK3 in chronic inflammatory diseases, where the LPS concentrations are much lower when compared to infectious stimulations, needs to be carefully investigated (Zhou et al., 2016).

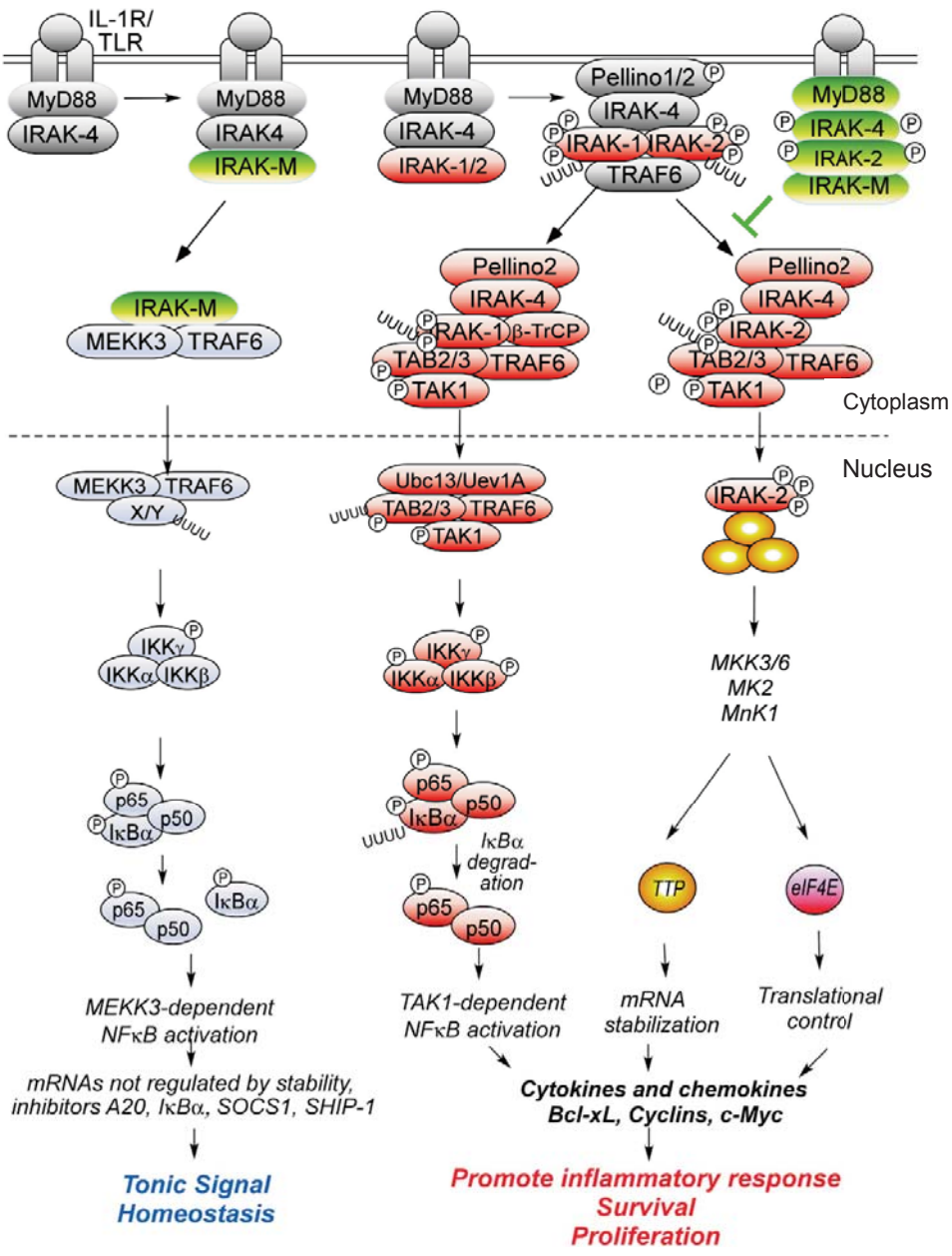

Figure 1.5 Regulatory role of IRAK3 in TLR/IL-1R signalling

IRAK3 (referred to as IRAK-M in this figure) acts either by interacting with IRAK2, therefore, suppressing downstream cytokine and chemokine translation. Or alternatively by interacting with MyD88 and IRAK4 to form an IRAK3 myddosome complex, activating NFκB through a MEKK3 second wave induction. This pathway induces expression of genes that are not regulated at the post-transcriptional levels which function to inhibit the inflammatory response. (Zhou et al., 2013).

1.3 IRAK3 FUNCTION IN DIFFERENT DISEASE STATES

1.3.1 IRAK3 in respiratory diseases

A number of studies have been conducted investigating IRAK3's roles in various inflammation-associated disorders such as lung injury, metabolic syndrome and tumour growth (Hubbard and Moore, 2010). Mouse studies have demonstrated irregularities in IRAK3 function may cause a disruption of immune system homeostasis (Rosati and Martin, 2002).

A study conducted on IRAK3 knockout mice demonstrated increased survival of these mice to pneumococcal pneumonia infection. The absence of IRAK3 as a proximal inhibitor of TLR signalling is implicated in macrophages producing elevated levels of pro-inflammatory cytokines when various pathogens bind to the TLR. Therefore, NFκB is able to elicit a regulatory immune response to the bacterial respiratory tract infection, when exposed to pathogens (van der Windt et al., 2012).

Sepsis is a devastating clinical syndrome characterised by systemic inflammation due to a severe infection. Elevated IRAK3 expression was observed in patients with septic melioidosis, an infectious disease caused by a gram-negative bacteria. The resultant immunosuppression was correlated with increased mortality. Higher IRAK3 mRNA levels was observed in patients that did not survive the infection. This significant increase in IRAK3 mRNA levels was not evident in patients that survived the infection (Wiersinga et al., 2009). During the innate immune response of the respiratory tract, it has been found that IRAK3 has an imperative role in regulating protective responses in the lungs. A study done by Pino-Yanes et al. (2011) examined the connection of IRAK3 with acute lung injury which is caused by over-inflammation during sepsis. IRAK3 impairs host defence during pneumococcal pneumonia at the primary site of infection by inhibiting the early immune response (Pino-Yanes et al.,

2011). The study revealed that increased expression levels of the IRAK3 gene were correlated with poorer outcomes during severe sepsis (Pino-Yanes et al., 2011).

Airway epithelial cells are the first line of defence against inhaled pathogens, this is through a number of defence mechanisms that also include TLR signalling pathways (Wu et al., 2012). IRAK3 protein expression was examined in human airway epithelia of both asthmatic and non-asthmatic patients. Significantly higher levels of IRAK3 were found in the airway epithelial cells of asthmatic subjects. Persistent upregulation of IRAK3 may increase exposure to inflammatory pathogens, thus compromising innate immunity (Wu et al., 2012). Furthermore, the chromosome region 12q13-14 is linked with early-onset asthma, and IRAK3 is critical to this connection. Rare mutations in the IRAK3 gene may predispose someone to asthma. Polymorphism of the IRAK3 gene had shown that variations in the gene could be linked to developing acute lung injury (Lyn-Kew et al., 2010). This was due to over-inflammation of the lung epithelia, however; without IRAK3, a pro-inflammatory response may lead to aggravated lung damage and may compromise multiple organs, therefore a balance is necessary (Villar et al., 2010). With this knowledge, IRAK3 may serve as a potential target for modifying the development of persistent asthma (Balaci et al., 2007).

1.3.2 IRAK3 in metabolic diseases

Wu et al. (2012) also provided data concerning the activation of the Phosphatidylinositide 3-kinases (PI3K) pathway. The PI3K/Akt family of kinases has been involved in the negative regulation of macrophage activation (Zacharioudaki et al., 2009), together with IRAK3 could synergistically dampen the immune response (Zacharioudaki et al., 2009). It was shown that the activation of the PI3K pathway is required for interleukin-13 (IL-13) induced IRAK3 expression, IL-13 is a protein secreted mainly by T-helper type 2 (Th2) cells. Th2 cells are an essential mediator of both inflammation and associated disorders (Wu et al., 2012).

IRAK3 is a critical factor contributing to endotoxin tolerance (Lech et al., 2011). A study on mouse macrophages showed that IRAK3 upregulation in endotoxin tolerance is induced by adiponectin which is dependent on the PI3K pathway (Zacharioudaki et al., 2009). Adiponectin is a hormone mainly involved in regulating blood glucose levels and fatty acid breakdown. High levels of adiponectin are often associated with a high body fat percentage in people, correlating closely with obesity and metabolic syndrome. It is shown by Hulsmans et al. (2012) that a down regulation of IRAK3 in obese people is associated with metabolic syndrome. Constant down regulation of IRAK3 was linked to chronic systemic inflammation and is associated with low adiponectin levels combined with high glucose and interleukin-6 (Hulsmans et al., 2012). Hulsman et al. (2012) showed a direct link between weight loss and the increase in IRAK3 expression, displaying the ability of IRAK3 to inhibit inflammation in the TLR-NFκB pathway. This study was able to link low adiponectin levels with a reduction in IRAK3 expression, and vice versa. This correlates with the knowledge that greater activation of blood monocytes occurs with obesity (Hulsmans et al., 2012). Hence, up regulation of IRAK3, and consequently the reduced activation of macrophages and monocytes may partially prevent insulin resistance and metabolic syndrome (Hulsmans et al., 2012).

IRAK3 deficiency was also correlated with promoting early onset type 1 diabetes in non-obese diabetic mice (Tan et al., 2014). Loss of IRAK3 expression in mice is linked to the development of several autoimmune diseases including lupus, colitis and inflammatory bowel disease. Type 1 diabetes mellitus is characterised by the loss of the insulin producing β-cells due to an autoimmune attack. Non-obese diabetic mice lacking IRAK3 displayed early onset and rapid progression of type 1 diabetes mellitus with impaired glucose tolerance possibly due to the unregulated activation of the TLRs which can lead to uncontrolled inflammatory responses that can predispose autoimmune responses (Tan et al., 2014).

1.3.3 IRAK3 in cancer

Chronic inflammation and dysregulation of inflammatory signalling components have been increasingly recognised to be associated with tumourigenesis and tumour progression (Jain et al., 2014; Rhyasen and Starczynowski, 2015). Depending on the tumour type IRAK3 expression can increase or decrease. A number of studies indicated that specific tumours can increase IRAK3 expression to suppress the innate immune response, therefore, allowing tumour growth. Knock out mice studies demonstrated that IRAK3 deficiency leads to enhanced host protection against tumour growth due to an increase in inflammation (del Fresno et al., 2005; Standiford et al., 2011; Xie et al., 2007). An increase in IRAK3 mRNA and protein expression was observed in tumour associated macrophages induced by factors found in the tumour microenvironment such as TGF-β. By increasing the levels of IRAK3, cancer cells can exploit IRAK3s inhibitory function, therefore permit them to escape from anti-tumour responses by macrophages, allowing tumour growth and metastasis (Standiford et al., 2011). Earlier studies had shown that tumour cells and soluble factors released by these cells induced transcription of the IRAK3 gene in human monocytes (del Fresno et al., 2005). Monocytes isolated from patients suffering from chronic myeloid leukaemia had increased IRAK3 mRNA due to the monocytes continuous contact with the tumour cells. This was not the case however for patients suffering from solid colon cancers (del Fresno et al., 2005; Hubbard and Moore, 2010). Recently this was further emphasised by Kesselring et al (2016) where IRAK3 was shown to be expressed in colorectal cancer cells. IRAK3 promotes colitis associated colon cancer by stabilising STAT3 which is activated in colorectal cancer leading to the induction of genes that function in cell proliferation and survival. IRAK3 was also shown to regulate microbial colonisation by reducing the antimicrobial defence, allowing for cancer progression (Kesselring et al., 2016). However, in another study on driver epigenetic events on cancer cell survival, IRAK3 expression

was shown to be reduced in specific cancers, namely colon adenocarcinoma (De Carvalho et al., 2012). Cancer cells can downregulate the IRAK3 gene by DNA methylation causing gene silencing. Silencing of the IRAK3 gene is essential for cancer cell survival due to IRAK3's indirect inhibitory function on the 3 essential pathways NFκB, STAT3 and MAPK especially required by cancer cells. These pathways consequently go on to regulate the expression of the antiapoptotic gene, survivin. DNA methylation is an epigenetic process that can change the gene expression but not the DNA sequence. Induced silencing by cancer cells of tumour suppressor genes including the IRAK3 gene can make a good target for epigenetic therapy (De Carvalho et al., 2012).

1.4 AIMS

The discovery of the GC catalytic centres within the kinase domain of proteins which includes IRAK3 has led our group into developing a new classification of GCs. To date the novel class of GCs have only been studied using plant proteins, however; other molecules were identified which are involved in defence and inflammatory processes in other non-plant species including humans. This observation suggests that these molecular domains have conserved evolutionary significance in defence responses. In order to test the widespread nature of these observations, it is essential to extend the work to other systems. The human protein, IRAK3 identified as a soluble GC is further studied in this thesis. Identifying the signalling mechanism in regards to its distinctive GC centre might explain some of the unanswered questions in regards to its selective binding to the other IRAKs as well as the myddosome complex. The selective interaction/binding of IRAK3 to the other signalling proteins to either suppress NFκB activity or otherwise through the alternative pathway to activate NFκB is still largely unclear. It is hypothesised that the GC centre of IRAK3, through the production of cGMP can modulate the IRAK3 function in the innate immune signalling

cascade. By mutating specific residues in the IRAK3 GC centre, the GC activity may be abolished, therefore reducing cGMP production. Such a malfunctioning GC mutant is hypothesised to have an alternative or reduced activity in the innate immune signalling pathway.

The aim of this project is to examine the GC centre of IRAK3 by assaying the GC activity of recombinant proteins *in vitro* and *in vivo* cell studies. Key amino acid residues in the catalytic centre will be identified and used in a mutagenesis study to investigate the effect the GC centre may have on IRAK3 signalling.

In the investigation of IRAK3 and its GC activity, repeated assays are needed for the detection of cGMP in this novel class of GCs, therefore; a reliable cGMP screening tool is ideal. Available cGMP detection kits can get quite expensive and time consuming when repeated and large screens are needed. To assist our GC research a cGMP sensitive OPTX-promoter system was designed and is shown to be a good option for the initial screening assays of potential novel guanylate cyclases as described in chapter 3 (Wheeler et al., 2013).

To explain how the novel GC centre may fit into the pseudokinase domain of IRAK3, a model is needed. Since a crystal structure is not yet available for IRAK3, we constructed a homology model based on the IRAK4 kinase domain crystal structure as detailed in chapter 4. This model is also used as a guide for further GTP docking and mutagenesis studies.

The inhibitory function of IRAK3 in the innate immune signalling cascade is of particular interest in terms of its guanylate cyclase activity. Therefore; we hypothesise that the novel GC activity of IRAK3 may modulate its inhibitory functions in the innate immune signalling cascade. The IRAK3 GC activity is investigated using different biological systems with different quantification techniques are used to detect cGMP, as outlined in chapter 5.

How the GC function of IRAK3 may affect downstream NFκB activity is investigated in chapter 6. Mutagenesis is used to investigate the importance of the GC centre on downstream signalling by looking at NFκB activity in the presence of IRAK3 or its GC mutants. The outcomes may explain some of the gaps in the knowledge of IRAK3s signalling mechanism. There are many opportunities for further investigations and potential therapy targets concerned with IRAK3, and some of these are suggested in chapter 7.

CHAPTER 2

GENERAL METHODS

CHAPTER 2

GENERAL METHODS

The rationale for this chapter is to provide a single site for all the common methods used throughout this thesis.

2.1 MOLECULAR CLONING OF GENES

2.1.1 IRAK3 constructs

The IRAK3 gene was obtained in a pBluescriptR plasmid (MHS1010-9204142, clone ID 30335802) and cloned using Gateway cloning technology, cloning of the first IRAK3 entry and destination clones were done in the Irving lab by Lubna Freihat prior to the start of the PhD. The gateway primers were designed in accordance with the guidelines for PCR primers in the Gateway technology manual, five primers were designed in total to make four constructs; two forward primers, each containing the Kozak sequence and three reverse primers to either incorporate a Myc tag or a STOP codon (Table 2.1). The gene of interest was cloned into the entry clone pDONR207 using the Gateway® BP Clonase™ II Enzyme Mix (Invitrogen, Thermo Scientific USA).

The gene of interest was then transferred using the Gateway® LR Clonase™ II Enzyme mix into the appropriate Gateway expression vector, either the pDEST17 for bacterial expression or pCDNA™ 6.2/C-EmGFP-DEST or pCDNA-DEST40 for mammalian cell expression (Invitrogen, Thermo Scientific USA).

2.1.2 IRAK4 constructs

The IRAK4 gene was obtained in a pDONR223 plasmid (Plasmid 23749: PDONR223-IRAK4, Addgene) (Johannessen et al., 2010) and cloned using the Gateway cloning technology. The gene of interest was transferred using the Gateway® LR Clonase™ II Enzyme Mix - into the appropriate Gateway expression vector, either the pDEST17 for bacterial expression or pCDNA™ 6.2/C-EmGFP-DEST or pCDNA-DEST40 for mammalian cell expression (Invitrogen, Thermo Scientific USA).

IRAK3-1-FWD 5'-**ggg gac aag ttt gta caa aaa agc agg ctt cac cat ggg gat ggc ggg gaa ctg tgg ggc c**-3'
IRAK3-3-FWD 5'-**ggg gac aag ttt gta caa aaa agc agg ctt cac cat ggg gga aca gaa act gat tag cga aga aga tct gat ggc ggg gaa ctg tgg ggc c**-3'
IRAK3-2-REV 5'-**ggg gac cac ttt gta caa gaa agc tgg gtc cta ttc ttt ttt gta ctg ttc ata**-3'
IRAK3-2NS-REV 5'-**ggg gac cac ttt gta caa gaa agc tgg gtc ttc ttt ttt gta ctg ttc ata**-3'
IRAK3-4-REV 5'-**ggg gac cac ttt gta caa gaa agc tgg gtc cta cag atc ttc ttc gct aat cag ttt ctg ttc ttc ttt ttt gta ctg ttc ata**-3'

201-FWD	5' - **tcg cgt taa cgc tag cat gga tct c** - 3'
201-REV	5' - **gta aca tca gag att ttg aga cac** - 3'
TK polyA REV	5' - **ctt ccg tgt ttc agt tag c** - 3'
T7 FWD	5' - **taa tac gac tca cta tag gg** - 3'
GFP-REV	5' – **tgg tgc aga tga act tca gg** - 3'

Table 2.1 Primer sequences for gateway cloning

The primer sequences in the top table are highlighted/coloured as follows, the specific gateway sequence for recombination with entry clone is in purple, the Kozak sequence is green, the Myc tag is blue, the gene specific sequence is in black and the stop codon is in red. The sequencing primers used to sequence the genes of interest in the gateway clones are in the bottom table.

2.2 GENERAL MOLECULAR CLONING METHODS

2.2.1 Media preparations and bacterial culturing

Luria Broth (LB) agar plates were prepared, 25 g/l of Luria Broth premade (Sigma-Aldrich, Australia) and 15g/l of the agar (Sigma-Aldrich, Australia) was used. The preparation was autoclaved at 121ºC for 20 min. The appropriate antibiotic is added just before the liquid is poured into the Petri dishes. The LB liquid medium is prepared in the same way, but no agar is added. The appropriate antibiotic is added as needed. Three strains of *Escherichia coli* bacteria were used in this project, One Shot® ccdB Survival™ 2 T1R Chemically Competent Cells, One Shot® Max Efficiency® DH5α™-T1R Competent Cells and One Shot® BL21-AI™ *E. coli* all from Invitrogen™ (Thermo Fisher Scientific, USA). These bacteria are sensitive to ampicillin 50-100 µg/ml unless the *E. coli* contained plasmids carrying the ampicillin resistance gene. Bacteria were grown using three different techniques. Transformed chemically competent cells are spread over a LB agar plate, separate single colonies are streaked on another LB agar plate. Liquid LB media cultures were prepared by the inoculation of a single colony from the streak LB agar plate in the LB media containing the appropriate antibiotic.

2.2.2 Transforming chemically competent cells

Competent *E. coli* bacteria are utilised to replicate a specific plasmid DNA. The transformation process was carried out according to the manufacturers' protocol. In general 1-10 ng/µl of a specific plasmid was added to 10-50 µl of competent cells. In this project, heat shock was used for all transformations. Transformed cultures are spread onto LB agar plates containing the appropriate antibiotic (e.g. ampicillin 100 µg/ml and gentamycin 15 µg/ml) and incubated overnight at 37 ºC.

2.2.3 Extraction and purification of DNA

To extract and purify the DNA from the bacterial cultures the PureLink® Quick Plasmid Miniprep Kit (Thermo Fisher Scientific, USA) for small scale purification and the PureLink® HiPure Plasmid Filter Midiprep Kit for larger scale purification were used.

2.2.4 DNA quantification

The Nanodrop® ND-1000 Spectrophotometer (Thermo Fischer Scientific, USA) was used to quantify the amount of DNA.

2.2.5 Plasmid digestion with appropriate restriction enzyme

To confirm the identity of the plasmids used and cloned in this study, plasmids were digested with selected restriction enzymes. The aim was to cut the plasmid at different points, so as to achieve at least two fragments, with a predicted length. To observe the fragment length, agarose gel electrophoresis was used as described in part 2.2.7.

2.2.6 Polymerase chain reaction (PCR)

PCR reactions are generally carried out to amplify and/or verify DNA samples. The primers used in this project are listed in Table 2.1 and 2.2. A standard PCR mixture contained 1 X Coral load buffer, 200 µM dNTPs (deoxynucleotide triphosphates), 0.1 µM primers and 0.5 units of Taq DNA polymerase (QIAGEN, Germany) and 2.5 fM DNA per 25 µl reaction. The MyCycler Thermal Cycler System (Bio-Rad, USA) was used to perform the PCR reactions. Generally, the samples were denatured at 95ºC for 15 minutes, followed by 30 cycles of amplification, which included denaturation at 95ºC for 30 seconds, annealing at 55ºC (variable) for 30 sec, an extension at 72ºC for 30 sec - 1 min and a final extension at 72ºC for 5 min. The annealing temperature is about 5ºC below the melting temperature (Tm) of the primers. The extension time depends on the size of the product expected; the time may need to be increased if the expected products are larger than 1000 base pairs.

2.2.7 Agarose gel electrophoresis

Agarose gel electrophoresis is used to observe the success of molecular cloning experiments. Agarose is a polysaccharide which forms a matrix, DNA fragments move through with a speed that is proportional to their size allowing for separation of DNA fragments of different length. To make the DNA visible, fluorescent nucleic acid gel stain GelRed™ (Biotium, USA) was used. For this purpose, 1% Agarose was dissolved in TAE (Tris-acetate-EDTA) buffer. DNA was mixed with Gel Loading Dye, Purple (6X) (NEB, Australia) except for PCR products which already contain the 1 x Coral load PCR buffer (QIAGEN, Germany). The gel was run at 90 volts for 40 to 60 minutes.

2.2.8 Gel extraction and PCR spin purification cleanup

The QIAquick Gel extraction kit from QIAGEN (QIAGEN, Germany), was used following the manufacturers' protocol. This technique is used to extract and purify specific DNA bands from an agarose gel. The UltraClean™ PCR Clean-Up Kit (Mo Bio Laboratories, USA) was used to purify the PCR products. The protocol was followed as outlined in the manufacturers' manual.

*2.*3 GATEWAY CLONING

2.3.1 BP recombination of PCR products

PCR products were purified using the UltraClean™ PCR Clean-Up DNA Purification Kit and quantified using the Nanodrop® ND-1000 Spectrophotometer. For the recombination reaction into entry clone pDONR207 (Invitrogen, Australia) 75 ng of PCR product and 75 ng of entry clone were combined with 1 µl BP clonase II enzyme (Invitrogen) and made up to a total volume of 10µl with water. Reaction was incubated at 25°C for two hours; 1µl proteinase K solution (2 µg/µl) (Invitrogen, Australia) was added to the mix to inactivate the BP clonase II enzyme and incubated for 15 minutes at 37°C. One Shot® MAX Efficiency® DH5α™-T1R Competent Cells (Invitrogen) were transformed with 1 µL of the BP reaction products. The clones were selected and purified. Samples were sent for sequencing to Micromon DNA sequencing facility Monash University to verify suitable constructs.

2.3.2 LR recombination of entry clone and expression vector

The gene of interest was transferred from the entry clone into the destination/expression vectors using an LR recombination reaction. For this reaction, 75 ng of entry clone and 75 ng of destination vector were combined with 1 µl of LR clonase II (Invitrogen) and water was added to a total volume of 10 µl. The reaction was incubated at 25ºC for 2 hours; 1 µl proteinase K solution (2 µg/µl) (Invitrogen) was added to the mix to inactivate the LR clonase enzyme. 1 µl of the LR products were transformed into chemically competent DH5α cells. The identity of derived clones was verified via PCR, restriction enzyme digest and sequencing.

2.4 MUTAGENESIS

2.4.1 Primer design

Primers were designed to mutate specific residues in the kinase domain of the IRAK3 and IRAK4 gene. The Agilent Technologies Quick change primer design program was used to design the mutagenesis primers (Table 2.2).

2.4.2 PCR and mutagenesis

To mutate the specific residues in the IRAK gene, a master mix was prepared containing the specific primers at a final concentration of 0.5 µM. The Phusion® High-Fidelity DNA Polymerase was used to catalyse the reaction mix. The Phusion PCR conditions included an initial denaturation at 98^{o}C for 30 seconds, followed by 20 cycles of 98^{o}C denaturation for 10 seconds, 68^{o}C Annealing for 30 seconds and an extension at 72^{o}C for 4 min. The final step was a final extension at 72^{o}C for 10 min. The PCR products were digested with the restriction enzyme DpnI (NEB, Australia) at 37°C, this was done to select for the mutated clones, DpnI cleaves only at methylated DNA purified from a dam+ strain like DH5α. Mutant clones were transformed into One Shot® Max Efficiency® DH5α™-T1R competent cells and were grown in ampicillin (100 µg/ml) containing media for selection, specific clones were chosen, purified and sent for sequencing for verification. Successfully mutated clones were then transferred to the appropriate expression vector via an LR reaction as described in part 2.3.2.

IRAK3G361LFwd 5'-**tcc att aaa aca gat gtc tac agc ttt tta att gta ata atg gaa gtt cta aca gg**-3'
IRAK3G361L_antisense 5'-**cct gtt aga act tcc att att aca att aaa aag ctg tag aca tct gtt tta atg ga** -3'
IRAK3R372LFwd 5'-**gga att gta ata atg gaa gtt cta aca gga tgt tta gta gtg tta gat gat c**-3'
IRAK3R372L_antisense 5'-**gat cat cta aca cta cta aac atc ctg tta gaa ctt cca tta tta caa ttc c**-3'
IRAK3S359L_G361LFwd 5'-**ggg gaa act ttc cat taa aac aga tgt cta cct ctt ttt aat tgt aat aat gga agt tct aac agg atg t**-3'
IRAK3S359L_G361L_antisense 5'-**aca tcc tgt tag aac ttc cat tat tac aat taa aaa gag gta gac atc tgt ttt aat gga aag ttt ccc c**-3'

IRAK4-C1154G-Fwd 5'-**aaa taa taa ctg gac ttc gag ctg tgg atg aac acc g**-3'
IRAK4-C1154G_antisense 5'-**cgg tgt tca tcc aca gct cga agt cca gtt att att t** -3'

Table 2.2 The IRAK3 and IRAK4 mutagenesis primer sequences

The IRAK3 mutagenesis primers are at the top of the table showing the gene specific forward primer and the antisense primer each with the associated mutation underlined in red. The IRAK4 mutagenesis forward primer and the antisense primer are in the bottom table with the associated mutation underlined in red.

2.5 RECOMBINANT PROTEIN EXPRESSION

2.5.1 Bacterial transformation

The pDEST17 vector (Invitrogen) containing the gene of interest was used for the expression of the recombinant proteins in *E. coli*. The procedure was followed as outlined in the *E. coli* Expression System with Gateway Technology manual (Invitrogen, USA). The purified expression vector was transformed into competent BL21-AI *E. coli* cells (Invitrogen, USA).

2.5.2 Protein expression

One shot BL21-AI cells (Invitrogen) were used to transform the expression clone of IRAK3, IRAK3 Mutant G361>L, IRAK3 Mutant R372>L and IRAK4 all in pDEST17. High expressing cultures were selected before the chosen cultures were upscaled to 500ml. Upscaled liquid cultures were grown to an OD600 of ~0.4 before they were induced with 0.2% L-arabinose (Sigma-Aldrich, Australia) and allowed to grow for a further 3 hours at 20ºC. Cells were harvested by centrifugation.

2.5.3 Protein purification

The proteins of interest were purified by affinity chromatography using the Ni-NTA agarose beads (QIAGEN, Germany). The purification was done under native conditions following protocol 12 of the QIAexpressionist manual (QIAGEN, Germany) in the presence of 30 mM imidazole to decrease the unspecific binding onto the Ni-NTA beads and in the presence of complete EDTA-free protease inhibitor cocktail tablets (Roche, Australia). Once the protein is eluted, the protein is concentrated using Vivaspin® 20 centrifugal concentrators (Sartorius Stedim Biotech, Germany) with a molecular weight cut-off of 30 kDa in the presence of 1 mM Phenylmethylsulfonyl fluoride (PMSF). The Nanodrop® ND-1000 Spectrophotometer protein A_{280} was used to quantify the protein amount at A_{280} nm.

2.5.4 Polyacrylamide SDS gel electrophoresis

To separate protein samples a 16% separating and 4% stacking gel SDS-PAGE was used. The electrophoresis instruments used are from Bio-Rad (Bio-Rad Laboratories, USA). SDS sample pellets were resuspended in SDS-PAGE sample buffer (Tris-HCl (pH 6.8) 120 mM, Glycerol 20% v/v, 4% SDS w/v, 2- Mercaptoethanol 10% v/v, Bromophenol blue 0.03% w/v). Samples were boiled for 5 min and then centrifuged briefly; samples are loaded on an SDS-PAGE gel. The gel was run at 200 volts for 50 minutes.

2.5.5 Coomassie blue staining

Polyacrylamide gel were stained with Coomassie blue (0.1% Coomassie Brilliant blue, 50% methanol, 10% glacial acetic acid and 40% distilled water), and destained with destain buffer (40% Methanol, 10% Acetic acid and 50% distilled water).

2.5.6 Immunoblot

To confirm the presence of the proteins post purification, a immunoblot analysis was done. Immediately after the polyacrylamide gel was run, the proteins were transferred from the gels to a nitrocellulose membrane (Whatman, GE Healthcare, Australia). The proteins were detected using either the mouse anti-His (Invitrogen, USA) or the rabbit IRAK3 antibody (Cell signalling technologies, USA) primary antibody and the corresponding secondary antibody. IRDye infrared dyes 680 or 800, the protocol used was from the Odyssey western blot detection (Li-Cor Biosciences, USA), the Odyssey (Li-Cor Biosciences – Li-Cor Odyssey Model 9120, USA) was used to observe the bands at the corresponding secondary antibody fluorescence of either 700 nm (red channel) or 800 nm channel (green channel).

2.6 cGMP ANALYSIS

2.6.1 cGMP preparation

2.6.1.1 cGMP sample preparation from recombinant purified protein

cGMP samples were prepared by incubating 5 µg – 10 µg protein in 50 mM Tris-HCl pH 8.0, 5 mM $MgCl_2$ or 5 mM $MnCl_2$, 2 mM of the phosphodiesterase inhibitor isobutyl methyl xanthine (IBMX) and 1 mM GTP in a final reaction volume of 100 µl. cGMP samples requiring calcium in the reaction were prepared as mentioned above, however calcium ion concentrations were controlled by adding 1 mM EGTA and total $CaCl_2$ calculated to contain free Ca^{2+} ion levels at 0.01, 0.1 and 1 µM (physiological range) using the Maxchelator WebMaxC Extended computational program (http://www-leland.stanford.edu/~cpatton/webmaxc/webmaxcE.htm ; last accessed 14 December 2016) taking into account the temperature, pH and ionic strength of the calcium buffer. As a negative control incubation medium was prepared with no protein added. Reactions were incubated for 15 min at room temperature (~25ºC). The reaction was terminated with 10 mM EDTA. Tubes were boiled for 3 min, cooled on ice for 2 min and centrifuged at 4300 × g for 3 min at 4ºC (Muleya et al., 2014). The clarified supernatant was retained and assayed for cGMP content as described in part 2.6.2.

2.6.1.2 cGMP sample preparation from mammalian cells

HEK 293T cells were grown for 48 hours post transfection in a Corning® Costar® cell culture 6 well plate (Sigma Aldrich, Australia), cells were lysed by the addition of 0.5% dodecyl ltrimethylammonium bromide supplied in the Amersham cGMP Enzyme immunoassay Biotrak (EIA) System kit. Cells were agitated on a microplate shaker for 10 minutes to facilitate lysis. Lysed cells are used immediately in the immunoassay, however cell lysates can be stored for up to 5 days at -80 ºC.

2.6.2 cGMP ELISA assay

The Amersham cGMP Enzyme immunoassay Biotrak (EIA) System (GE Healthcare, UK) was used to detect cGMP in the protein preparation and cell lysates, following the protocol which measures total cellular cGMP using novel lysis reagents, described by the supplier. The New East monoclonal Anti-cGMP Antibody Based Direct cGMP ELISA kit (Non-acetylated) (New East Biosciences, USA) was also used for comparison following the manufacturer's protocol. Absorbance was measured as optical density readings at 405 or 450 nm. All cGMP quantification assays were carried out as independent triplicate experiments.

2.6.3 Mass spectrometry

The cGMP samples were prepared as outlined in part 2.6.1. Samples were dried by Freeze-drying using the Dynavac freeze dryer and sent to Professor Christoph Gehring's lab at the King Abdullah University of Technology (KAUST) in Saudi Arabia for liquid chromatography–tandem mass spectrometry (LC - MS/MS) where the analysis was done by Dr Aloysius Wong.

2.7 KINASE ACTIVITY ASSAY

Recombinant purified protein was used in the kinase assay, 1 µg of protein per 75 µl reaction mix was prepared. The reaction mix is made up of a final concentration of 1 x Omnia® Ser/Thr reaction buffer, 1 mM ATP, 0.2 mM DTT and 10 µM Omnia® Ser/Thr Peptide 1 (Invitrogen, Thermo Fisher Scientific, USA).

To test the kinase activity of IRAK3, the Omnia® Ser/Thr Peptide 1 kit (Invitrogen, Thermo Fisher Scientific, USA) was used following the manufacturer's protocol. The serine/threonine kinase activity of IRAK3 was investigated where phosphorylation is detected as an increase in fluorescence of the SOX chemophore using the Ser/Thr peptide 1 as a substrate. Reactions were set up in triplicates in a white Nunc 96 well

plates (Nunc, Thermo Fisher Scientific) and fluorescence was measured with an Envision 2101 plate reader (PerkinElmer, Melbourne Australia) with excitation at 355 nm and emission at 470 nm for 10 minutes.

2.8 TISSUE CULTURE

2.8.1 HEK 293 cells

2.8.1.1 293T cells

Human embryonic kidney 293T (HEK 293T) cells (American Type Culture Collection ATCC: CRL-11268) were used in the cGMP assay experiments, they were grown in Dulbecco's Modified Eagle Medium (DMEM) with 10% Fetal Bovine Serum (FBS).

2.8.1.2 HEK BLUE hTLR4

HEK BLUE™ hTLR4 cells were obtained from InvivoGen (InvivoGen, USA). These cells contain the human toll-like receptor 4 (TLR4), lymphocyte antigen 96 (MD-2) and the cluster of differentiation (CD14) co-receptor genes, and an inducible secreted embryonic alkaline phosphatase (SEAP) reporter gene. The SEAP reporter gene is under the control of the IL-12 p40 promoter fused to five NFκB (nuclear factor kappa-light-chain-enhancer of activated B cells) and AP-1 (activator protein 1) binding sites. Levels of SEAP can be determined with QUANTI Blue™ Detection (InvivoGen (USA)). HEK BLUE™ hTLR4 cells were grown as described in the cell maintenance protocol provided using HEK BLUE selection antibiotics. The TLR4 stimulation with lipopolysaccharide (LPS) (Escherichia coli 055:B5, Sigma-Aldrich) and NFκB activation was determined using QUANTI Blue™ Detection as described in the TLR4 stimulation determined using QUANTI Blue protocol (InvivoGen).

2.8.2 Culture and passaging of adherent cells

All cells were tested for mycoplasma before use; cells were split for 3 passages once taken from the frozen stock before testing for mycoplasma using the MycoAlert™ Mycoplasma Detection Kit (Lonza Australia). HEK 293T cells were grown in Dulbecco's Modified Eagle Medium (DMEM; Gibco) with 10% (v/v) Fetal Bovine Serum (FBS; Gibco) at 37°C, in a 5% CO2 tissue culture incubator. Cells were grown to 70-80% confluency before they were split, cells were only used up to a maximum passage of 30. Cells were washed with 1x PBS and lifted with 1x PBS and 2 mM EDTA. Cells were spun down at 350 g for 4 minutes and the supernatant was removed, cells were re-plated as needed in fresh DMEM and FBS. Antibiotics were not used in the tissue culture.

2.8.3 Transient transfection of cells

Cells were transfected using the Fugene HD (Promega, Australia) transfection reagent, the protocol was followed as outlined in the Promega Fugene HD manual. The Fugene database program was used to calculate the concentration of DNA and Fugene HD depending on cell type and plate used.

2.8.4 Stable transfection of cells

HEK BLUE™ hTLR4 cells were transfected as described in part 2.8.3, using the IRAK clones in the pCDNA-DEST40 vector which gives Neomycin (G418) resistance to the transfected cells, a pCDNA 6.2/nGFP-DEST control vector was also double transfected into cells at 1:10 to observe transfection efficiency, Neomycin (Sigma Aldrich, Australia) was added to the growth media and cells were split 4 times post transfection to select for the neomycin resistant transfected cells. Cells were checked for stable transfection of clones by western blot and RT-qPCR.

2.8.5 Transfection efficiency analysis

The efficiency was observed under the microscope, by visualising the green fluorescence of the reporter GFP (Green Fluorescent Protein) attached to the C-terminal of the gene of interest.

2.8.5.1 Imaging of live cells

Images were taken with a CoolSNAPFX camera (Photometrics, Arizona) attached to an Eclipse TE-2000E microscope (Nikon, Japan).

2.8.5.2 FACS analysis

FACS analysis was performed with a FACS Canto II analyser (BD Science, Australia). Before analysis, cell suspensions were cleared of clumps by passing through a 70µm strainer (BD Biosciences, Australia). GFP positive cells were compared to non-transfected cells and the percentage of transfected live cells were observed.

2.8.5.3 Immunoblot of cell culture samples

Adherent cells were grown in a 6 well plate to a confluency of about 70-80%. The cells were washed with 1X PBS and lifted using 1X PBS with 2 mM EDTA. Cells were spun down at 350 g for 4 min and the supernatant was removed. The cell pellet was resuspended in lysis buffer which consists of 150 mM NaCl, 1% (v/v) Triton X -100, 0.1% (w/v) SDS, 50 mM Tris base at pH 8 and protease inhibitor. The polyacrylamide gel was run and proteins transferred to a nitrocellulose membrane as outlined in parts 2.5.4 and 2.5.6.

2.9 SEAP ASSAY

HEK BLUE™ hTLR4 cells (Invivogen) were split at about 1.4 x10^5 cells per ml in a Corning® Costar® cell culture clear flat bottom 96 well plate and induced with 10 ng/µl of LPS (*Escherichia coli* 055:B5, Sigma-Aldrich). Control HEK BLUE™ hTLR4 cells were not induced with LPS. Cells were grown for 20-24 hours at 37°C, in a 5% CO_2 tissue culture incubator. In another clear flat bottom 96 well plate, post induction 20 µl of cell supernatant was taken in triplicate from each well and 180 µl of QUANTI Blue was added as described in the HEK BLUE™ hTLR4 QUANTI Blue™, TLR4 stimulation protocol. The plate was then incubated at 37°C for 1 hour. SEAP levels were determined using the Envision plate reader to read absorbance at 660 nm.

2.10 RT-qPCR

2.10.1 Cell preparations for RNA extraction

Transfected as well as non-transfected HEK BLUE™ hTLR4 cells were split at ~ 2 x10^5 cells per ml in a flat bottom 6 well plate and induced with 10 ng/µl of LPS, control cells were not induced with LPS. Cells were grown at 37°C, in a 5% CO2 tissue culture incubator for 24 hours. Cells were lifted with 1 X PBS and 2 mM EDTA, cell pellets were collected and stored at -80 ºC for RNA extraction.

2.10.2 RNA extraction

The RNA was extracted from the cell lysates using the QIAGEN RNeasy mini kit (QIAGEN, Germany). The extraction was done as recommended in the QIAGEN RNeasy mini kit protocol. A cleanup was done to clear DNA contamination from RNA samples using the TURBO DNAse treatment (Ambion, Life technologies. Germany). The amount of RNA extracted was quantified using the Nanodrop® ND-1000 Spectrophotometer. The RNA was stored at -80ºC till use

2.10.3 cDNA synthesis

First-Strand cDNA was synthesised from 1 µg of total RNA using the Superscript™ III Reverse transcriptase (Invitrogen, Australia). Supplied oligo-dTs and dNTPs were used during reverse transcription. The cDNA was stored at -80ºC till use.

2.10.4 PCR conditions and primer sequences

The mastermix was prepared using the SensiMix™ SYBR® Hi-ROX Kit (Bioline, Australia). The IRAK primer pairs (see Table 2.3) were designed using the IDT (Integrated DNA technologies) qPCR primer design website (http://www.idtdna.com/Primerquest/Home/Index), the specific exons of each sequence were obtained from the NCBI website. The primers were chosen from the

recommended list of primers based on the expected size of the product (100-300 bp). All primer pairs were checked with BLAST (http://blast.ncbi.nlm.nih.gov/Blast.cgi).

2.10.5 qPCR and analysis of data

Non-template controls were prepared for each qPCR analysis, consisting of RNA samples where reverse transcriptase was not added to ensure that DNA contamination of samples was not affecting qPCR results. Each sample was analysed in triplicate. The efficiency of reactions was determined using linear regression of the Log (fluorescence) per cycle number data with the LinRegPCR program version 2015.2 which considers the amplification with the efficiency of the primer pairs. Baseline correction was performed by subtracting the fluorescence value of the mean for the first five cycles to all values. Expression data of samples was calculated relative to the two housekeeping genes (β-actin and GAPDH) expressed as the following ratio, where Ct is the crossing point threshold of the sample for the amplified genes:

$$\text{Ratio} = (\text{Efficiency}_{\text{reference}})^{\text{Ct, reference}} / (\text{Efficiency}_{\text{sample}})^{\text{Ct, sample}}$$

2.11 Statistical analysis

Data was analysed using the GraphPad prism 7 software (GraphPad Software, USA). Data was analysed by t-test or ANOVA followed by multiple comparison post hoc tests. ($P<0.05$ was considered to be significant).

IRAK3 FWD 305	**gaa caa gag aat tac ttt ggt cct g**
IRAK3 FWD 974	**gtg gca gta tat caa gtg caa ac**
IRAK3 REV 414	**gga ctc aac act gct cca tag**
IRAK3 REV 1519	**ctc cag gaa tag agg aga agg a**
IRAK4 FWD 428	**ttg ctc cca gat gct gtt c**
IRAK4 FWD 885	**caa gtg atg gag atg acc tct g**
IRAK4 REV 532	**aga ttc tgc aca ggt gtc atc**
IRAK4 REV 1492	**agc agc tgt tga acc ttc tta**
GAPDH Fwd	**gaa ggt gaa ggt cgg agt c**
GAPDH Rev	**gaa gat ggt gat ggg att tc**
β-actin Fwd	**gcc ctg agg cac tct tcc a**
β-actin Rev	**ttg cgg atg tcc acg tca**

Table 2.3 The qPCR primer sequences

Top section displays the IRAK gene specific primers. The housekeeping gene sequences are displayed at the bottom of the section.

CHAPTER 3

DEVELOPING A CYCLIC NUCLEOTIDE SENSITIVE LUCIFERASE REPORTER SYSTEM

CHAPTER 3

DEVELOPING A CYCLIC NUCLEOTIDE SENSITIVE LUCIFERASE REPORTER SYSTEM

3.1 INTRODUCTION

Cyclic adenosine monophosphate (cAMP) and cGMP are major signalling molecules generated from adenosine triphosphate (ATP) or GTP by the action of adenylate or guanylate cyclases, respectively. cAMP is an established signalling molecule and second messenger ranging from Dictyostelium to Homo sapiens, however, its presence in higher plants was under debate (Assmann, 1995; Gehring, 2010). cAMP was shown to have a fundamental role in cellular response to many hormones and neurotransmitters regulation, it affects many different physiological and biochemical processes including the activity of kinases and phosphodiesterases (Fimia and Sassone-Corsi, 2001; Gehring, 2010). Guanylate cyclases and cGMP are well represented in various invertebrates such as insects, nematodes, echindermata and the amoeba Dictyostelium which use cGMP as well as cAMP as a chemoattractant (Biswas et al., 2009; Hanna et al., 1984; Schaap, 2005). The role of cGMP in bacteria, fungi and plants is controversial in part because levels of this cyclic nucleotide were considerably lower than cAMP (Gomelsky, 2011; Lemtiri-Chlieh et al., 2011; Linder, 2010; Newton and Smith, 2004; Schaap, 2005). However cGMP is now a relatively well characterised second messenger in higher plants regulating a wide variety of physiological effects ranging from plant hormone dependent responses to induction of plant defence responses (Lemtiri-Chlieh et al., 2011; Newton and Smith, 2004) and currently novel plant guanylate cyclases have been partly characterised (Kwezi et al., 2011; Meier et al., 2010; Muleya et al., 2014; Qi et al., 2010; Szmidt-Jaworska et al.,

2009). Studies on bacteria had shown that a guanylate cyclase and cGMP system is involved in bacterial encystment in *Rhodospirillum centenum* and by homology in other members of the α-proteabacteria such as *Rhizobium NGR234* (Marden et al., 2011). A guanylate cyclase found in cyanobacteria has also been crystallised (Rauch et al., 2008). Therefore cGMP appears to be a universal signalling molecule in eukaryotic cells and to have roles in at least some prokaryotes.

Part of the controversy relating to cGMP being a second messenger in non-animal cells is due to its transitory nature and generally lower levels compared to cAMP. The most reliable method to detect cGMP is by mass spectrometry (Lemtiri-Chlieh et al., 2011; Newton and Smith, 2004), which is limited in its utility for time course measurements essential for detecting molecules transiently present in limited numbers of cells. Various antibody-based assays have been developed but these were tailored for animal cells and the early assays detected false components in non-animal cells (Newton and Smith, 2004). Newer ELISA based kits are more specific for cGMP but tend to under report amounts of cGMP present in non-animal cells (Meier et al., 2010). To measure endogenous cGMP levels at a cellular level in real time in mammalian cells a fluorescent biosensor FlincG was developed. FlincG contains the regulatory domain of protein kinase G type I fused to the circular permuted enhanced green fluorescent protein and is used in transfected mammalian cells to detect intracellular changes in cGMP over native dynamic ranges (Nausch et al., 2009). Constructs of FlincG placed under the control of a plant promoter have been expressed in plant cells and detect endogenous changes in cGMP levels (Isner and Maathius, 2011; Isner et al., 2012). Alternative protein cGMP biosensors have been constructed using cGMP binding domains in phosphodiesterases (e.g. PDE5) and the blue fluorescent protein (mTagBFP) that can be used in multiple parameter imaging with FRET-based cAMP reporters (Niino et al., 2010). A luciferase reporter system making use of cross-talk between cAMP and cGMP pathways using the cAMP response element and

overexpressed protein kinase G has been developed that detects both cyclic nucleotides (Okano et al., 2011). However, a routine screening reporter assay detecting endogenous cGMP or cAMP levels in different systems is still lacking.

Using plant root cells several genes were identified that were up-regulated following exposure to membrane permeable cGMP (Maathius, 2006). Using this knowledge three genes were selected by Janet I Wheeler and Helen R Irving as being suitable candidates to design a suitable reporter construct to measure changes in cGMP in plant cells (Wheeler et al., 2013). Interestingly one of these genes, AtOPTX has recently been annotated as a member of the plant oligopeptide transporter family (although it was originally annotated as AtNTL1 (low affinity nitrate transporter)) and is predicted to be a membrane bound transporter of small peptides, contained a cGMP response element within its promoter. This cGMP response element was earlier identified in mammalian cells as a cGMP-sensitive element (Hum et al., 2004; Wheeler et al., 2013); therefore this gene was chosen as a suitable candidate to design a cGMP sensitive promoter and to investigate if this promoter system reported changes in cGMP levels in mammalian cells.

This PhD project involves repeated assays in the detection of cGMP produced by members of a novel class of GC kinases, therefore; a reliable cGMP screening tool would be ideal, to test cGMP production in different cell types and possibly from different systems. Therefore the effectiveness of these promoters was tested in bacterial and mammalian cells. Simultaneously the system was also tested in plant protoplasts by Dr Janet I Wheeler. Co-transformation of these constructs with a guanylate cyclase into the cell of choice allows for altered gene transcription and luciferase activity. Luciferase is produced if there is an increase in intracellular cGMP levels due to guanylate cyclase activity (Figure 3.1).

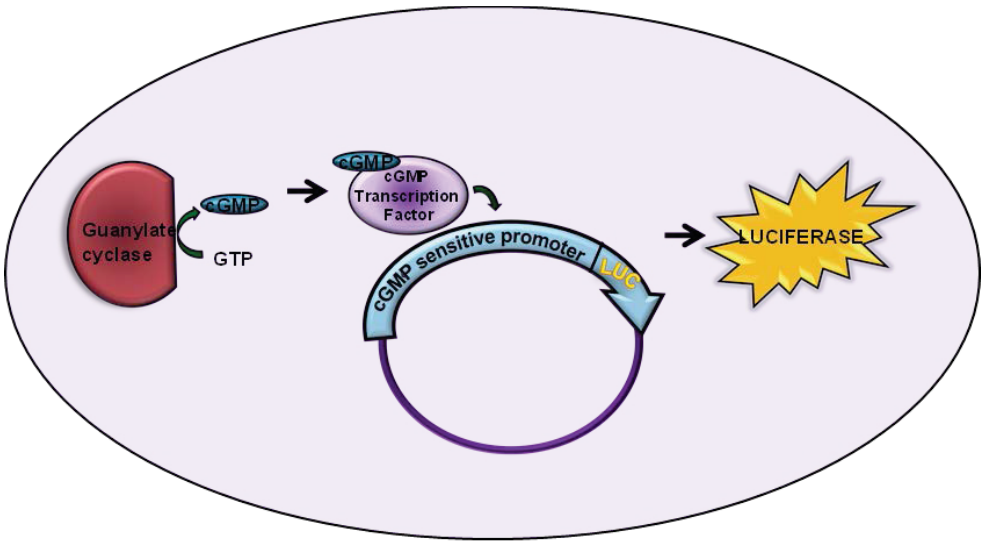

Figure 3.1 Concept diagram: Induction of the cGMP sensitive promoter with cGMP produced by a guanylate cyclase.

Induction of the cGMP sensitive promoter induces the gene transcription of luciferase which can be measured by luminescence.

3.2 MATERIALS AND METHODS

3.2.1 Plasmid construction

3.2.1.1 OPTX reporter constructs

The constructs were designed and prepared by Dr Janet I Wheeler and are summarised here. The 1000 bp promoter sequence for the OLIGOPEPTIDE TRANSPORTER X (OPTX; **TAIR: AT1G33440** was recombined into pLUCTrap3 (**GenBank: DQ073044.1**) (Calderon-Villalobos et al., 2006) resulting in pOPTXLUC. Three copies of the cGMP response element (Hum et al., 2004) and five copies of the GARE (Bastian et al., 2010) were incorporated into the AtOPTX promoter to make pOPTXcGMPRELUC and pOPTXGARELUC (Wheeler et al., 2013).

3.2.2 Transfection of HEK 293T cells and treatment

For quantification purposes, cells were co-transfected with pcDNA6.2/EmGFP-DEST (Invitrogen) as well as the specific constructs at a 1:5 (GFP:LUC) ratio respectively using Lipofectamine LTX (Invitrogen) following the manufacturer's instructions. Transfected cells were incubated in OPTI-MEM and the media was changed to DMEM with 10% FBS the following day. The cells were incubated at 37°C for 2-3 hours before they were treated with various concentrations of 8-bromo-cGMP, dibutyryl cAMP, DEA/NONOate or forskolin (all from Sigma). Treated cells were incubated for a further 18 hours at 37°C and then the media was removed before 400 µl of 1X Reporter Lysis Buffer (RLB, Promega) at room temperature was added to cover the cells. The cells detached after 5-10 minutes. The lysate from each well was placed into individual 1.5 ml tubes, each tube was vortexed for 10 seconds and then centrifuged for 30 seconds at 12,000 x *g*. Lysates were frozen on dry ice and kept at -80ºC till analysis.

The Promega Luciferase assay system (Promega, Australia) is used to analyse the cells. Lysates are brought to room temperature in a water bath, 20 µl of lysate is loaded

in triplicates into a 96 well white Nunc plate (Thermo Scientific). 100 µl of Luciferase assay reagent was added to each well just before analysis. The LUMIstar Omega multidetection microplate reader is used to measure the luciferase activity. Using the GFP 96 well plate program (A_{488}, FITC mirror 492 excitation, 520 emission) on the Envision 2101 plate reader (PerkinElmer, Melbourne, Australia). GFP fluorescence is measured by loading 120 µl of each lysate into a black 96 well plate. The average luciferase luminescence reading was divided by the GFP reading to account for the transfection efficiency.

3.2.3 Bacterial transformation and treatments

One shot BL21-AI cells (Invitrogen) were used to transform either pLUCTRAP3, OPTX, OPTXcGMPRE or OPTXGARE. At least four isolated colonies were chosen from each transformation and used to inoculate 10 ml LB broth with kanamycin (50 µg/ml) and grown with shaking at 225 rpm overnight at 37ºC. Overnight cultures were diluted 1 in 10 ml LB broth and were incubated in a shaking incubator 225 rpm at 37°C until an OD_{600} of about 0.5. Then 1 ml aliquots of each of the cultures were taken and treated with various concentrations of 8-bromo-cGMP (8-bromoguanosine-3′,5′-cyclic monophosphate from Sigma Aldrich, Australia), or cAMP (N^6,2′-O-Dibutyryladenosine 3′,5′-cyclic monophosphate from Sigma Aldrich, Australia) for 3 hours with shaking in 1.5 ml tubes. The OD_{600} of each culture was measured to quantify the cell number using a spectrophotometer (WPA Lightwave personal UV/VIS from Spectum®).

For the proof of concept experiments, BL21-AI cells were co-transformed with either pOPTXcGMPRELUC or pOPTXGARELUC (kanamycin resistance) and the cytoplasmic domain of the phytosulfokine receptor 1 (PSKR1; **TAIR: AT2G02220**) in pDEST17 (pDEST17PSKR1cd; ampicillin/carbenicillin resistance) (Kwezi et al., 2011). Colonies were selected with kanamycin (100 µg/ml) and carbenicillin (200 µg/ml) and separately inoculated into SOC media and grown to OD_{600} of 0.4 - 0.5 when the BL21-

AI cells were induced with 0.2% L-arabinose and 1 mM IPTG to express the PSKR1 protein over the next 3 to 5 hours.

3.2.4 Bacterial treatment and Luciferase assay

Bacterial cells are lysed after the specific treatment, 90 µl of each bacterial sample was taken, 10 µL of buffer (1 M K_2HPO_4 at pH 7.8 and 20 mM EDTA) was added and the cultures were frozen on dry ice and then brought to room temperature in a water bath (alternatively samples were stored at -80ºC). The Promega Luciferase assay system (Promega, Australia) is used to analyse the cells. Lysis mix (1X Cell Culture Lysis Reagent and 1.25 mg/ml lysozyme) (300 µl) is added to each culture as recommended in the Promega Luciferase assay (Promega, Australia) and incubated for 10 min. Lysate (20 µl) is loaded in triplicate into a 96 well white plate. Luciferase assay reagent (100 µl) is added to each well just before analysis. The LUMIstar Omega multidetection microplate reader is used to measure the luciferase activity. The average luciferase reading was divided by the individual OD_{600} after the 3 hours induction.

3.2.5 Statistical analyses

Data was analysed using one way analysis of variance (ANOVA) followed by either Dunnett's multiple comparison test ($P < 0.05$) or Tukey-Kramer multiple comparison test ($P < 0.05$) using GraphPad Prism 5.0 (GraphPad Software). Data for each treatment contains at least 3 biological replicates ($n \geq 3$) and each experiment was repeated at least twice.

3.3 RESULTS AND DISCUSSION

3.3.1 Generation of cyclic nucleotide responsive promoter:Luciferase plasmid constructs

The promoter fragment of approximately 1000 bp of OPTX was amplified and cloned into the plant luciferase reporter vector pLucTrap3 (Calderon-Villalobos et al., 2006) to create pOPTX:LUC (Figure 3.2 A, C) by Dr Janet I Wheeler.

3.3.2 Augmentation of the cyclic nucleotide sensitive promoter OPTX

DNA sequence analysis had shown that the OPTX promoter contained the mammalian cGMP response element (AxAxxxxxTTCxAxAxT) (Figure 3.2 B) identified by (Hum et al., 2004). To potentially enhance cGMP sensitivity of the OPTX promoter, Dr Janet I Wheeler used mutagenesis to incorporate an additional three mammalian cGMP response elements to make OPTXcGMPRE:LUC (Figure 3.2 C). A recent promoter analysis study identified a putative gibberellic acid response element TAACAAA/G (Figure 3.2 B) which is found at a higher frequency in promoters of genes responsive to gibberellic acid (Bastian et al., 2010). Since gibberellic acid induces transient increases in cGMP in plants (Penson et al., 1996), Dr Janet I Wheeler used mutagenesis to incorporate five additional GAREs into the OPTX promoter to make OPTXGARE:LUC (Figure 3.2 C).

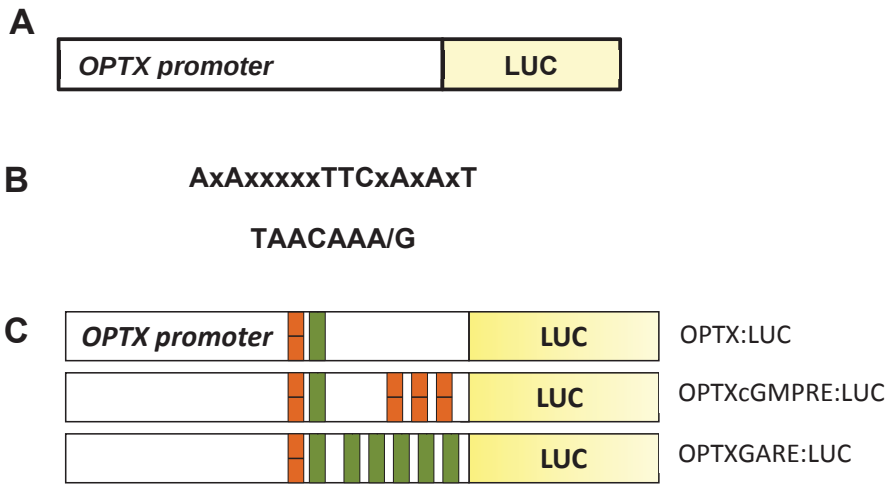

Figure 3.2 Schematic diagrams of plasmids used and the response elements incorporated.

(A) cGMP responsive promoter - Luciferase plasmid used for transfection. (B) Mammalian cGMP response element (cGMPRE) DNA sequence described in (Hum et al., 2004) top and gibberellic acid response element (GARE) DNA sequence described in (Bastian et al., 2010) bottom. (C) Schematic diagram of plasmids used for transfection. OPTX promoter showing the mammalian cGMPRE present in all three constructs (orange), cGMPRE inserted (orange) and GARE inserted (green).

3.3.3 Testing the OPTX promoters for cGMP sensitivity in mammalian cells

The mammalian cGMP response element was first identified in the promoter of the natriuretic peptide receptor 1 (NPR1 or GCA) where it induced downregulation of the receptor transcript when cGMP levels were raised (Hum et al., 2004; Martel et al., 2010). We hypothesised that this element would be responsive in mammalian cells. Therefore we tested the sensitivity of the OPTX and augmented promoters using transiently transfected HEK 293T cells. The OPTX:LUC, OPTXcGMPRE:LUC and OPTXGARE:LUC were transfected separately into HEK 293T cells which were co-transfected with pcDNA 6.2/EmGFP-DEST. Luciferase activity and GFP fluorescence

were measured after 18 hours of treatment and the samples were normalised by the corresponding transfection efficiency with GFP. Luciferase activity was expressed as a percentage of the cGMP untreated control which was set at 100%.

Nitric oxide has been shown to increase cytosolic cGMP levels (Arnold et al., 1977; Nausch et al., 2009). To test whether the promoter luciferase construct OPTX:LUC could be used to show physiological differences in cGMP levels we used the nitric oxide donor DEA/NONOate which is shown to induce cytosolic cGMP (Nausch et al., 2009). The OPTX:LUC showed no response to treatments with various concentrations of 8-bromo-cGMP but a significant decrease in luciferase activity occurred when treated with 0.1 μM DEA/NONOate (Figure 3.3 A). Treatments with dibutyryl cAMP also showed no significant differences in luciferase activity. Only small changes were detected in HEK 293T cells transfected with the OPTXcGMPRE:LUC promoter where there was a significant increase in luciferase activity with the NO donor and a decrease in activity following treatment with forskolin which activates adenylate cyclase to increase endogenous cAMP (Figure 3.3 B). We speculate that this may be due to the positioning of the augmented response elements close to the transcription start site (Martel et al., 2010). This may negatively/incorrectly modulate the transcriptional machinery, as the cGMP response element is over 1000 bp upstream of NPR1/GCA (Hum et al., 2004).

The OPTXGARE:LUC transfections resulted in a significant increase in luciferase activity when compared with the untreated control at 0.1 μM cGMP but not at 1 μM cGMP (Figure 3.3 C). However, there was no significant change in response to the NO donor possibly because this stimulated the generation of too much endogenous cGMP. Interestingly, this augmented promoter differentiated between cAMP and cGMP in mammalian cells and this appeared to be concentration dependent. Forskolin which strongly activates adenylate cyclase to continuously produce cAMP significantly reduced luciferase activity confirming the trend we observed with dibutyryl cAMP

treatments (Figure 3.3 C). This is an interesting observation as it suggests that the OPTXGARE:LUC could be used to report transient increases in cGMP independently of cAMP in mammalian cells. Significant cross-talk occurs between the cAMP and cGMP transcription regulatory pathways in mammalian cells (Lucas et al., 2000), which has led to the development of a mammalian cGMP reporter system that does not discriminate between cAMP and cGMP (Okano et al., 2011).

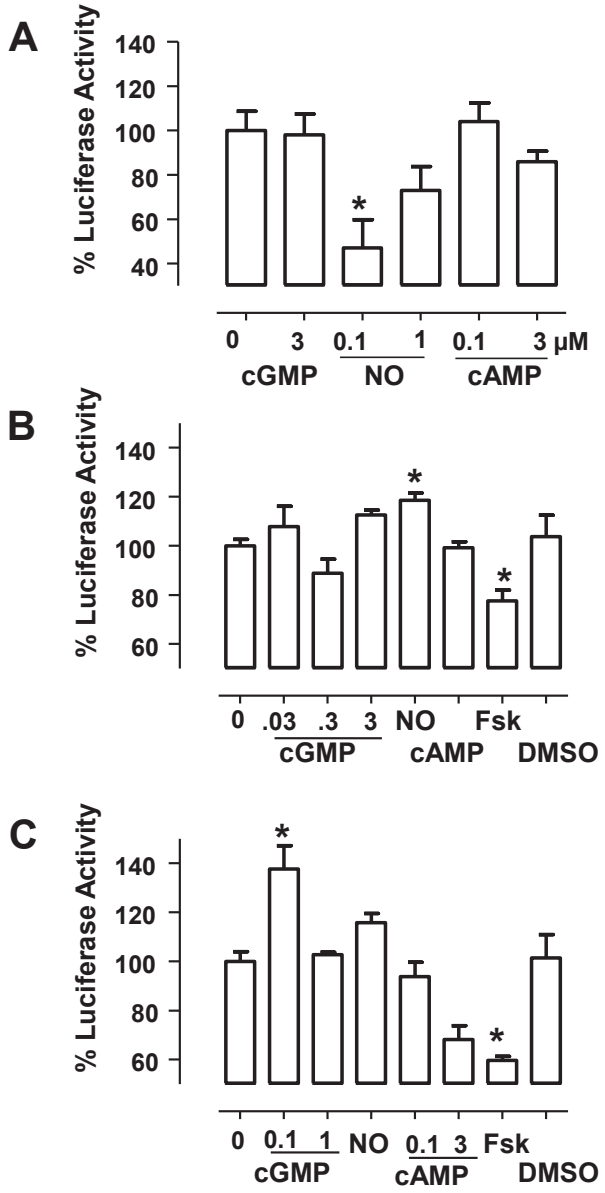

Figure 3.3 Cyclic nucleotide-induced luciferase activity in HEK 293T cells transiently transfected with the promoter constructs.

The results are from separate transfections tested for each promoter/treatment combination. (A) Effect of 8-bromo-cGMP (3 µM), DEA/NONOate (NO, 0.1 and 1 µM), dibutyryl cAMP (0.1 and 3 µM) on cells transfected with OPTX:LUC (n = 3 - 5); (B) Effect of 8-bromo-cGMP (0.03, 0.3 and 3 µM), DEA/NONOate (1 µM), dibutyryl cAMP (3 µM) and forskolin (Fsk, 0.1 µM) and the DMSO vehicle on cells transfected with OPTXcGMPRE:LUC (n = 4 - 13); (C) Effect of 8-bromo-cGMP (0.1 and 1 µM), DEA/NONOate (1 µM), dibutyryl cAMP (0.1 and 3 µM) and forskolin (0.1 µM) and the DMSO vehicle on cells transfected with OPTXGARE:LUC (n = 4 - 15). Asterisks indicate treatments significantly different from the control ($P < 0.05$; one way ANOVA, Dunnett's multiple comparison post test).

3.3.4 Testing the OPTX promoters for cGMP sensitivity in bacterial cells

To date, only members of the α-proteabacteria are known to naturally synthesise cGMP although other bacteria are well known to express cAMP and the di-cyclic nucleotides c-di-AMP and c-di-GMP (Gomelsky, 2011; Marden et al., 2011). Therefore a system that detects cGMP in bacteria would be particularly useful to screen for novel recombinant guanylate cyclases from other organisms. Our goal is to develop a screening assay that we can use to detect novel guanylate cyclases expressed in bacteria. With this aim in mind, the three OPTX constructs were tested in the BL21-AI *E. coli* strain which we selected as a representative bacterium because it is suitable for high-level recombinant protein expression. The OPTX:LUC, OPTXcGMPRE:LUC and OPTXGARE:LUC were transformed separately into the BL21-AI *E. coli*. At least 4 independently transformed colonies were grown and tested for each promoter/ treatment combination. In these experiments, 1 ml cultures were induced in a 1.5 ml tube, as only a small amount of protein is needed to be produced, this may also be a good option in case we want to grow and induce the cultures on multi well plates. Each sample was normalised using the OD_{600} reflecting cell number for each sample, the luciferase activity is expressed as a percentage of the untreated control which was set at 100%. The promoter OPTX:LUC showed some difference in luciferase activity from the untreated control only at the 1 μM cGMP treatment, hence this construct was not used to test for cGMP in bacteria due to its concentration specificity (Figure 3.4).

The OPTXcGMPRE:LUC transformants showed a significant increase in luciferase activity when treated with 0.3 μM, 1 μM and 3 μM 8-bromo-cGMP but not 0.01 μM and 0.1 μM 8-bromo cGMP (Figure 3.5 A). However, this increase in luciferase activity appears to be independent of the purine base as similar changes were seen with treatments containing dibutyryl cAMP (Figure 3.5 B).

The OPTXGARE:LUC showed a significant increase in luciferase activity when compared to the untreated control when 8-bromo-cGMP was between 0.1 µM and 0.3 µM, but not at 0.01 µM or 1 µM (Figure 3.5 C). Again similar increases were observed in response to dibutyryl cAMP in BL21-AI cells transformed with OPTXGARE:LUC (Figure 3.5 D). As *E. coli* has no known guanylate cyclases and cGMP signalling system but highly characterised cAMP signal networks (Gomelsky, 2011), it is possible that the native bacterial transcription factors recognise both purine nucleotides and does not discriminate between them.

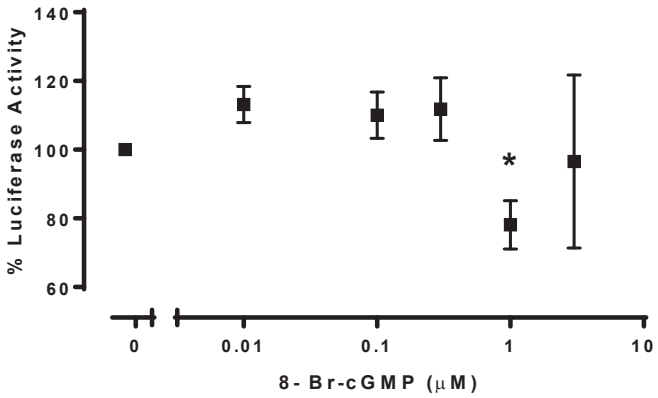

Figure 3.4 Cyclic nucleotide-induced luciferase activity in E. coli BL21-AI cells transformed with the OPTX-LUC reporter.

BL21-AI transformed with the OPTX-LUC promoter luciferase reporter construct and treated with different concentrations of 8-bromo-cGMP. At least 3 separate colonies were tested (n = 3 - 4). Asterisks indicate treatments significantly different from control time points (P < 0.05; one way ANOVA, Tukey-Kramer post test).

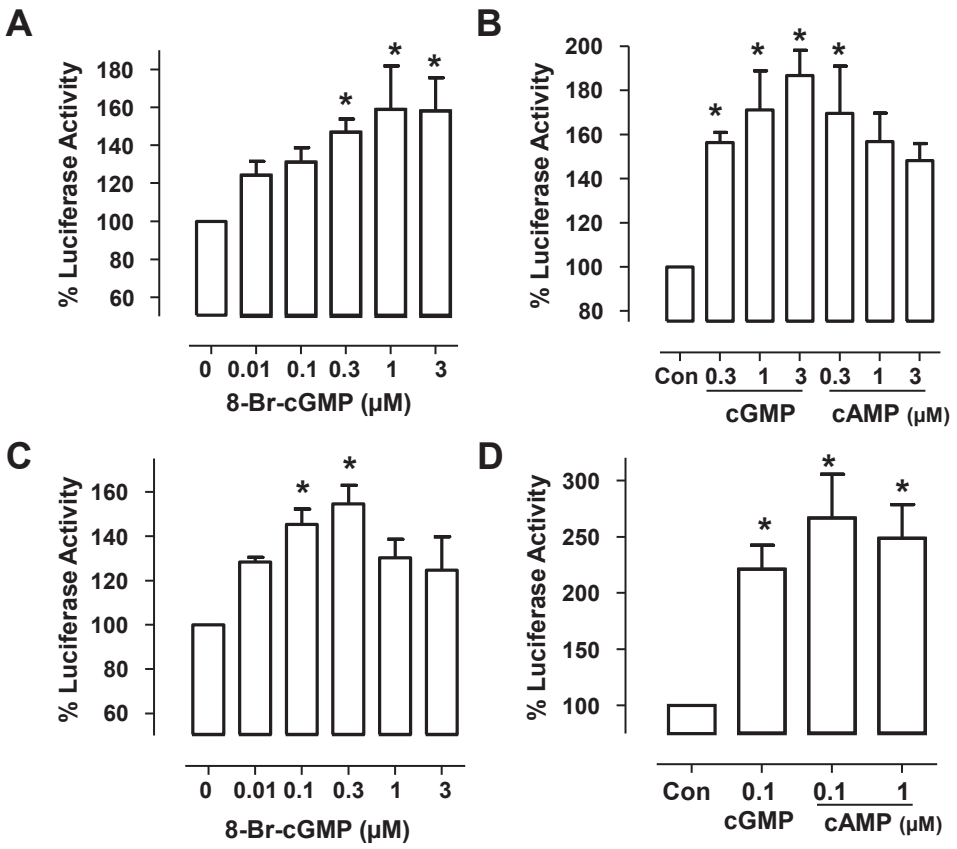

Figure 3.5 Cyclic nucleotide-induced luciferase activity in E. coli BL21-AI cells transformed with the OPTXcGMPRE:LUC and the OPTXGARE:LUC reporter.

At least 3 separate colonies were tested for each promoter/treatment combination. (A) Effect of different concentrations of 8-bromo-cGMP on BL21-AI cells transformed with OPTXcGMPRE:LUC (n = 3 - 4); (B) Effect of dibutyryl cAMP on BL21-AI cells transformed with OPTXcGMPRE:LUC (n = 3 - 4); (C) Effect of different concentrations of 8-bromo-cGMP on BL21-AI cells transformed with OPTX-GARE:LUC (n = 4). (D) Effect of dibutyryl cAMP on BL21-AI cells transformed with OPTXGARE:LUC (n = 6). Asterisks indicate treatments significantly different from the control (P < 0.05; one way ANOVA, Dunnett's multiple comparison post test).

3.3.5 Using OPTXcGMPRE:LUC to report cyclic nucleotide production in bacterial cells

We tested the constructs to see if we could detect cGMP in BL21-AI cells expressing a novel guanylate cyclase. Previous work has shown that BL21-AI cells expressing the novel plant cytoplasmic guanylate cyclase GC1 indicates that cGMP is produced by bacteria during induction of protein expression (Ludidi and Gehring, 2003; Szmidt-Jaworska et al., 2009). Our group has demonstrated that the cytoplasmic domain of the plant phytosulfokine receptor (PSKR1) contains guanylate cyclase but not adenylate cyclase activity (Kwezi et al., 2011). The PSKR1 cytoplasmic domain (PSKR1cd) protein is relatively stable, it shows relatively high expression in BL21 cells (Figure 5.1) in the soluble fraction (Muleya et al., 2014). Therefore PSKR1cd was chosen as the test protein. PSKR1cd was co-transformed with either OPTXcGMPRE:LUC or OPTXGARE:LUC into BL21-AI. To test if PSKR1cd generates cGMP, luciferase activity was measured 3 and 5 hours following induction of PSKR1 expression. Luciferase activity increased for both constructs relative to the control uninduced treatments, a significant effect was also seen 3 and 5 hours post induction (Figure 3.6 A and B). Therefore, these bacterial reporter assays could be used as a preliminary screen for novel guanylate cyclase enzymes.

To further test the bacterial cGMP detection system, mammalian proteins were also tested. The mammalian protein NTRK1 (neurotrophic receptor tyrosine kinase 1) is predicted to contain a novel guanylate cyclase centre (H.R.Irving, personal communication 2012), therefore, the cytoplasmic domain of NTRK1 was tested using the OPTXcGMPRE system (Figure 3.6 C). A significant increase of about 20% in luciferase activity is seen 3 hours post induction of NTRK1 expression when compared to the uninduced cells. This is currently the only data available to show that the predicted novel GC NTRK1, may produce cGMP *in vitro*., however, further investigation is necessary on this protein.

The IRAK3 protein which is the focus of this thesis is believed to be a novel GC and has been shown to produce cGMP *in vitro* (Freihat et al, 2014). IRAK3 was examined using the OPTXcGMPRE system, however the system did not pick up a clear significant difference in the presence of IRAK3 post 3 hour induction when compared to the uninduced control (Figure 3.6 D), this discrepancy with alternative cGMP assays may be due to IRAK3s instability. The instability index is computed to be 59.95 which classifies the protein as unstable on EXPASY Bioinformatics resource portal, (http://web.expasy.org/cgi-bin/protparam/prot_param1?Q9Y616@1-596@). IRAK3 is also difficult to express in bacteria, as it is expressed mainly as an insoluble protein, see chapter 5 for IRAK3 expression in bacterial cells. Therefore this system is best used for proteins that can be expressed in bacterial cells.

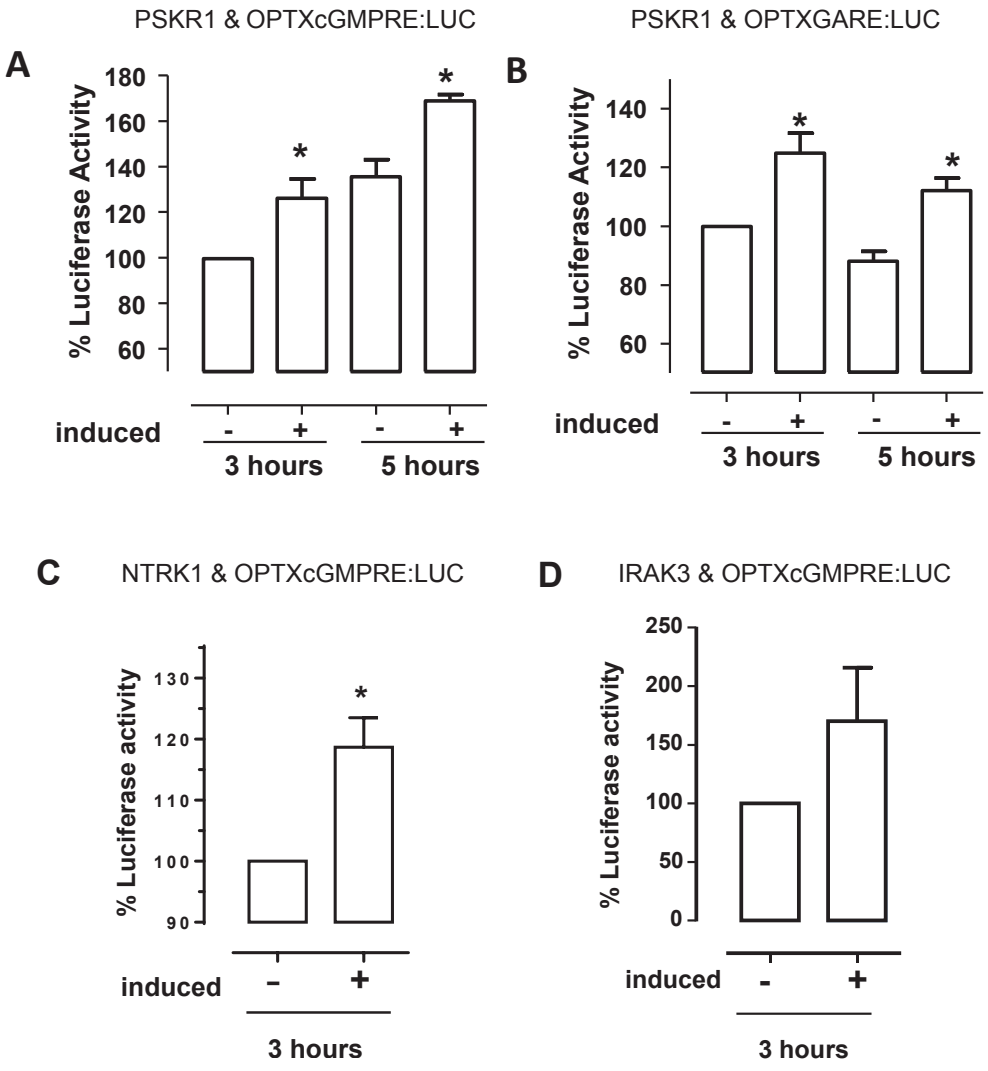

Figure 3.6 Detection of cGMP-induced by the novel GCs in bacteria.

BL21-AI cells were co-transformed with a promoter luciferase reporter construct and a plasmid containing a novel guanylate cyclase enzyme (pDESTPSKR1cd). Expression of PSKR1 was induced in at least 4 separate colonies and then luciferase activity was tested and expressed relative to culture optical density. (A) Effect of PSKR1 expression on OPTXcGMPRE:LUC activity (n = 4 – 5); (B) Effect of PSKR1 expression on OPTXGARE:LUC activity (n = 4). Asterisks indicate treatments significantly different from control time points (P < 0.05; one way ANOVA, Tukey-Kramer post test). (C) Effect of NTRK1 expression on OPTXcGMPRE:LUC activity (n=4) (P < 0.05; unpaired student t-test). (D) Effect of IRAK3 expression on OPTXcGMPRE:LUC activity (n=5) (P > 0.05; unpaired student t-test).

3.4 CONCLUSION

The developed promoter reporter systems based on the plant OPTX promoter can be successfully employed in bacterial cells to test for cyclic nucleotide production. The OPTX system may also be an alternative technique we can use in mammalian cells to report endogenous cyclic nucleotide levels, however further optimisation may be necessary for use in different cell lines. Since the OPTX promoter is a plant gene, augmentation of the promoter with the different cGMP response elements resulted in changes of efficacy in the different cell types. Surprisingly, augmentation with the predicted response element to the plant hormone GA (OPTXGARE:LUC) effectively reported changes in cyclic nucleotides in both systems tested. In mammalian cells, the OPTX:LUC reporter detected endogenous cGMP. The OPTXGARE:LUC reporter, however, differentiated between the low cGMP and high cAMP levels in the mammalian cells. In bacteria (BL21-AI), both the OPTXGARE:LUC reporter and the separate OPTXcGMPRE:LUC reporter responded to increased levels of cyclic nucleotides.

The respective constructs were employed to detect novel recombinant guanylate cyclase activity in the bacterial system. The OPTXGARE:LUC reporter used to detect cGMP production of the novel GC PSKR1 showed significant luciferase activity, representing an increase in cGMP production in the presence of PSKR1. This was also the case for PSKR1 when the alternative OPTXcGMPRE:LUC reporter was used.
NTRK1 was shown to significantly induce luciferase activity in the presence of the OPTXcGMPRE:LUC construct, this was also the first report that NTRK1 may produce cGMP *in vitro*. IRAK3 was also investigated for cGMP production using the OPTXcGMPRE:LUC construct, however, a clear significant increase in luciferase activity was not observed, possibly due to the instability of the IRAK3 protein in bacteria.

CHAPTER 4

EXPLORING THE STRUCTURE OF IRAK3

CHAPTER 4

EXPLORING THE STRUCTURE OF IRAK3

4.1 INTRODUCTION

The IRAK family consisting of IRAK1,2,3 and 4 share a common and important death domain which is used in the interaction of the signalling proteins (Du et al., 2014; Rhyasen and Starczynowski, 2015). Once TLR/IL-1R are activated there are a sequence of molecular recruitments that occur, which involve the assembly of signalling molecules and complexes. This includes MyD88 a necessary adaptor protein in the TLR/IL-1R signalling cascade, subsequently recruiting the IRAK proteins. The death domain plays a key part in complex formation, the structure is termed a myddosome complex and is crystallised (Lin et al., 2010). The MyD88-IRAK4-IRAK2 death domain myddosome complex shows a left-handed helical oligomer consisting of six MyD88, four IRAK4 and four IRAK2 molecules interacting via the death domain. Formations of these myddosomes allow the kinase domain of the IRAK proteins to be in close proximity for both trans and autophosphorylation and activation (Lin et al., 2010). IRAK3 negatively regulates this pathway; it also binds via its death domain to the other members of the IRAK family, in other words, IRAK3 forms heterodimers with IRAK1 and IRAK2 to disable downstream TRAF6 and NFκB activation and consequent inflammatory response (Lin et al., 2010). A single amino acid mutation of E71A or Q78G in the IRAK3 death domain can result in partial defects to binding, however, if both mutations occur there is a significant decrease in the binding of IRAK3 to IRAK4 (Zhou et al., 2013). Mutation of W74A in the IRAK3 death domain caused a complete loss in interaction with IRAK4, affecting the function of IRAK3 as a negative regulator of inflammation (Zhou et al., 2013).

The kinase activities of the IRAK family members are important in the signalling and the activation of other signalling molecules in the signalling cascade. For example, IRAK4 is autophosphorylated once it is activated, IRAK4 phosphorylates downstream kinases like IRAK1 and IRAK2 (Cushing et al., 2014; Li et al., 2002). IRAK4 kinase inactive clones K213A/K214A in the kinase VAVKK domain, expressed in IRAK4 deficient cell lines revealed that the mutation caused a significant reduction in the interleukin-1 receptor-induced signals. This includes a reduction in the activation of IRAK1, nuclear factor kappa-light-chain-enhancer of activated B cells (NF-κB), and c-Jun NH2-terminal kinase (JNK) (Lye et al., 2004).

IRAK3 is a pseudokinase in humans, IRAK3 is defined as a class I pseudokinase as it does not display nucleotide or cation binding. It is thought that this is mainly due to the absence of the conserved aspartic acid (D) in the HRD motif sequence of the kinase domain, which is replaced by a (Ser293) in IRAK3 (Murphy et al., 2014; Wesche et al., 1999). IRAK3 was however shown to bind ATP-competitive small-molecule inhibitors, indicating perhaps the presence of an intact ATP binding cleft. Therefore, it is possible that IRAK3 can bind nucleotides and cations, but the binding affinities may be below the limit of detection used (Murphy et al., 2014).

The IRAKs also contain a C-terminal domain except for IRAK4, the IRAK3 C-terminal domain was shown to be necessary for interaction with TRAF6 (TNF receptor-associated factor) a signalling molecule in the signalling cascade. IRAK3 was unearthed as a potential novel guanylate cyclase using a GC search motif in computational searches. The GC motif used is an amino acid sequence homologous to GC catalytic centres found in lower eukaryotes (Figure 4.1 A, B) (Kwezi et al. 2011). Such novel GC centres had previously been found in the cytoplasmic kinase domain of receptor like proteins in plants, including Arabidopsis BRASSINOSTEROID INSENSITIVE 1 (BRI1) receptor kinase, phytosulfokine receptor 1 (PSKR1) and wall associated kinase like 10 (WAKL10) (Irving et al., 2012; Kwezi et al., 2007; Kwezi et

al., 2011; Meier et al., 2010). IRAK3, however, is a soluble cytoplasmic protein that contains a GC centre believed to catalyse the formation of cGMP.

A crystal structure of IRAK3 is not yet available; therefore, to explain the GC centre of IRAK3, a model is required. Constructing a homology model of IRAK3 can assist us in explaining how the GC centre may fit in and guide mutagenesis studies. Therefore, the aim of this chapter was to construct a homology model of the IRAK3 kinase domain, based on the crystal structure of the IRAK4 kinase domain (Wang et al., 2006).

4.2 MATERIAL AND METHODS

4.2.1 Construction of the IRAK3 homology model

4.2.1.1 Sequence alignments

The protein sequences of the human IRAK3 (http://www.uniprot.org/uniprot/Q9Y616) and the human IRAK4 (http://www.uniprot.org/uniprot/Q9NWZ3) were obtained from the UniProtKB database. The sequences were aligned using the Clustal W2 multiple sequence alignment website, the kinase domain of the IRAK3 sequence was aligned to the IRAK4 kinase domain sequence (Figure 4.2). The IRAK4 crystal structure of 2NRU (Wang et al., 2006) was used in the alignment and homology model design of IRAK3. Alignment of the IRAK3 amino acid sequence in different species was done using the Clustal W2 multiple sequence alignment website. The IRAK3 sequences used in the alignment were taken from the gene bank NCBI database. The IRAK3 database search for SNP variants was done using the ExAC Browser (Beta), Exome Aggregation Consortium (Lek et al., 2015).

4.2.1.2 Model building and minimisation

The homology model was generated using Prime version 3.1 (Maestro 9.3, Schrödinger, LLC, New York, USA) using the relevant aligned sequences. An energy minimisation of the IRAK3 homology model was done to relax the overall structure; first, the hydrogen atoms were relaxed where the energy decreased significantly. Second, a macro-model minimisation was done by constraining the protein backbone and allowing the side chains to relax. Another macro-model minimisation was done by constraining the α-carbons and thus allowing the relaxation of the rest of the structure. A final minimisation/relaxation was done were the α-carbons of the KHLW (residues 336-339) loop were allowed to move/relax while the rest of the α-carbons of the structure were kept rigid.

4.2.2 Mutant constructs

The IRAK3 mutants were constructed by mutating the specific residues in the IRAK3 homology model and then observing the effect on the surrounding residues and the effect on the overall structure. Once the mutation was added to the sequence, a minimisation of all the hydrogens was done, followed by minimisation of the side chains of either the mutation or the surrounding molecules.

4.2.3 GTP docking

Molecular docking was performed using the glide module within the Maestro molecular modelling package (Maestro version 9.3, Schrödinger, LLC, New York, USA). GTP was docked using the XP algorithm into the homology model that was developed for IRAK3. To initially position GTP in the binding site, the location of GTP within the structure of a related protein, cAMP-dependent protein kinase (pdb code 1ATP) was used as a guide. Default parameters were used for each docking experiment. The same methods were applied for the R372>L mutant of IRAK3.

4.3 RESULTS AND DISCUSSION

4.3.1 Alignment of IRAK family members

The IRAK members have a similar domain architecture where they all contain a death domain, a kinase homology domain and all except IRAK4 contain a C-terminal domain. The domain architecture of IRAK3 is presented in (Figure 4.1 A) showing the different domains as well as a distinct GC centre within its kinase domain.

To check if the other members of the IRAK family also contained a GC centre, the IRAK members were aligned. The GC centre of IRAK3 is highlighted in green and the GC-like centres of the other IRAK members are highlighted in purple (Figure 4.1 C). Underlined in red text are residues that do not follow the GC search motif, these GC centre residues are believed to be required for GC function and were used to identify IRAK3 as well as other novel GCs (Figure 4.1 B and C). Due to the lack of these essential residues in the GC-like centre of IRAK1, 2 and 4, these members are possibly non-functional, as they do not encompass a complete GC centre; therefore, the GC centre is unique to IRAK3 amongst the IRAK family (Figure 4.1 C).

To determine if the GC centre was conserved amongst other species, an alignment was done comparing the amino acid sequence of IRAK3 close to the GC centre in different species. This included the amino acid sequence of a mouse, zebrafish, wolf, gibbon, orangutan, rat and cattle, (Figure 4.1 D). As can be seen, IRAK3 maintains its GC centre sequence in all the species presented, particularly within the mammalian species, the amino acid sequence is also quite conserved in the GC vicinity, which is part of the pseudokinase domain. Such marked conservation is suggestive that the GC centre may be important in the function of IRAK3. Regions conserved mainly due to low mutation rates are usually functionally important (Carlton et al., 2006; Hardison, 2003).

In our search of IRAK3 in different species, we also compared the IRAK3 domain architecture. Interestingly, of all the species, looked at, only cattle *(Bos Taurus*) lack the usual death domain seen in IRAK3 as well as the rest of the IRAK family members (NCBI http://www.ncbi.nlm.nih.gov/homologene/36215# 25/08/16). Since the death domain of the human IRAK3 is important in protein-protein interaction in the signalling cascade, it would be interesting to find out how IRAK3 functions in cattle. This can be done experimentally by expressing the bovine IRAK3 protein and observing its binding patterns and how this feature affects downstream signalling in the cell.

A

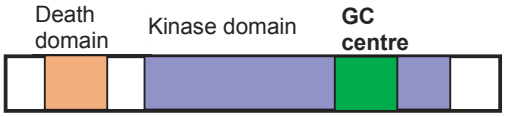

B

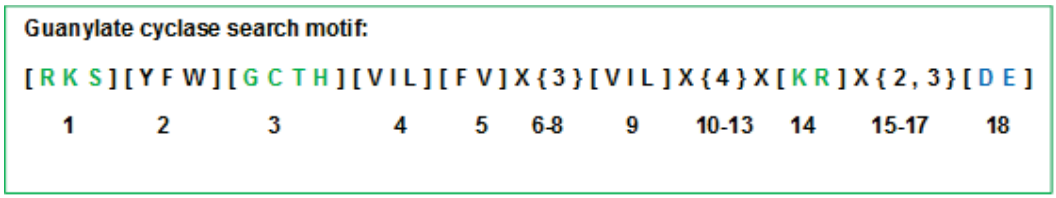

C

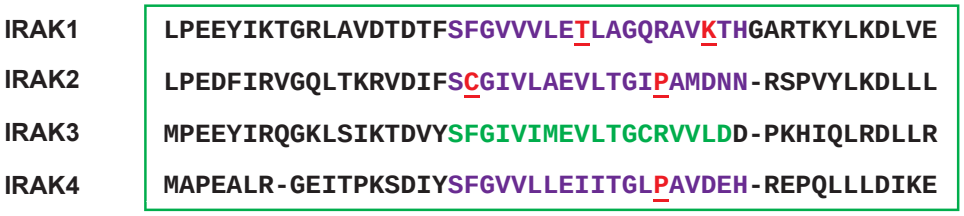

D

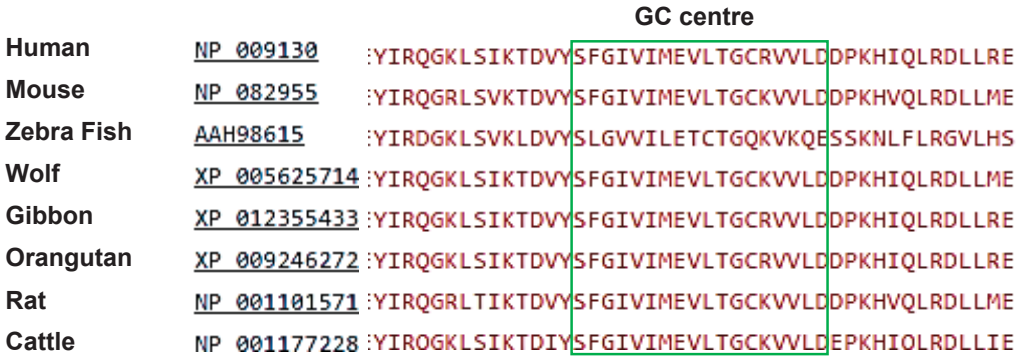

Figure 4.1 Sequence alignment of the IRAK family members, alignment of IRAK3 in different species and the GC search motif.

(A) Domain architecture of IRAK3 showing the death domain in orange, the kinase homology domain in purple and the GC centre in green. (B) The guanylate cyclase search motif highlighting the numbering of the residues in the GC centre (Kwezi et al., 2011) used to reveal IRAK3. Highlighted in green are the functionally assigned residues and in blue are the predicted Mg^{2+} or Mn^{2+} binding residues. (C) Alignment of the amino acid sequence of the different human IRAK family members in the GC vicinity. The IRAK3 GC centre is in green text and the GC-like centre of the other IRAK members are in purple text. The residues that are different to the GC search motif are in red text and underlined. (D) Alignment of the amino acid sequence of IRAK3 in different species around the GC vicinity, the GC centre is boxed in green.

4.3.2 Building of structure

The human IRAK4 kinase domain crystal structure has been crystallised by two different groups. Wang et al. (2006) used a synthetic potent kinase inhibitor (termed compound 1) to yield a structure at 2 Å, and staurosporine another kinase inhibitor to yield a structure at 2.2 Å, the two structures were claimed to be almost identical, with the exception of a few loops in the binding vicinity. The structures revealed a tyrosine gatekeeper residue which is a unique feature of the IRAK family (Wang et al., 2006). Another crystal structure by Kuglstatter et al. (2007) revealed that in the apo or unbound form, IRAK4 coexists as two conformations, differing in the two kinase lobes and the position of α-helix C, α-helix C is a conserved structural feature of all protein kinases (Taylor et al., 2012). However, in the presence of ATP, only one conformation was observed which is believed to be the active form of the enzyme (Kuglstatter et al., 2007). So far, crystal structures are not available for the kinase domain of the other IRAK proteins. The 2NRU crystal structure of IRAK4 was chosen as a suitable template, as, the crystal structure available was the most complete in terms of the kinase domain and had about 28.14% similarity to IRAK3 (Gosu et al., 2012; Wang et al., 2006). Other IRAK4 crystallised homologs were also considered however, they were disregarded due to either missing parts of the sequence structure or less similarity with IRAK3.

To build the IRAK3 homology model the knowledge-based method was originally selected. The alignments of the two sequences were used to build the predicted homology model. The main difference between the two models was that an α-helix originally present in the IRAK4 model in the GC-like domain region was replaced by a loop in the IRAK3 model, the loop was coloured red indicating that it is strained or that there is a potential error. The reason for this is possibly due to the extra four amino acid sequence (KHLW (residue 336-339)) found in IRAK3 but not in IRAK4, highlighted in pale red in Figure 4.2. To try to overcome these obstacles, we rebuilt the model

using the energy-based method instead of the knowledge-based method. A model of IRAK3 was constructed by removing all of the extra amino acid residues highlighted in pale red from the IRAK3 sequence, the structure was then minimised in energy by minimising/relaxing the atoms. These amino acid portions were then reinserted individually and then a homology model was built for each addition. Each of these IRAK3 homology structures had an α-helix in the GC area, similar to the IRAK4 structure. However once the KHLW (residues 336 – 339) amino acid portion was inserted into the model, the α-helix was automatically disrupted and transformed into a loop. This may be due to the extra amino acid portion pushing the α-helix out of place, making it a loop, or that the alignments of the specific amino acids are not correctly aligned. By performing a final minimisation of the energy, it allows the complete structure to relax causing the α-helix to reform. A final check of the structure was done to check for any strains in the structure (Fig 4.3).

It is noteworthy that in the homology model of IRAK3, the GC centre is in part an internal α-helix while the remainder emerges as a loop (Figure 4.3 A and C). In IRAK3 the loop section of the GC centre and the KHLW loop (residues 336 – 339) can easily adopt alternative structures (Figure 4.3 D). The KHLW (residues 336–339) loop is adjacent to the GC centre section (Figure 4.3 D). There is a possible cation π interaction between arginine 372 of the GC centre and the adjacent histidine 337 whereas tryptophan 339 (part of KHLW (residue 336-339)) sticks out into space and possibly has a role in protein–protein interactions as most nearby amino acids are polar. The loop region of IRAK3 from 383 to 398 includes part of the GC centre and this was refined via iterative molecular dynamics to generate ten possible loop configurations that were overlaid on the IRAK3 model confirming that a number of possible conformations exist that may alter the GC centre configuration (Figure 4.3 D). The IRAK3 homology model is quite similar to the IRAK4 crystal structure with very few noticeable differences in the presented ribbon model. The main differences in the

GC centre vicinity between the IRAK3 model and IRAK4 are highlighted in cyan and green and transposed onto the silver IRAK4 model (Figure 4.3 B). The fact that there is an extended loop in IRAK3 can make the loop even more dynamic. IRAK4 is an active kinase unlike IRAK3, which is a pseudokinase, and the activation segment pointed at by a blue arrow is an important part of its kinase activity regulation (Nolen et al., 2004) (Figure 4.3 B). Previous studies on crystal structures of different inactive kinase have suggested that their kinase inactivity may be due to the altered positioning of the lobes and the cleft opening in the activation segment. Elusive changes in the activation loop have also been shown to disrupt precise points which can be amplified into major structural changes that reduce their activity (Nolen et al., 2004).

```
h-IRAK3     LKSSISFQNIIEGTRNFHK------DFLIGEGEIFEVYRVEIQNLTYAVK 192
h-IRAK4     RFHSFSFYELKNVTNNFDERPISVGGNKMGEGGFGVVYKGYVNNTTVAVK 213 (213)
               *:** :: : *.**.:      .  :*** :  **:  ::* * ***

h-IRAK3     LFKQEKKMQCKKHWKRFLSELEVLLLFHHPNILELAAYFTETEKFCLIYP 242
h-IRAK4     KLAAMVDITTEELKQQFDQEIKVMAKCQHENLVELLGFSSDGDDLCLVYV 263 (263)
             :    .:  ::  ::* .*::*:   :* *::** .: :: :.:**:*

h-IRAK3    YMRNGTLFDRLQCVGDTAPLPWHIRIGILIGISKAIHYLHNVQPCSVICG 292
h-IRAK4    YMPNGSLLDRLSCLDGTPPLSWHMRCKIAQGAANGINFLHENH---HIHR 310  (310)
           ** **:*:***.*:..*.**.**:*  *  * ::.*::**: :    *

h-IRAK3     SISSANILLDDQFQPKLTDFAMAHFRSHLEHQSCTINMTSSSSKHLWYMP 342
h-IRAK4     DIKSANILLDEAFTAKISDFGLARASEKFAQTVMTSRIVGTTA----YMA 356 (356)
            .*.*******: * .*::**.:*:  .:: :   * .:..:::    **.

h-IRAK3     EEYIRQGKLSIKTDVYSFGIVIMEVLTGCRVVLDDPKHIQLRDLLRELME 392
h-IRAK4     PEALR-GEITPKSDIYSFGVVLLEIITGLPAVDEHREPQLLLDIKEEIED 405 (405)
             * :* *::: *:*:****:*::*::**  .* :. :   * *: .*: :

h-IRAK3     KRGLDSCLSFLDKKVPPCPRNFSAKLFCLAGRCAATRAKLRPSMDEVLNT 442
h-IRAK4     EE--KTIEDYIDKKMNDADSTSVEAMYSVASQCLHEKKNKRPDIKKVQQL 453 (453)
            :.  .:  .::***:  .  .    ::.:*.:*   : : **.:.:* :

h-IRAK3     LESTQ 447
h-IRAK4     LQEMT 458 (458)
            *:.
```

Figure 4.2 Amino acid sequence alignment of IRAK4 and IRAK3

Alignment of the kinase domain of IRAK3 and IRAK4 amino acid sequence using the Clustal W2 program. A score of 28.14 was achieved. Important kinase residues are highlighted in yellow the main gaps are highlighted in pale red. Possible GC residues and the novel GC centre is highlighted in blue. In brackets highlighted in green are the amino acids numbering according to the homology model of IRAK4, similar numbering was used in the IRAK3 model.

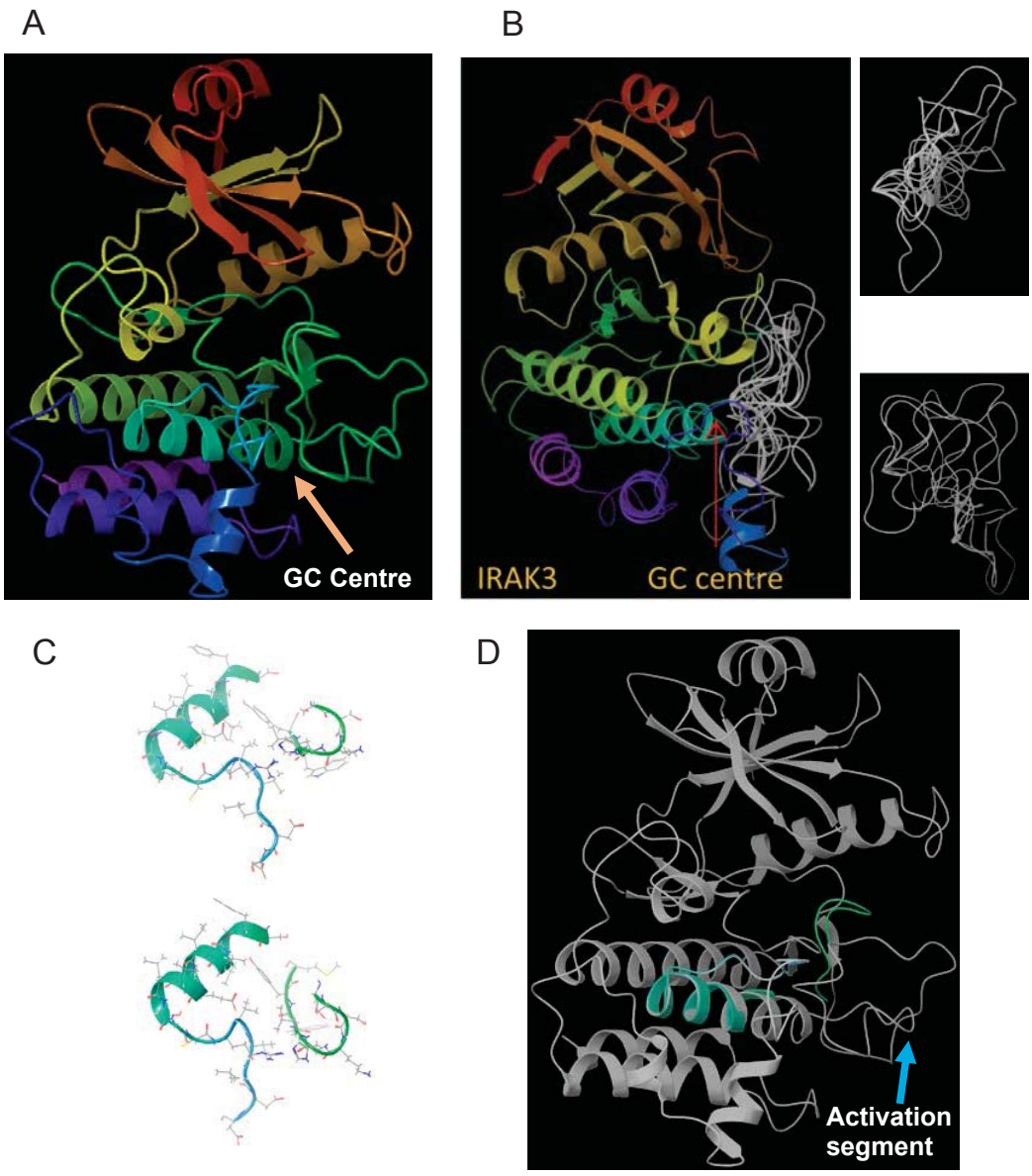

Figure 4.3 IRAK3 homology model

(A) The IRAK3 kinase domain homology model, the GC centres is pointed at by an orange arrow. (B) IRAK3 showing ten possible configurations (silver) of the loop containing the C-terminal part of the GC centre of IRAK3 (383–398). In addition, two alternative views of the loop configurations are shown demonstrating the potential for large movements associated with this section of the protein. (C) The GC centre part of the IRAK3 homology model at slightly different angles showing the GC centre as well as the nearby KHLW loop, displaying possible interactions. (D) The IRAK4 crystal structure in silver (2NRU) (Wang et al., 2006) with the transposed extra loops of IRAK3 in cyan and green showing the main differences between the two structures in the GC vicinity. The blue arrow points to the IRAK4 activation segment

4.3.3 Comparison of IRAK3 and PSKR1 homology models

We wanted to see if IRAK3 has a similar homology structure to other novel GCs, therefore we aligned the amino acid sequence of the kinase domain of IRAK3 to the amino acid sequence of the kinase domain of PSKR1. PSKR1 was used as it is a novel GC previously characterised within our group with a previously prepared homology model. The model for PSKR1 was based on its 41.2% identity with the crystal structure of tomato resistance protein Pto (for *Pseudomonas syringae* pv. tomato) kinase (PDB code 3HGK). (Freihat et al., 2014; Muleya et al., 2016; Muleya et al., 2014) (Figure 4.4). The two sequences were aligned at the five key kinase amino acid residues that are conserved between the kinase families (highlighted in yellow in Figure 4.4. The histidine residue of the HRD motif of PSKR1 was aligned to the corresponding cysteine 291 of the CGS in IRAK3. Using the amino acid sequence alignment the two homology models were then aligned to observe the overall architecture of the GC centre of the two protein. (Freihat et al., 2014; Kwezi et al., 2011).

Both IRAK3 and PSKR1 homology models show a typical kinase structure that is in agreement with these molecules being primarily kinase in nature, although human IRAK3 is a pseudokinase (Murphy et al., 2014; Wesche et al., 1999). The overall structures have a high degree of similarity (RMSD of 0.72A°; 1A° = 0.1 nm) demonstrating the predominant kinase shape (Figure 4.5 A). The main differences are that the PSKR1 model does not show an N-terminal α helix, a number of loop configuration differences are seen throughout the model and the C-terminal α helices do not align. The GC centre is in part an internal α-helix, whereas the remainder emerges as a loop (Figure 4.5 A).

Surface models of PSKR1 and IRAK3 indicate that the GC centre is associated with a small groove leading into the kinase cleft (Figure 4.5 C). The groove alters with the different loop configurations and potentially with dimerization, a catalytic or binding site

is developed. Transient dimerization that depends upon interactions at the C-terminus is observed in PSKR1 (Muleya et al., 2016) and it may be that the transient nature of this dimerization is an important regulatory component of the GC response (Freihat et al., 2014). Classical nucleotide cyclases are known to dimerize to form functional complexes essential for their activity (Winger et al., 2008). In GCs, the dimerization can produce a catalytic groove for GTP binding. Dimerization is less documented in the novel GC class, and further evidence is needed to document the necessity of dimerization in this class. To date the novel GC BRI1 has demonstrated homodimer formation; however, this has not yet been seen with the other characterised novel GCs (Muleya et al., 2016). Dimerization in the case of this novel class of GCs however, may not be essential; therefore, further experimental evidence is necessary to address the matter. IRAK3 is not known to form homodimers, however, IRAK3 does bind to other IRAKs in the signalling cascade through its death domain, as well as through its C-terminal domain to TRAF6. Therefore, it is of interest to observe the effect the binding to the other IRAKs, TRAF6 and the formation of myddosome complexes may have on IRAK3s GC activity.

```
PSKR1-KD    -------DDLLDSTNSFDQANIIGCGGFGMVYKATLPDG---KKVAIKKLSGDCGQIERE  774
IRAK3-KD    LKSSISFQNIIEGTRNFHKDFLIGEGEIFEVYRVEIQNLTYAVKLFKQEKKMQCKKHWKR  208
                   ::::::.*..*.:  :** * :  **:. : :     *:  :: . :* :  :.

PSKR1-KD    FEAEVETLSRAQHPNLVLLRGFCFYKNDRLLIYSYMENGSLDYWLHERNDGPALLKWKTR  834
IRAK3-KD    FLSELEVLLLFHHPNILELAAYFTETEKFCLIYPYMRNGTLFDRLQCVG-DTAPLPWHIR  267
            * :*:*.*   :***:: * .:   .:.  *** **.**:*   *:      * * *: *

PSKR1-KD    LRIAQGAAKGLLYLHEGCDPHILHRDIKSSNILLDENFNSHLADFGLARLMSPYETHV—   892
IRAK3-KD    IGILIGISKAIHYLHNVQPCSVICGSISSANILLDDQFQPKLTDFAMAHFRSHLEHQSCT  327
            : *  * :*.: ***:     ::  .*.*:*****::*: :*:**.:*:: *  * :

PSKR1-KD    ---STDLVGTLGYIPPEYGQASVATYKGDVYSFGVVLLELLTDKRPVDM-CKPKGCRDLI  948
IRAK3-KD    INMTSSSSKHLWYMPEEYIRQGKLSIKTDVYSFGIVIMEVLTGCRVVLDDPKHIQLRDLL  387
               ::.    * *:* ** : .  : * ******:*::*:**  * *    *    ***:

PSKR1-KD    SWVVKMKHESRASEVFDPLIYSKENDKEMFRVLEIACLCLSENPKQRPTTQQLVSWLDDV-1008
IRAK3-KD    RELMEKRGLDSCLSFLDKKVPP-CPRNFSAKLFCLAGRCAATRAKLRPSMDEVLNTLESTQ 447
              ::: :  . . ..:*  :      :   ::: :*  * : . * **: ::::. *:..
```

Figure 4.4 Amino acid sequence alignment of the PSKR1 kinase domain and the IRAK3 kinase domain

Alignment of the amino acid sequences of the PSKR1 kinase domain and the IRAK3 kinase domain using the Clustal W2 program. Important kinase residues/domain are highlighted in yellow, the novel GC centre is highlighted in blue.

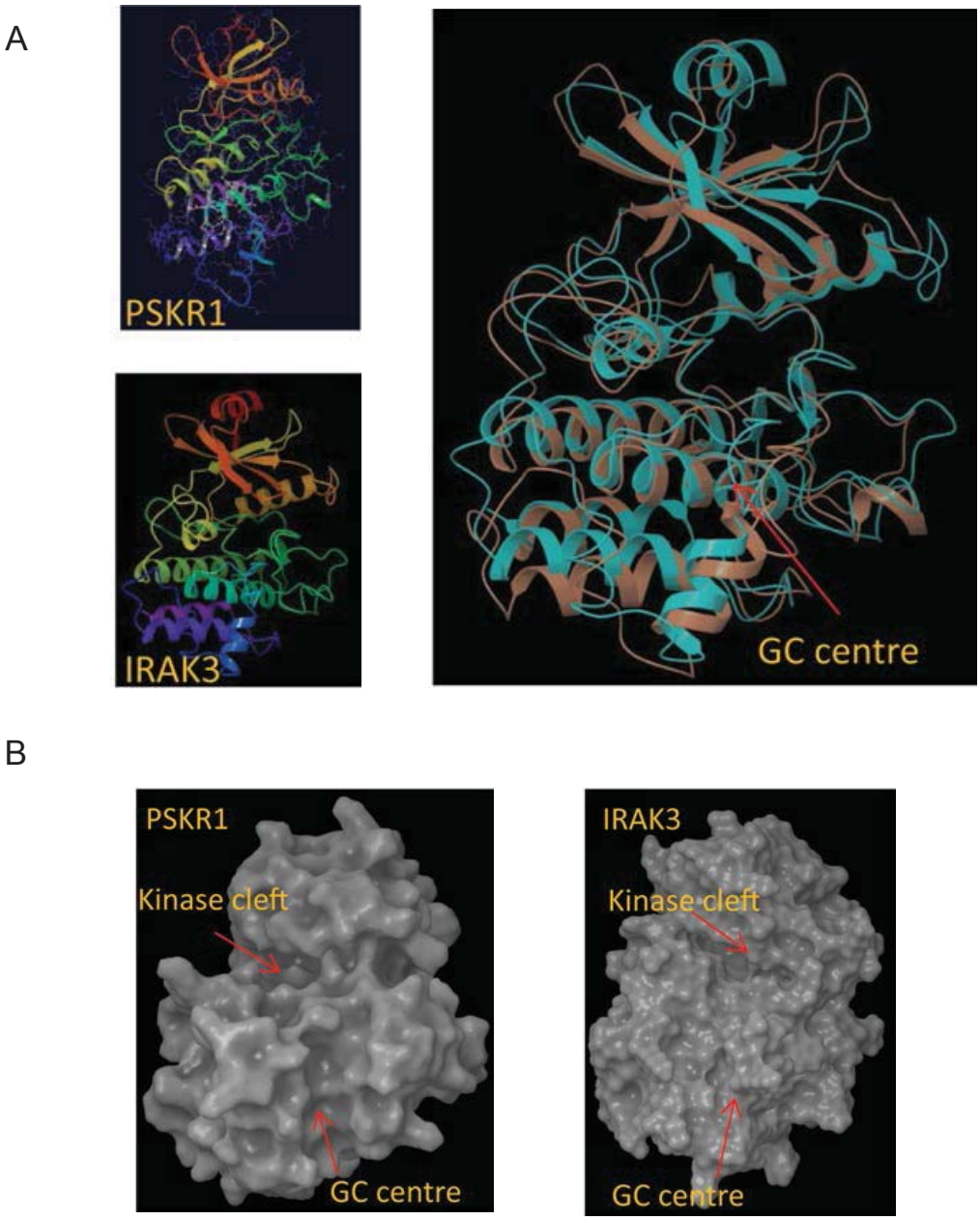

Figure 4.5 Comparison of PSKR1 and IRAK3 homology models

(A) Homology models of the kinase domain of PSKR1 and IRAK3 are overlaid following alignment at key amino acid residues, PSKR1 is brown and IRAK3 is cyan. The GC centre is indicated IRAK3. (B) Comparison of the surface topology of homology models of PSKR1 and IRAK3 showing the kinase cleft and the catalytic GC groove adapted from (Freihat et al., 2014).

4.3.4 Natural mutations in IRAK3

A number of natural mutations occur throughout the gene that may affect IRAK3 function. For instance, SNPs in the IRAK3 gene may be determinants of sepsis-induced acute lung injury (Pino-Yanes et al., 2011). Early onset asthma was also shown to be connected to SNPs at P22L in the death domain as well L400V and R429Q in the kinase homology domain (Balaci et al., 2007). Other polymorphisms are present in the kinase homology domain of IRAK3 that have relevance to this study, in particular, there are mutations in the GC centre. Table 4.1 highlights these mutations in the GC vicinity. The natural SNPs within the GC centre are highlighted in blue and those SNPs in the vicinity are highlighted in green. The investigation of the clinical variations would be of particular interest, however, due to the rarity of these mutations, no clinical information is available yet. The fact that the natural mutations in the GC centre and vicinity are so rare indicates the likely importance of these residues in the GC centre and vicinity, which are also quite conserved within the mammalian species (Carlton et al., 2006) (Table 4.1).

4.3.5 Mutation of the guanylate cyclase centre

To observe the effect specific residues in the GC centre have on the GC function, three different residues were chosen to be mutated in the GC centre to leucine. This was based on previous docking simulation studies done with GTP on the PSKR1 homology model. The amino acids in green are functionally assigned residues, while the blue residues are associated in binding with Mg^{2+} or Mn^{2+} ions (Figure 4.1 B). In these docking experiments done by Wong et al. (2013), the negatively charged hydrophilic triphosphates tail of the GTP is understood to interact with the arginine (or lysine) at position 14 of the motif which is positively charged (Ludidi and Gehring, 2003; Wong and Gehring, 2013). Wong et al. (2013) showed that mutating specific functionally assigned residues in the GC centre either had caused disruption in the homology model in the GC vicinity, or affected GTP docking. In this same study, it was

hypothesised that the amino acid in position 1 may form a hydrogen bond with the guanine of GTP, while in position 3 it confers specificity for GTP. The amino acid in position 14 is understood to stabilise the transition state from GTP to cGMP (Figure 4.1 B) (Wong and Gehring, 2013; Wong et al., 2015).

To observe these mutations in our IRAK3 homology model, we changed the specific residues, Serine359>Leucine and Glycine361>Leucine, Glycine361>Leucine only and Arginine372>Leucine only in the GC centre and observed the effects on the overall structure and surrounding molecules (Figure 4.6). The mutation of G361>L which is residue number 3 in the GC centre of IRAK3 to leucine showed a major steric clash, the leucine side chain clashed with the adjacent C425, A426, and somewhat with G423, R424, A427 and T428. To relieve the clash the α-helix (413-425) may shift or alternatively a loop can commence from about residue 424 or earlier which may allow some room for the leucine (Figure 4.6 A). The mutation of R372, which is residue number 14 in the GC centre to leucine, may not have a major effect on the surrounding molecules, as L372 may fit in adjacent to F419. The side chain of L372 can form a hydrophobic interaction with F419 and may still have an acceptable conformation so it may not have an effect on the overall structure (Figure 4.6 B). However if the GTP molecule interacts with the arginine as predicted in the PSKR1 docking model, then this may affect the affinity of GTP to the protein. A mutation at position 14 of the GC centre of PSKR1 effects binding to the phosphate acyl group and stabilises the transition of GTP to cGMP (Wong et al., 2015). Adding a serine 359 leucine mutation to the model had no major effect on the overall structure, the combination of the S359>L and G361>L mutation had no major effect other than that observed with the G361 leucine mutation alone (Figure 4.6 C).

Variant		Consequence	Transcript Consequence	Annotation	Allele Frequency
G	A	p.Ser359Asn	c.1076G>A	missense	0.000008246
T	G	p.Phe360Cys	c.1079T>G	missense	0.000008247
A	G	p.Glu366Gly	c.1097A>G	missense	0.000008248
C	T	p.Thr369Ile	c.1106C>T	missense	0.000008245
A	G	p.Gly370Gly	c.1110A>G	synonymous	0.00002473
A	T	p.Gly370Gly	c.1110A>T	synonymous	0.000008243
G	C	p.Arg372Thr	c.1115G>C	missense	0.000008242
T	C	p.Val373Ala	c.1118T>C	missense	0.000008241
A	G	p.Val373Val	c.1119A>G	synonymous	0.000008241
A	C	p.Asp376Ala	c.1127A>C	missense	0.000008241
CAT	C	p.Ile381ProfsTer7	c.1141_1142delAT	frameshift	0.000008239
A	G	p.His380Arg	c.1139A>G	missense	0.0000412
C	T	p.Ile381Ile	c.1143C>T	synonymous	0.0003625
C	CT	p.Arg384AlafsTer5	c.1148dupT	frameshift	0.000008238
C	T	p.Arg384Trp	c.1150C>T	missense	0.0003048
G	A	p.Arg384Gln	c.1151G>A	missense	0.0003295
A	T	p.Asp385Val	c.1154A>T	missense	0.000008237
T	A	p.Asp385Glu	c.1155T>A	missense	0.000008237
C	A	p.Leu386Ile	c.1156C>A	missense	0.000008237
C	G	p.Leu386Leu	c.1158C>G	synonymous	0.00004942
T	G	p.Leu387Arg	c.1160T>G	missense	0.000008237
T	C	p.Leu390Leu	c.1168T>C	synonymous	0.000008237
T	C	p.Met391Thr	c.1172T>C	missense	0.0006672
C	G	p.Leu400Val	c.1198C>G	missense	0.001161
G	A	p.Arg429Gln	c.1286G>A	missense	0.0001323

```
      360        370        380        390        400
.IKTDVYSF GIVIMEVLTG CRVVLDDPKH IQLRDLLREL MEKRGLDSCL.
```

Table 4.1 SNP variants of IRAK3 around the GC centre.

SNP variants of IRAK3 around the GC vicinity using (The Exome Aggregation Consortium (ExAC) program) http://exac.broadinstitute.org/gene/ENSG00000090376. Highlighted in blue are the SNPs within the GC centre, highlighted in green are SNPs in the GC vicinity. Below the table, for clarity the SNP variants are highlighted in blue in the GC centre and green in the GC vicinity showing the numbering of the residues.

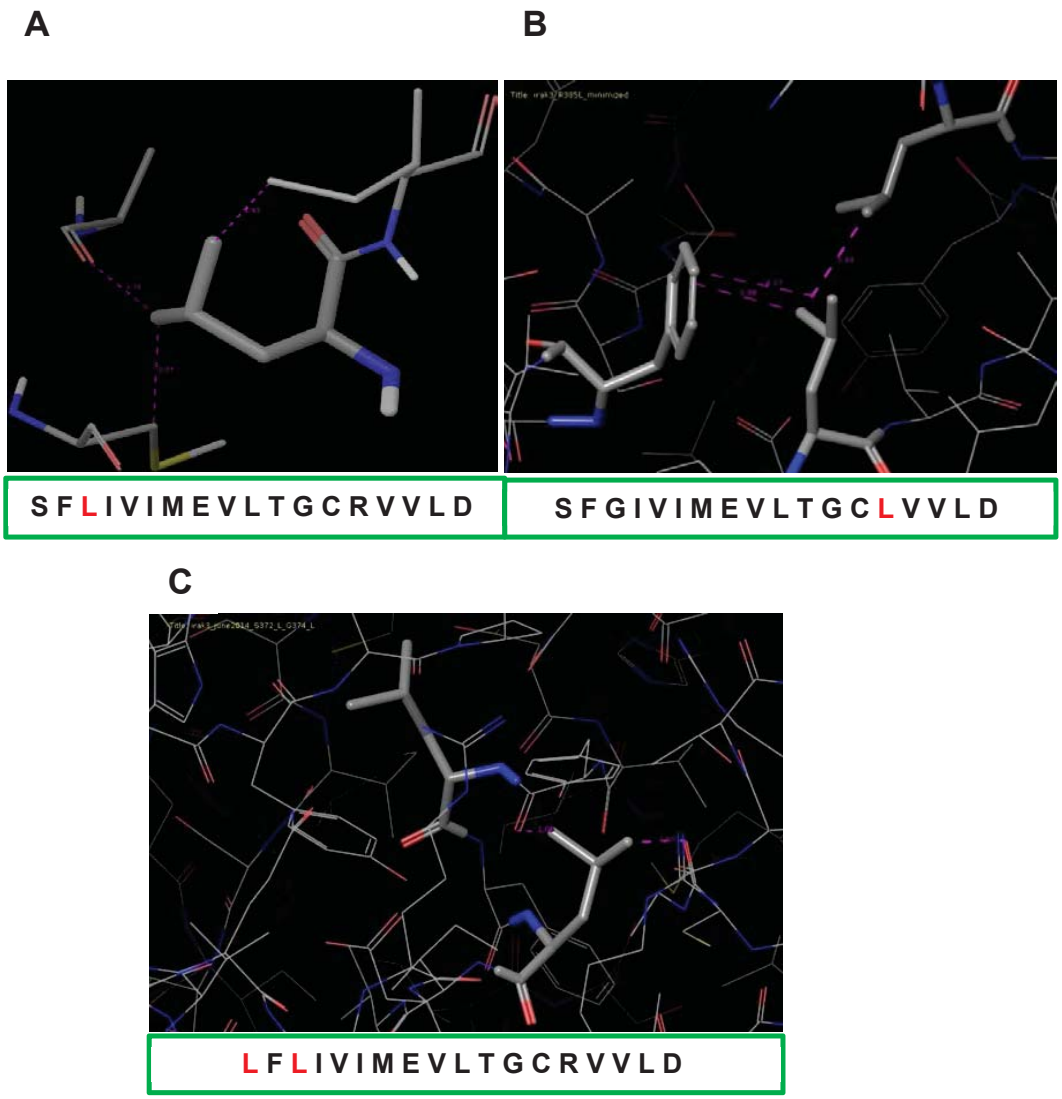

Figure 4.6 Mutation effects on the GC centre of IRAK3

(A) IRAK3 mutation of the G361 (position 3 in the GC search motif) to leucine indicating that may cause a disruption of the neighboring molecules. (B) Mutation of R372 (position 14 in the GC search motif) to leucine had no major effect on the structure. (C) IRAK3 mutation of the S359 and G361 (position 1 and 3 in the GC search motif) to leucine can cause a disruption of the neighboring molecules mainly due to the G361>L mutation.

4.3.6 GTP docking

To investigate if the mutations affected GTP binding, docking studies were done. GTP was docked into the homology model of IRAK3 and two molecular poses were observed. The first of these poses placed GTP in an orientation not usually observed in crystal structures of nucleotide cyclases. The second pose placed GTP in the active site in a manner similar to that found for the binding mode of ATP in a cAMP dependent protein kinase (pdb code 1ATP). Based on the study done by Wong et al. (2013) it is predicted that there may be an interaction between the GTP phosphate tail, which is negatively charged, and the positively charged arginine in the GC centre.

From this binding mode in our IRAK3 homology model it was noted that the terminal phosphate groups of the GTP was about 9 Å away from the guanidine group of R372. And in this position an interaction is unlikely, however this separation is due to H337 was located in between the two groups of interest (Figure 4.7 A). To explain the possibility of interaction between the phosphate group and R372, a number of manipulations were made. These included moving the H337 imidazole ring out of the way and adjusting the conformation of the triphosphate chain (Figure 4.7 B). This placed the phosphate and guanidine at a distance of close to 4 Å. It could be predicted that an interaction may be formed between these residues but this remains speculative and requires further experimental work (Figure 4.7 C). However, when R372 was mutated to leucine and a GTP dock was done on the R372>L mutant we can see that it is unlikely that the methyl group of the leucine can interact with the polar phosphate group of GTP (Figure 4.7 D). Therefore, from this docking result we can predict that mutant R372>L may no longer be able to catalyse the production of cGMP due to the decreased chance of interaction and stabilisation of the GTP.

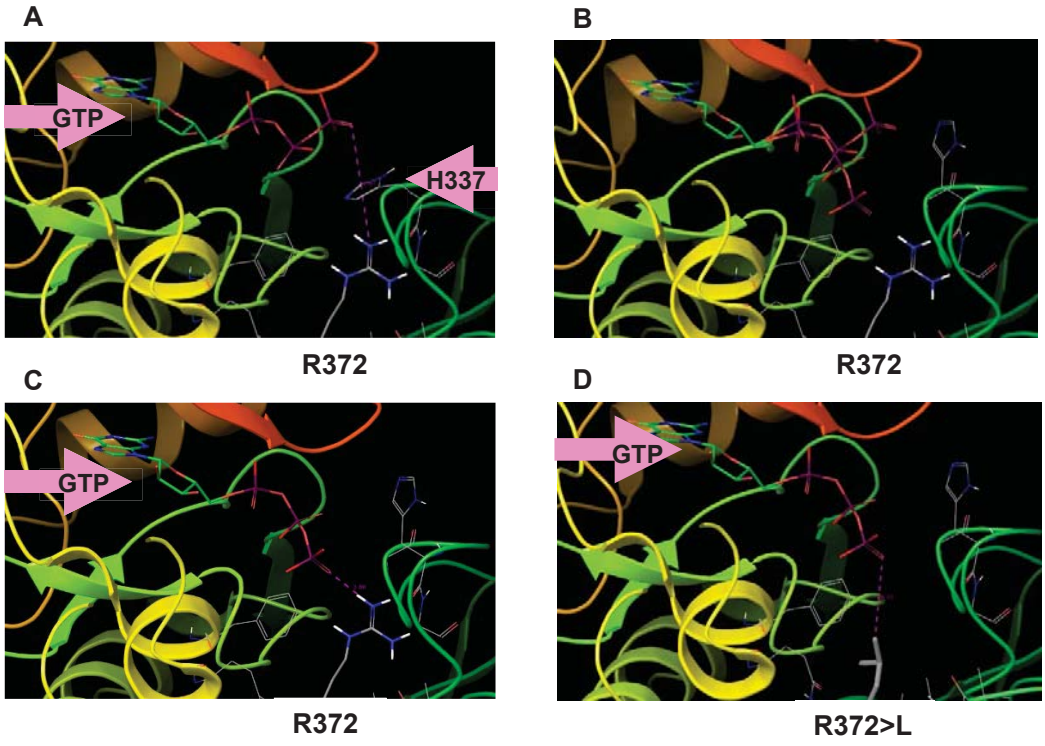

Figure 4.7 GTP docking interactions

(A) Interaction between the triphosphate of the GTP and the arginine side chain when histidine 337 interferes. (B) Interaction between the triphosphate of the GTP and the arginine side chain when the histidine side chain is moved. (C) Interaction between the triphosphate of the GTP and the arginine side chain at distance of close to 4 Å. (D) Mutant R372>L with the GTP docked showing that the two residues are quite far from each other (distance of about 6 Å) and an interaction is less likely.

4.4 CONCLUSION

We have explored the nature of IRAK3 in different species and observed the conservative nature of the GC centre in the different mammalian species. Looking at the SNPs in the GC centre had also shown the conservative nature of the GC centre and its vicinity, with very rare SNPs observed. This highlights the possible significance of the GC centre within the pseudokinase domain. We modelled and observed the structures of IRAK3 using homology modelling which was built based on the crystal structure of IRAK4 (2NRU). The homology model of IRAK3 was used to note the GC centre structure and possible interactions in the GC vicinity. IRAK3 was also aligned to the PSKR1 model, and both of these kinase GCs adopt a similar architecture. The GC centre of the kinase GCs is rather hidden and not easily recognized as a GC centre.

Our homology model was used to predict mutations that may interfere with the GC function. Three separate residues were mutated, and structural changes were observed. The G361>L mutant model structure, the double S359>L and G361>L mutant model structure as well as the R372>L mutant model structure was prepared. The G361>L mutation had revealed possible steric hindrance in the GC centre which may affect the overall GC function, while the other mutations did not affect the overall structure. GTP docking was done in the GC centre to observe potential interactions between the GTP and the arginine in the GC centre of the IRAK3 model. Possible interactions are observed between the two residues, this is suggestive that R372 is potentially important in catalysis of GTP to cGMP. This interaction however, may not be possible in the IRAK3 R372>L mutant model due to the noticeable distance between the residues. Since the IRAK3 structure is a homology model, we cannot be sure of our predictions and still remains quite speculative, therefore mutagenesis studies and experimental data is needed to confirm these predictions.

CHAPTER 5

INVESTIGATING THE GUANYLATE CYCLASE ACTIVITY OF IRAK3

CHAPTER 5

INVESTIGATING THE GUANYLATE CYCLASE ACTIVITY OF IRAK3

5.1 INTRODUCTION

The nucleotide cyclases are a family of enzymes with a similar conserved catalytic domain that convert nucleotide triphosphates like GTP and ATP to the cyclic nucleotide monophosphates cGMP and cAMP respectively. There are three characterised nucleotide cyclase families, adenylate cyclase (AC), classical transmembrane guanylate cyclase and soluble guanylate cyclase. These enzymes are involved in a broad array of signal transduction pathways mediated by the cyclic nucleotides as discussed in chapter 1 (Section 1.1.2 and 1.1.3).

Guanylate cyclases are known to be mediated by a number of factors such as nitric oxide, peptide ligands and fluxes in intracellular calcium (Gerzer et al., 1983; Hardman and Sutherland, 1969; Lucas et al., 2000; Schultz et al., 1969; White and Aurbach, 1969). Calcium is known to act as a substrate cofactor to support transmembrane guanylyl cyclase catalytic activity through calcium dependent guanylate cyclase activating protein (Duda et al., 2016). Research within our lab shows that, calcium has a direct effect on the GC activity of phytosulfokine receptor 1 (PSKR1) a novel transmembrane kinase GC, where increasing amounts of calcium increased cGMP production (Muleya et al., 2014). In the case of soluble GCs however, calcium has a negative effect on cGMP production, inactivation of soluble GCs by intracellular calcium works to decrease the stimulatory effect of nitric oxide on guanylate cyclase activity. (Andric et al., 2001; Levine et al., 1979; Lucas et al., 2000). Divalent cations

such as Mg^{2+} and Mn^{2+} that complex with GTP are required as substrates for guanylate cyclase catalysis. *In vivo,* Mg^{2+} is believed to be the GC physiological cation due to its higher concentration in cells of about 3 mM compared to Mn^{2+} which is at a concentration of 10 µM (Padh and Brenner, 1984; Veltman et al., 2005). Veltman et al. (2005) had shown that the *Dictyostelium* soluble GC which is a homologue of mammalian soluble GCs reside mainly in the cytosol in an inactive uncoupled state, a small fraction however is associated with the cell membrane. It was shown that the GC activity in the supernatant preferred Mn^{2+}, however the GC activity in the membrane fraction was 2–3 fold higher in the presence of Mg^{2+} (Veltman et al., 2005). Bocanera et al. (1999) used bovine thymus extracts of supernatant and particulate fractions to show that replacing Mn^{2+} for Mg^{2+} considerably decreased the GC activity of both the transmembrane as well as the soluble GC activity. (Bocanera et al., 1999; Lucas et al., 2000; Potter, 2011a) .

Classical transmembrane guanylate cyclases contain a kinase homology domain and a separate guanylate cyclase domain parted by a linker region. The structure and function of transmembrane GC are described in greater detail in chapter 1. IRAK3 is believed to be a member of the novel class of GCs as described in more detail in chapter 4. This class is unique in the fact that it contains a GC centre within its kinase domain. IRAK3 is a soluble protein with a conserved GC centre within its kinase homology domain. Therefore, the aim of this chapter was to test the GC activity of recombinant IRAK3 protein. Both *in vitro* and cellular studies were undertaken to look at IRAK3 GC activity through cGMP production. In chapter 4 key amino acid residues in the catalytic centre were identified. These residues were mutated by site directed mutagenesis to test if the molecular changes altered cGMP production as predicted.

5.2 RESULTS AND DISCUSSION

5.2.1 cGMP production by recombinant IRAK3

To investigate the GC activity of the proteins of interest, recombinant protein was prepared as described in chapter 2 section 2.5. To test for GC activity, cGMP production by recombinant IRAK3 protein was determined using ELISA or mass spectrometry (MS). All reactions contained guanosine triphosphate (GTP) and a divalent cation either Mg^{2+} or Mn^{2+}. Reactions were completed over 5 minutes, as described in chapter 2 section 2.6. Divalent cations such as Mg^{2+} and Mn^{2+} can act as substrate cofactors or allosteric modulators for maximal GC activity of transmembrane and soluble GC catalytic activity (Lucas et al., 2000). GCs can have different cofactor preferences for cGMP production. Therefore, the ability of IRAK3 to generate cGMP was tested in the presence of either Mg^{2+} or Mn^{2+}. The preferred cofactor for IRAK3 cGMP production is Mn^{2+} (Figure 5.1A), Mn^{2+} was therefore used as the cofactor in subsequent experiments unless otherwise stated.

Initial experiments to test if recombinant IRAK3 could generate cGMP used ELISA based systems from two different companies; either GE Amersham cGMP Enzyme immunoassay Biotrak (EIA) System or NEW EAST monoclonal Anti-cGMP Antibody Based Direct cGMP (Non-acetylated) ELISA kit. Figure 5.1, shows a comparison between the two kits using Mn^{2+} as the metal cofactor where the Amersham GE-kit is used in figure 5.1 A and the NEW EAST kit in figure 5.1 B. Similar amounts of cGMP generated by recombinant IRAK3 were detected by both kits and therefore both appear suitable to use but for any one experiment 2-4 separate protein preparations were used with a specific kit. Interestingly, it appears that GTP partially interferes with cGMP detection when combined with Mn^{2+} as seen in the negative no protein control (Figure 5.1 B). Therefore, the no protein control value was subtracted from data in subsequent experiments. The amount of cGMP generated by IRAK3 was similar to the amount

produced by the cytoplasmic domain of PSKR1 which was used as a positive control for GC activity (Figure 5.1B). PSKR1 has no preference for either Mg^{2+} or Mn^{2+} ions as metal cofactor (Kwezi et al., 2011) unlike IRAK3 which prefers Mn^{2+} (Figure 5.1 A).

Prior studies on GCs by different groups have shown high variability cGMP production (Table 5.1), GC activity is presented as picomol per mg protein per minute (pmol/mg protein/min). Different methods showed variability in cGMP production between similar and different types of GCs, which ranged from 0.12 pmol/mg protein/min to 1000 pmol/mg protein/min (Bachiller et al., 2013; Chester et al., 2011; Gukovskaya et al., 2000; Gustafsson and Brunton, 2002; Murthy, 2008). However, in a study by Klaiber et al. (2011), GC activity was shown to be as high as 45,000 pmol/mg protein/min, highlighting the extent of the variability depending on the technique used (Table 5.1). The Arabidopsis members of the novel class of GCs fall within this range when measured using ELISA or mass spectrometry and expressed either recombinantly or in cell (Kwezi et al., 2011; Meier et al., 2010). IRAK3 also falls in the range and is similar to PSKR1 (Figure 5.1 B).

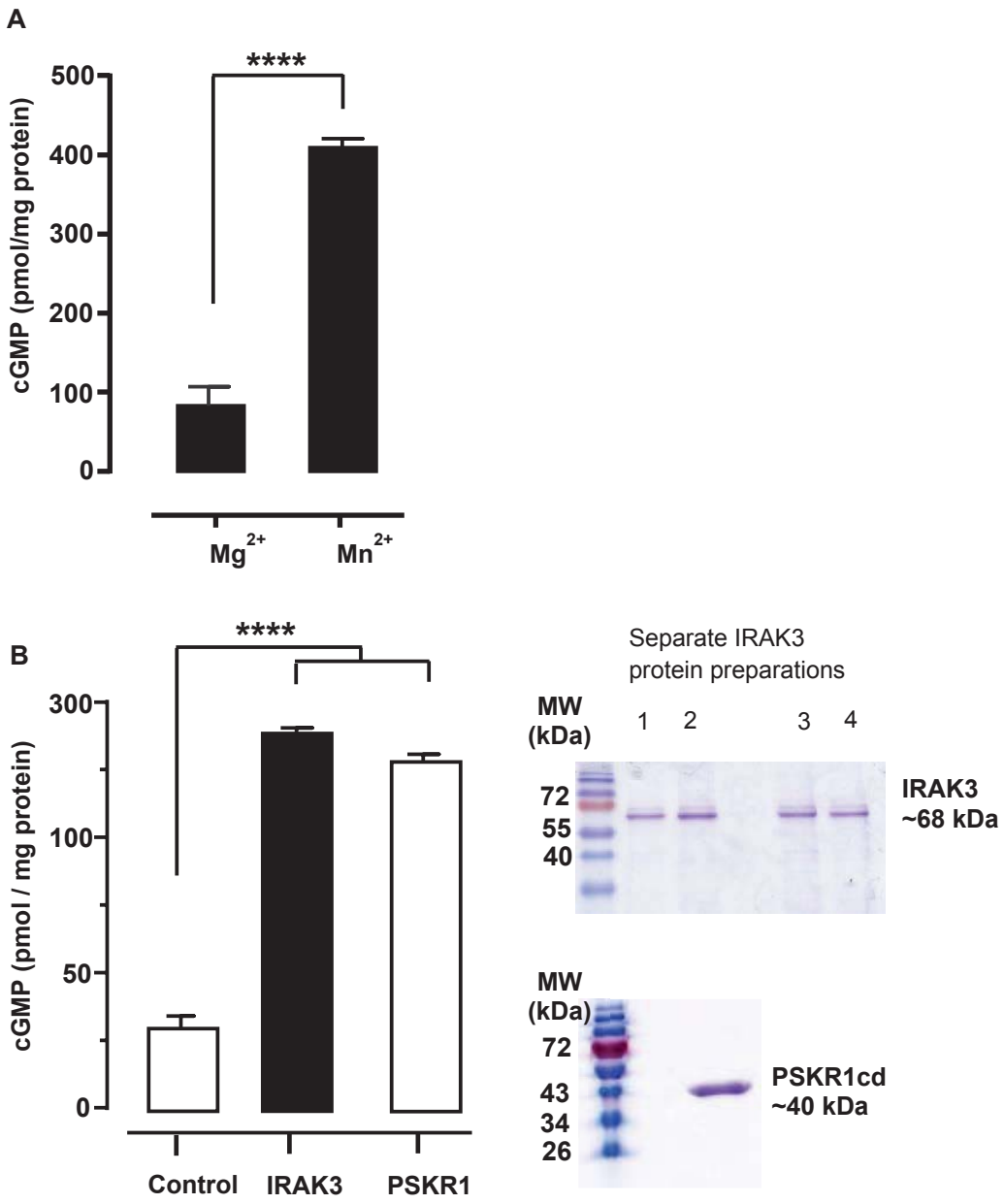

Figure 5.1 cGMP production by IRAK3

(A) Recombinantly expressed IRAK3 GC activity is tested after a *5 minute reaction in the presence of divalent cations Mg^{2+} or Mn^{2+}. The divalent cation Mn^{2+} is preferred for cGMP production. The Amersham GE cGMP kit was used (n=4-5, Unpaired t test P<0.0001).*

(B) Comparison of cGMP production between recombinant IRAK3 and the recombinant cytoplasmic domain of PSKR1. Similar levels of cGMP are produced (5 minute) and are significantly different to the no GTP control. The purified proteins are shown on Coomassie stained protein gels, four separate protein preparations were tested. cGMP was detected using the NEW EAST cGMP kit (n=4, ANOVA P<0.0001 Tukey's multiple comparisons test).

Guanylate cyclase name /type	Cell/Organism	Cation used	Technique used	Activity pmol/mg protein/min approx.	Reference
Soluble GC	Rabbit gastric smooth muscle cells	-	RIA	0.12	(Murthy, 2008)
Soluble GC	Pulmonary artery smooth muscle cells	Mg^{2+}	ELISA	1.5	(Chester et al., 2011)
Soluble GC	Solubilized lung protein	Mg^{2+}	ELISA	1000	(Bachiller et al., 2013)
Soluble GC	Rat cardiac fibroblast cells	-	RIA	22	(Gustafsson and Brunton, 2002)
Soluble GC	Bovine lung extract	Mg^{2+}	RIA	1.2- 2.4	(Humbert et al., 1990)
Soluble GC	Bovine lung extract	Mg^{2+}	RIA	15.7	(Gerzer et al., 1981)
Soluble/ Transmembrane	Dictyostelium cell line	Mg^{2+} /Mn^{2+}	RIA	35 pmol/min. /10^7 cells*	(Veltman et al., 2005)
Soluble/ Transmembrane	Bovine thyroid extracted proteins	Mn^{2+}	RIA	93-125	(Bocanera et al., 1999)
GC-A Transmembrane	Rat pancreatic aciner cells	Mg^{2+}	RIA	12	(Gukovskaya et al., 2000)
GC-A Transmembrane	HEK 293 cells	Mg^{2+}	RIA	45000	(Klaiber et al., 2011)
PSKR1 Novel transmembrane	Recombinant protein	Mg^{2+} /Mn^{2+} Mg^{2+} and Ca^{2+}	ELISA	4	(Kwezi et al., 2011; Muleya et al., 2016; Muleya et al., 2014)
BRI1 Novel transmembrane	Protoplasts	Mg^{2+} /Mn^{2+}	ELISA	2.5	(Irving et al., 2012; Kwezi et al., 2007)
AtWAKL10 Novel transmembrane	Recombinant protein	Mg^{2+}	ELISA	14	(Meier et al., 2010)

* This study expressed data as per 10^7 cells.

Table 5.1 cGMP production of different guanylate cyclases

Guanylate cyclase cGMP production measured using radioimmunoassays (RIA) or enzyme immune assays (ELISA) is presented. The amounts shown is in picomoles per milligram of protein per minute (pmol/mg protein/min) to account for reaction time. cGMP preparations were taken from either cell lysates or solubilized protein. The divalent cation used and preferred for each reaction is presented for the different guanylate cyclases. The amount of cGMP was measured in each study post induction with either nitric oxide or nitric oxide donors for soluble GCs or atrial natriuretic peptide for the transmembrane GCs.

Earlier studies on Arabidopsis members of the novel class of GCs showed that more cGMP was detected using mass spectrometry (MS) then ELISA (Kwezi et al., 2007; Kwezi et al., 2011). Therefore, a quantitative investigation using MS was undertaken to confirm cGMP production of IRAK3 compared to the immunoassays. Mass spectrometry cGMP analysis is more sensitive than the immunoassays (Gross and Durner, 2016; Marondedze et al., 2015; Spangler et al., 2009) and this can be seen by the increase in cGMP production by about 10 fold compared to the new east immunoassay kit, note that the amount is expressed as picomoles per microgram of protein (Figure 5.2). The amount produced by IRAK3 however is slightly less than the amount produced by the demonstrated novel GC control, cytoplasmic domain of brassinosteroid receptor (BRI1) (Figure 5.2). The mass spectrometry analysis and sample preparation are described in chapter 2 section 2.6.1. Samples were sent for LC- MS/MS analysis to be tested by Dr Aloysius Wong, at the same time BRI1 was also tested for activity using the MS analysis (Wheeler et al., 2017).

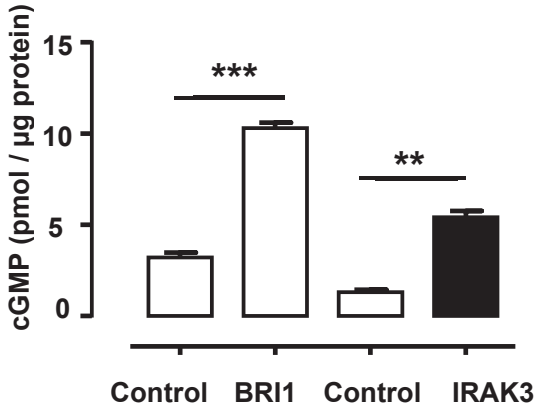

Figure 5.2 Mass spectrometry analysis of cGMP generated by recombinant proteins

Mass spectrometry (LC-MS/MS) analysis of cGMP produced by two separately expressed protein preparations of recombinant IRAK3 in the presence of Mn^{2+} and two separately expressed protein preparations of recombinant BRI1 in the presence of Mg^{2+}. Each separate protein was tested in three separate reactions (technical repeats). Compared to each no protein control both proteins produce significant amounts of cGMP (n=2, ANOVA P<0.0001, Tukey's multiple comparisons test).

The amount of cGMP produced by this novel class of GCs including IRAK3, PSKR1 and BRI1 is overall on the lower side of that produced by the classical transmembrane and soluble GCs ((Table 5.1) (Figure 5.1 and 5.2)). This novel class of GCs was shown to be activated by molecular switches such as calcium *in vitro* (Muleya et al., 2014). In addition as discussed in chapter 4, formation of cGMP may depend on the ability of the protein to homodimerize. Transient dimerization of recombinant PSKR1 occur (Muleya et al., 2016) and BRI1 (Bojar et al., 2014). However, Bojar et al. (2014) claimed that BRI1 does not produce cGMP using HPLC-based activity assays. These results are conflicting to previous studies that showed significant amounts of cGMP being produced *in vitro*. Mass spectrometry analysis as well ELISA had shown significantly increased cGMP production over multiple experiments (Kwezi et al., 2007; Wheeler et al., 2017) (Figure 5.2). Recombinant protein assays need to be optimised and the correct cofactors need to be considered. Bojar et al. (2014) used conditions that may have favoured kinase activity and the construct used did not contain the full kinase domain that allows for dimerization (Bojar et al., 2014); these factors may have further reduced any GC activity.

5.2.2 Stability of recombinant IRAK3

During the course of this study it became apparent that IRAK3 was quite unstable when expressed in bacterial cells. The recombinant IRAK3 protein post purification is also quite unstable *in vitro*. Despite much effort into optimisation of expression conditions, the expression was still quite variable in terms of the amount of soluble protein being produced and available for extraction. Purified protein preparations expressed under the same conditions on different days showed variability in the amount of protein purified as can be seen on the two different coomassie gels prepared separately (Figure 5.1 B and figure 5.3). This was also confirmed quantitatively using the Nanodrop® ND-1000 Spectrophotometer protein at A_{280} nm, (data is not shown). Previously prepared proteins also showed some degradation at -20ºC. Therefore, a

western blot was prepared to confirm if IRAK3 could be detected after a period of time (one month in this case) at -20 ºC. Using a 6xHis-tag antibody, the antibody only picked up the 6xHis-tag at about 25 kDa and no signal was seen at the expected mass of 68 kDa (Figure 5.3 B). A search on the stability of IRAK3 using the ExPASy - ProtParam program (Gasteiger et al., 2005) also showed that the protein is considered unstable. Therefore, freshly isolated protein was used in all the cGMP assays presented to avoid the degradation of the protein with time.

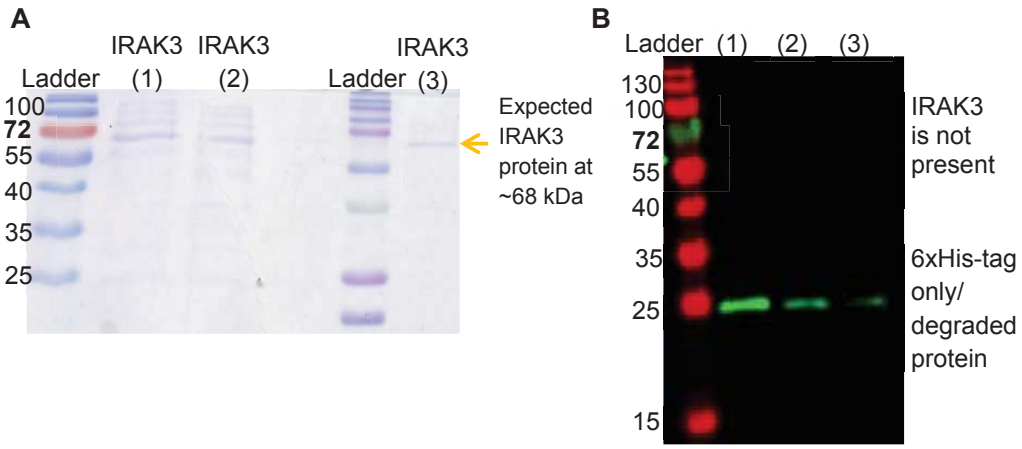

Figure 5.3 Stability of IRAK3 protein

(A) Coomassie gel showing IRAK3 protein the day after purification at about 68 kDa. (B) Western blot of IRAK3 concentrated purified protein is no longer present after freezing at -20ºC for over a month. A mouse anti- 6xHis-tag antibody was used to detect the tag, followed by an anti-mouse secondary antibody.

5.2.3 Effect of calcium on cGMP production

Calcium appears to have opposing effects on mammalian GCs. Calcium acts as a substrate cofactor to support GC activity of transmembrane associated GCs where it acts through a calcium dependent GC activating protein (Duda et al., 2016). Whereas calcium has a negative effect on soluble GCs, where it decreases the stimulatory effect of nitric oxide on the GC activity (Andric et al., 2001; Levine et al., 1979; Lucas et al.,

2000). Moreover, calcium appeared to act as a switch for PSKR1, at physiologically relevant calcium levels, the GC activity of the cytoplasmic domain of PSKR1 increased with an increase in Ca^{2+} levels in a concentration dependent manner (Muleya et al., 2014). The kinase activity of PSKR however was abolished with an increase in Ca^{2+} levels (Muleya et al., 2014). Therefore, it was of interest to investigate the effect of calcium on IRAK3 GC activity. cGMP production of recombinant IRAK3 was measured in the presence of Mn^{2+} and different concentrations of calcium. Free calcium ion concentrations were buffered by EGTA, and calculated using the Maxchelator WebMaxC Extended computational program conditions of experiment are explained in greater detail in the methods chapter 2 (2.6.1.1) (Bers et al., 2010).

The GE cGMP ELISA kit was used to measure cGMP production at different calcium concentrations. The data was calculated by taking away the background or negative control. A 10 fold reduction in cGMP production with the different protein batched prepared is observed (Figure 5.4), compared to previous ELISA assays under similar conditions (Figure 5.1A). This also confirms the variability in cGMP production between protein batches described in section 5.2.2. A decreasing trend in cGMP production by IRAK3 was observed in the presence of increasing amounts of calcium occurred; however, the decrease is not significant (Figure 5.4). This result is unlike the effects seen with PSKR1, where increasing calcium concentrations were shown to increase cGMP production. PSKR1 is an active kinase and calcium was shown to act as a modulating switch between the GC and kinase activity (Muleya et al., 2014). Figure 5.4 indicates that calcium may possibly have an alternative modulatory effect on IRAK3 when compared to PSKR1. Since IRAK3 is an inactive kinase, calcium is unlikely to affect IRAK3 in terms of its kinase activity. However, the decrease in cGMP production may modulate downstream signalling, therefore further investigation is necessary to observe the effect of calcium on IRAK3 in terms of the downstream signalling cascade.

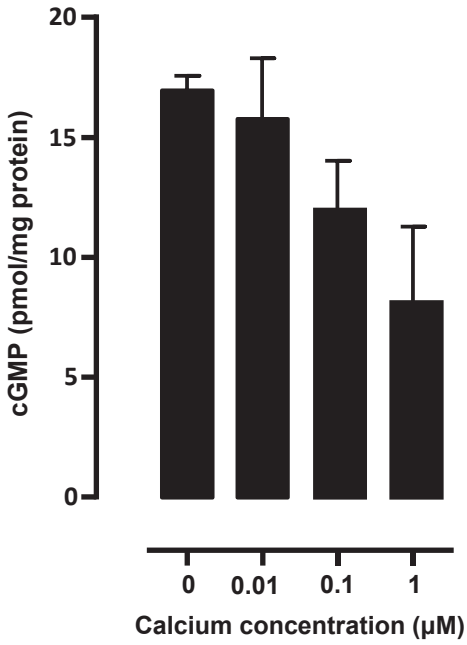

Figure 5.4 Effect of calcium on cGMP production by IRAK3

The effect of calcium on cGMP production of IRAK3 in the presence of Mn^{2+} was measured using the Amersham GE cGMP kit. Increasing free calcium ion concentrations were buffered by EGTA. A slight but non-significant decrease in cGMP production is observed with increasing calcium concentration ((n= 4-6, ANOVA P=0.092, Tukey's multiple comparisons test).

5.2.4 cGMP production of recombinant mutant IRAK3 protein

To test if the predicted GC centre is important in cGMP production a series of mutations were made to this region. The mutagenesis experiments were designed taking into account previous docking work done on potential mutation sites that may disrupt GC activity in PSKR1. If one or more key amino acid residues at position 1, 3 and/or 14 of the GC search motif (Figure 5.5 A) was replaced with leucine, disruptions in the docking orientations of GTP can occur in PSKR1 (Wong and Gehring, 2013). The

mutagenesis experimental design was also influenced by further modelling of IRAK3 discussed in chapter 4.

Site directed mutagenesis was used to create IRAK3 G361>L and IRAK3 R372>L. Wildtype (WT) and mutant recombinant IRAK3 proteins were expressed in bacteria and cGMP was measured using the GE ELISA kit. Our experimental data suggests that the G361>L mutation had no major effect on cGMP production, since a significant amount of cGMP was produced which is comparable to IRAK3 WT (Figure 5.5 B). Therefore the mutation of G361 to leucine did not affect cGMP production and the docking study can accommodate this result. The leucine therefore does not cause any hinderence as alternativley predicted by the IRAK3 docking study in chapter 4 section 4.3.5.

The docking study showed that the mutation of G361 to leucine initially caused a major steric clash. However this clash may be relieved by shifting the nearby α-helix or alternatively a loop can commence earlier which may allow some room for the leucine. The R372>L mutation significantly decreased cGMP production when compared to the IRAK3 WT (Figure 5.5 B). On the other hand previous docking done on PSKR1 and IRAK3 (chapter 4) also showed that the mutation of R372 to leucine, may affect GC activity. It is predicted that the GTP molecule may interact with the arginine in position 14 in the GC centre (Wong and Gehring, 2013; Wong et al., 2015). The experimental data is thus supported by the predicted docking studies done in chapter 4 and the previous docking study done on PSKR1 (Wong and Gehring, 2013).

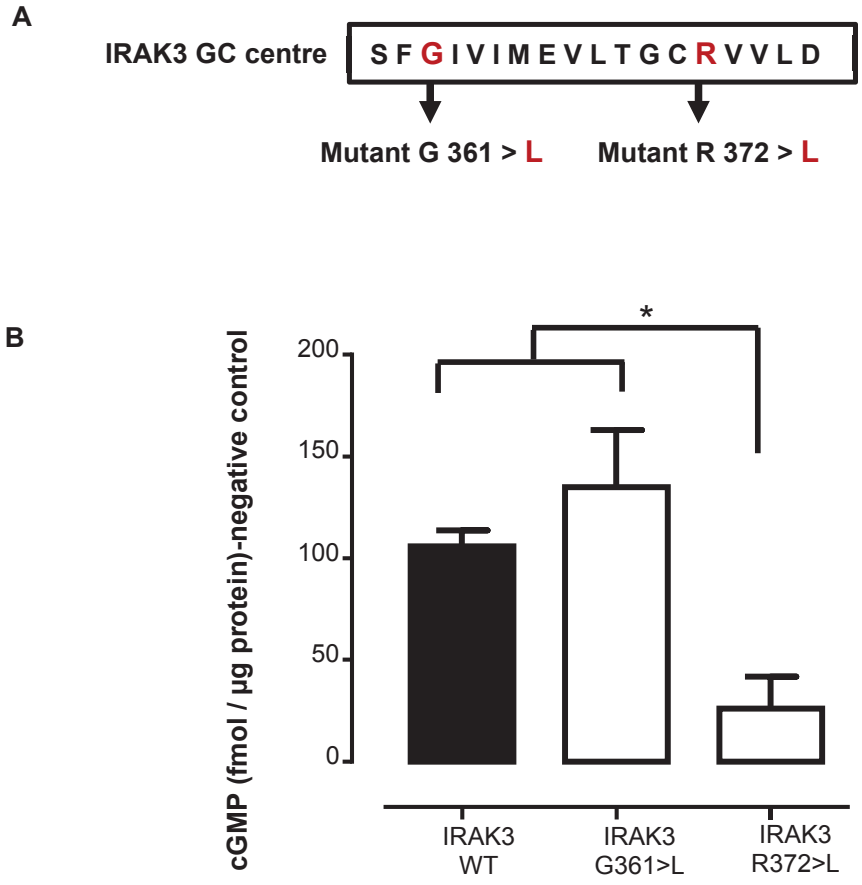

Figure 5.5 cGMP production by recombinant mutant IRAK3 proteins

(A) IRAK3 amino acid sequence highlighting the G361 and R372 to leucine mutation in red text. (B) IRAK3 protein was expressed as either wildtype IRAK3, IRAK3 mutant G361>L or IRAK3 mutant R372>L as previously described in chapter 2 section 2.5. Mutant G361>L produced significant amounts of cGMP which is comparable to the amount produced by IRAK3 WT. Mutant R372>L had significantly decreased cGMP production when compared to the IRAK3 WT and IRAK3 mutant G361>L (n=2-3, One way - ANOVA P<0.05 and Tukey's multiple comparison test).

5.2.5 Guanylate cyclase activity in cell

Since recombinant protein preparations of IRAK3 produce cGMP, it was of interest to see if such activity could be detected in cells. Transiently transfected HEK 293T cells (methods described in chapter 2 section 2.8.3 and 2.8.5) were used to test for cellular IRAK3 GC activity. HEK 293T cells do not contain IRAK3 (Du et al., 2014; Kobayashi et al., 2002; Wesche et al., 1999) therefore they were transiently transfected with IRAK3-GFP or IRAK4-GFP and induced with either Mn^{2+} or Mg^{2+} 24 hours post transfection. Cells transfected at similar efficiencies were lysed and tested for cGMP production using the GE cGMP immunoassay kit (chapter 2 section 2.6.2; section 2.8.5.1). In the presence of Mn^{2+}, IRAK3 transfected cells produced about two fold more cGMP compared to the GFP and IRAK4-GFP transfected cells. Mn^{2+} appears to be the preferred inducer for cGMP production, as in the presence of Mg^{2+} less cGMP was seen in all cells (Figure 5.6). Despite similarities at the GC site between IRAK3 and IRAK4, IRAK4 lacks specific residues in the GC centre, most importantly at residue 14 in the GC centre. The arginine is replaced by a proline, as discussed in chapter 4 section 4.3.1. IRAK4 only generated amounts of cGMP similar to the basal level of the GFP transfected cells control (Figure 5.6) and has no ability to produce cGMP. Together these results indicate that residues such as arginine at position 14 of the GC centre are important to generate cGMP within cells.

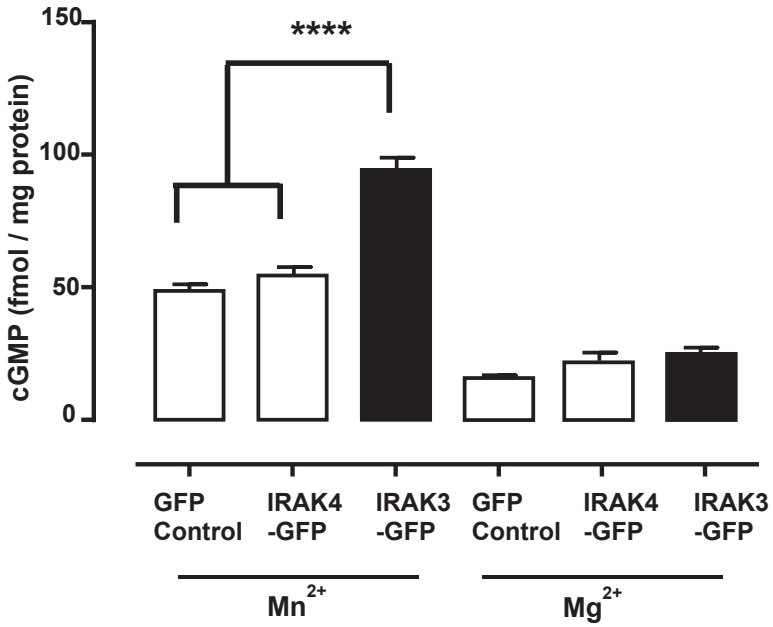

Figure 5.6 cGMP production by IRAK proteins in HEK 293T cells

HEK 293T cells were transiently transfected with GFP only, IRAK3-GFP and IRAK4-GFP vectors. Cells were induced with either Mn^{2+} or Mg^{2+} 24 hours post transfection. Cells transfected at similar efficiencies were lysed and assayed for cGMP production using the Amersham GE cGMP kit. Cells transfected with the IRAK3 gene produced significantly more cGMP when compared to the basal level of the GFP only transfected control cells and the GFP tagged IRAK4 transfected cells. IRAK3 cGMP production prefers Mn^{2+} over Mg^{2+} as a cofactor ((n=6-8, ANOVA P<0.0001) Tukey's multiple comparison test).

5.3 CONCLUSION

Using quantitative cGMP detection techniques including ELISA and mass spectrometry we show that recombinant IRAK3 protein is capable of producing cGMP at levels comparable to those produced by our positive controls the recombinant cytoplasmic domain of PSKR1 and BRI1. In separate experiments, calcium was shown to have a negative although not significant effect on cGMP production by IRAK3. This is unlike that seen with the cytoplasmic domain of PSKR1 which had shown an increase in cGMP production with an increase in calcium concentration (Muleya et al., 2014). Therefore, IRAK3 may be affected by calcium in a different manner to that seen with the transmembrane kinase GCs. Mutation of specific residues in the GC centre can effect cGMP production of IRAK3. Mutation of the arginine 372 of the GC centre to leucine abolished cGMP production confirming predictions of previous docking studies presented in chapter 4. HEK 293T cells transiently transfected with IRAK3 produced significantly higher levels of cGMP when compared to transfected control cells confirming GC activity of IRAK3. Importantly the inability of IRAK4 to generate cGMP is perhaps due to the fact that in this same position, the arginine is replaced by a proline. Together this data confirms that human IRAK3 is capable of cGMP production and that this novel class of GCs exists in other systems in addition to the previously recognized plant GCs. Further investigation is necessary to observe and explain the critical residues involved in the GC catalytic activity in IRAK3. Also it is important to learn if the GC activity of IRAK3 affects its regulation and downstream signalling in the innate immune signalling cascade, which is the focus of chapter 6.

CHAPTER 6

THE EFFECT OF THE IRAK3 GC CENTRE ON THE IMMUNE SIGNALLING CASCADE

CHAPTER 6

THE EFFECT OF THE IRAK3 GC CENTRE ON THE IMMUNE SIGNALLING CASCADE

6.1 INTRODUCTION

The IRAK family play an important part in the innate immune signalling cascade, by mediating IL-1 and TLR signalling. Humans have been shown to have 10 different forms of TLR, TLR1–TLR10, while mice have 12 forms, TLR1–TLR9 and TLR11–TLR13. TLR4 was the first member to be functionally characterised. TLR4 responds to bacterial lipopolysaccharides (LPS) through a multireceptor complex, which consists of a LPS-binding protein (LBP), cluster of differentiation 14 (CD14) (Zanoni et al., 2011) and myeloid differentiation protein-2 (MD-2) (Brubaker et al., 2015; Medzhitov et al., 1997; Pålsson-McDermott and O'Neill, 2004; Shimazu et al., 1999). All the TLRs except for TLR3 use the adapter protein MyD88 for signal transduction. The adaptor protein MyD88 interacts with the IRAKs through the IRAK N-terminal death domain (Gay et al., 2014; Lin et al., 2010; Wesche et al., 1997) (See Chapter 1 Figure 1.4 A). The activation of TLR4 causes MyD88 oligomerization to form a large signalling platform called a myddosome (Brubaker et al., 2015; Lin et al., 2010). A myddosome complex is an arrangement of the signalling molecules/adapters components into a MyD88–IRAK4–IRAK2/1 complex (Lin et al., 2010). Binding of the myddosome complex to the TNF receptor-associated factor 6 (TRAF-6) causes the dissociation from the TLR. This goes on to form a complex with TGF-beta activated kinase 1/MAP3K7 binding protein 2/3 (TAB2/3) and TGF-beta activated kinase 1 (TAK-1). Downstream phosphorylation and ubiquitination of nuclear factor of kappa light polypeptide gene enhancer in B-cells inhibitor, alpha (IκBα), activates NFκB and

transcription of inflammatory genes, this pathway is referred to as the TAK1-dependent pathway (Takeuchi and Akira, 2010). Alternatively, IRAK2 hyperphosphorylation post complex dissociation triggers a specific IRAK2 dependent mRNA stabilisation and translational control of pro-inflammatory mediators to also promote the inflammatory response (Chapter 1, Figure 1.5) (Wan et al., 2009; Zhou et al., 2013).

As a negative feedback protein in the innate immune signalling pathway, IRAK3 is stimulated to prevent excessive inflammation upon TLR activation. IRAK3 is thought to function by preventing the dissociation of the MyD88–IRAK4–IRAK2/1 myddosome complex, thereby inhibiting downstream signalling (Kobayashi et al., 2002; Zhou et al., 2013). Du et al. (2014) highlighted the importance of the myddosome complex formation through the IRAK death domain association. It was shown that a single mutation of the amino acid tryptophan 74 to alanine in the death domain of IRAK3 completely abolished IRAK3 function (Du et al., 2014).

Zhou et al. (2013) showed that in TLR7 signalling, IRAK3 is able to interact with MyD88–IRAK4, to form an IRAK3 myddosome, this exposed an alternative regulatory pathway through a TLR7-induced second wave NFκB activation. This pathway is uncoupled from post-transcriptional regulation, therefore it produces inhibitory molecules like suppressor of cytokine signalling 1 (SOCS1) and SH-2 containing inositol 5' polyphosphatase 1 (SHIP1), causing an overall inhibitory effect on the inflammatory response (Zhou et al., 2013).

Nitric oxide (NO) is a multifunctional free radical important in the modulation of inflammation. It is the main activator of sGC by binding directly to the heme group (see Chapter 1, Figure 1.2), and activating cGMP production (Lucas 2000). Nitric oxide (presumably via cGMP) was shown to inhibit TLR and IL-1 receptor-dependent signal transduction through the inhibition of the molecular interaction between IRAK-1 and TRAF-6, therefore inhibiting IRAK1 activity and downstream NFκB activation in mouse

macrophages and dendritic cells (Xiong et al., 2004). Del Fresno et al. (2004) showed that in the presence of NO, IRAK3 may be involved in the inhibition of IRAK1 activity. NO-induced IRAK3 mRNA and protein expression in human monocytes, however, this effect was shown to be dependent on the early NO-induced release of the cytokine TNFα by the monocytic cells (del Fresno et al., 2004).

Several studies have shown that increased levels of cGMP alone or in the presence of NO has an anti-inflammatory effect in different cell types and systems. A study on mouse hepatic inflammation investigated mice on a high fat diet that exhibited increased inflammation. This increased inflammatory effect, however, was not seen in mice treated with a phosphodiesterase inhibitor, sildenafil, which allows accumulation of cGMP by preventing its degradation. Sildenafil has a vasodilatory effect and is clinically used for erectile dysfunction and pulmonary artery hypertension (Singh, 2010; Tateya et al., 2011). Further work in the group had shown that in mouse peritoneal macrophages, diminished NFκB signalling was observed upon LPS stimulation in the presence of 10 μmol/L of either NO or 8-bromo-cGMP alone (Tateya et al., 2011). In an earlier study by the same group, human microvascular endothelial cells were used to look at vascular inflammation and insulin resistance. Stimulation of human microvascular endothelial cells by LPS in the presence of 50 μmol/L of 8-bromo-cGMP, decreased phosphorylated IκBα, signifying an anti-inflammatory effect (Rizzo et al., 2010). An earlier study, however, using an electrophoretic mobility shift assay, showed that nitric oxide inhibits NFκB activity in TNFα-induced human vascular endothelial cells. This same effect was not as pronounced when a cGMP analogue 8-bromo-cGMP (1 mM) was used, therefore it was proposed that nitric oxide may not act through a soluble guanylate cyclase in these cells when induced with TNFα (Peng et al., 1995).

A separate study looking at neuroinflammation and demyelination disorders used mice treated with sildenafil. Treated mice showed reduced inflammation compared to the untreated mice in several cell types investigated, including the neuronal resident cells,

astrocytes and microglial cells, as well as macrophages and leukocytes. Inflammatory factors explored included adhesion proteins and IL-2. Drugs targeting the NO-sGC-cGMP pathway are proving to be beneficial in the treatment of neuroinflammatory/demyelinating disorders like multiple sclerosis (Raposo et al., 2014). This was also emphasised by another study, clearly showing anti-inflammatory and neuroprotective effects of sildenafil on mice. Although the exact mechanism by which sildenafil causes the anti-inflammatory effect is unknown. Nunes et al. (2015) suggested that it may function by modulating endothelial nitric oxide synthase (eNOS)/NO signalling and hence NFκB activity, however AMP-activated protein kinase also induced by sildenafil was shown to activate eNOS/NO signalling (Nunes et al., 2015). Further studies are however necessary to understand how cGMP affects the inflammatory signalling cascade either in the presence or absence of NO. It is important to note that the effect of cGMP as an anti-inflammatory modulator is highly dependent on species as well as cell type. For instance, cGMP displayed a TNFα inducing effect in Kupffer cells in rats, the opposite was observed in mice (Harbrecht et al., 1995).

The inhibitory function of IRAK3 in the innate immune signalling cascade is of particular interest in terms of its guanylate cyclase activity. We hypothesise that the novel GC activity of IRAK3 may modulate its inhibitory functions in the innate immune response possibly through its cGMP production described in chapter 5. Therefore we aim to investigate the effect of the IRAK3 GC centre and how the cGMP produced by IRAK3 effects NFκB signalling. Furthermore, the effect of wildtype IRAK3 is compared to the IRAK3 GC mutants, IRAK3 R372>L and IRAK3 G361>L. The IRAK3 GC centre mutant R372>L showed abolished cGMP production described in chapter 5, the effect the IRAK3 R372>L mutant has on NFκB activity is of particular interest, and may aid in our understanding the role of the GC centre on NFκB signalling under TLR4 activation.

6.2 RESULTS AND DISCUSSION

6.2.1 LPS induction of HEK BLUE hTLR4 cells

Since NFκB has a key role in downstream signalling involving IRAK3, we employed an NFκB reporter system. The human embryonic kidney (HEK) BLUE hTLR4 cells stably express a secreted embryonic alkaline phosphatase (SEAP) NFκB reporter together with TLR4, CD14 and MD-2 which are essential for the LPS-TLR4 mediated response. Upon activation of the TLR4 by LPS, induction of NFκB occurs, which subsequently induces the SEAP reporter to produce alkaline phosphatase. The alkaline phosphatase released into the cell culture media causes a quantifiable change in colour of the QUANTI Blue reagent from its original pink (no LPS) to a blue colour (LPS) (Figure 6.1 A and B) (Chapter 2, Section 2.9). To check that the receptor-signalling pathway was operational, a LPS concentration response curve was generated. The change in the colour intensity by different concentration of LPS was measured quantitatively at 660 nm using the Envision plate reader (Figure 6.1 C). A significant increase in NFκB activity was observed in the presence of 0.1 ng/μl of LPS, with a maximal effect seen between 1-10 ng/μl of LPS.

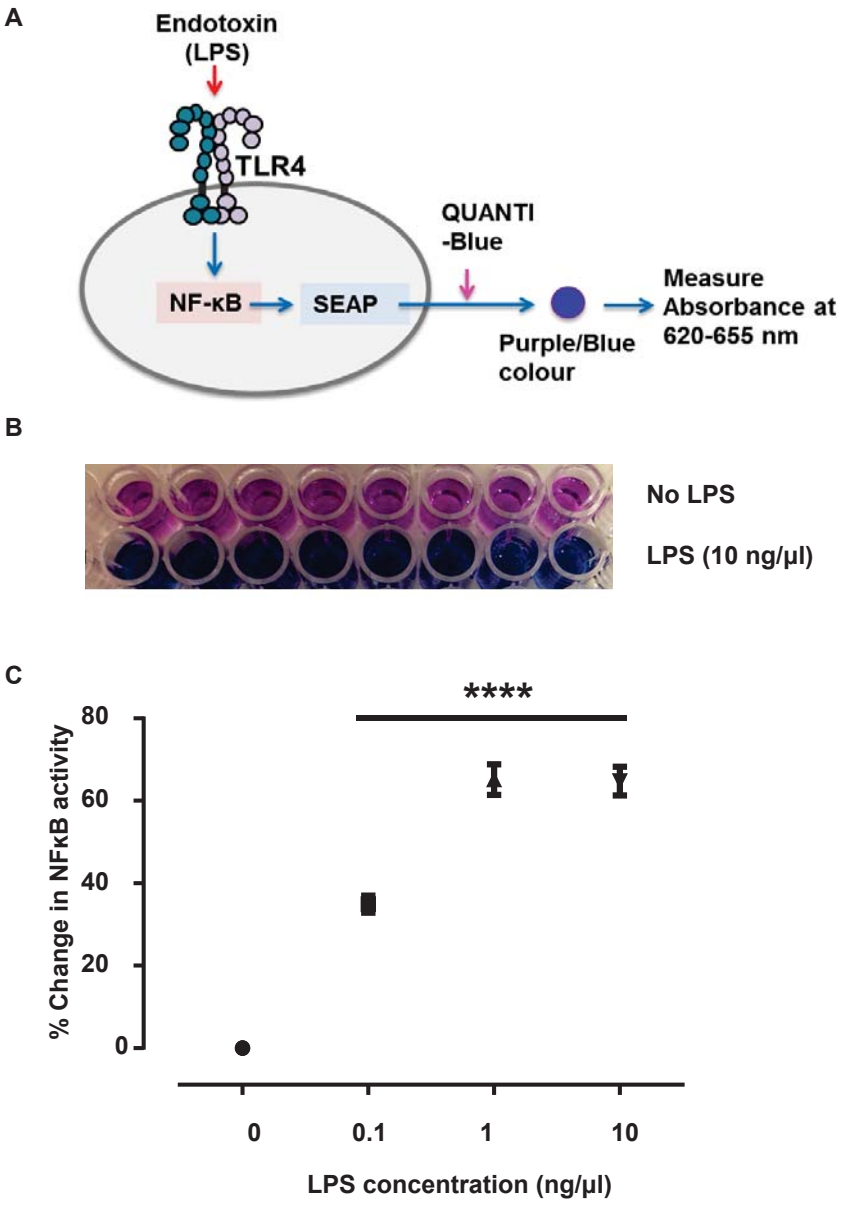

Figure 6.1 Control experiment showing NFκB activity measured after LPS induction of HEK BLUE hTLR4 cells

(A) Schematic diagram showing the Invivogen HEK BLUE hTLR4, NFκB - SEAP reporter system adapted from http://www.invivogen.com/ 01/04/17

(B) Supernatant/media taken from HEK BLUE hTLR4 cells that were not induced with LPS (negative control) remained pink and media taken from cells induced with LPS (positive controls) turned blue in the presence of QUANTI Blue reagent.

(C) HEK BLUE hTLR4 cells were induced with different concentrations of LPS or no LPS (negative control). The percent change in NFκB activity is reported in the presence of LPS compared to the non-induced cells, (n= 8, P value <0.0001 One-way ANOVA, Dunnetts multiple comparison test).

6.2.2 Induction of HEK BLUE hTLR4 cells with cGMP

To test the effect of cGMP on NFκB induction, HEK BLUE hTLR4 cells, NFκB/SEAP reporter system were used. HEK BLUE hTLR4 cells were induced with various concentrations of a cell permeable cGMP analogue, 8-bromo-cGMP. As a separate positive control, cells were induced with 10 ng/µl of LPS, NFκB activity was measured 24 hours post induction. No significant effect was observed on NFκB activity when cells where induced with 8-bromo-cGMP only, compared to the uninduced cells set at zero percent (Figure 6.2 A). Previous studies have also shown that membrane permeable cGMP alone had no effect on NFκB activation or suppression (Kim et al., 2008; Peng et al., 1995).

When 8-bromo-cGMP was added to LPS treated cells, a significant reduction in NFκB activity was seen in the presence of all concentrations of cGMP beginning at subnanomolar cGMP concentrations, this effect however was more pronounced at 0.1-10 µM (Figure 6.2 B). This result is supported by previous studies demonstrating that cell permeable cGMP has an anti-inflammatory effect (described in section 6.1). Tateya et al. (2011) showed that in the presence of 10 µM of 8-bromo-cGMP, mouse derived peritoneal macrophages and primary hepatocytes reduced NFκB signalling upon LPS induction (Tateya et al., 2011). Rizzo et al. (2010) also showed reduced NFκB signalling upon LPS Induction in human microvascular endothelial cells with 50 µM 8-bromo-cGMP (Rizzo et al., 2010).

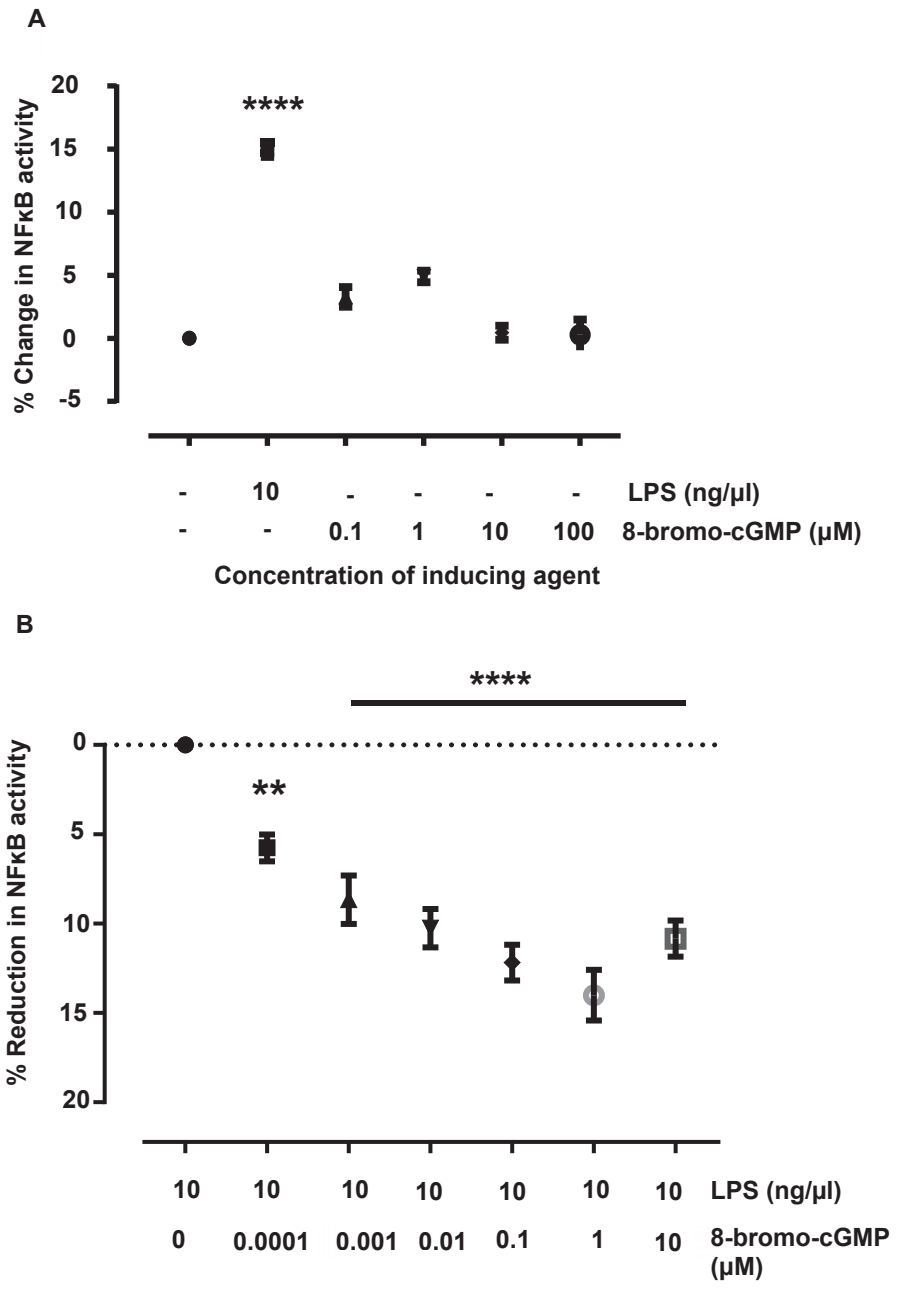

Figure 6.2 NFκB induction with membrane permeable 8-bromo-cGMP

(A) HEK BLUE hTLR4 cells were induced with increasing concentrations of 8-bromo-cGMP. Cell permeable 8-bromo-cGMP alone had no significant effect on NFκB activity. All values were compared to the uninduced control set at zero percent (n= 6-8, P value <0.0001 One-way ANOVA, Dunnetts multiple comparison test). (B) Effect of increasing concentrations of 8-bromo-cGMP on LPS induced cells. All values are compared to the 0 µM 8-bromo-cGMP concentration set at zero percent (n= 4-8, P value <0.0001 One-way ANOVA, Dunnetts multiple comparison test).

6.2.3 Effect of IRAK3 expression on HEK BLUE hTLR4 cells

To observe the effect IRAK3 may have on NFκB activation, we transiently transfected HEK BLUE hTLR4 cells with C-terminal GFP tagged IRAK3 and IRAK3 mutants. HEK BLUE hTLR4 cells do not contain IRAK3 as it is mainly found in macrophages, monocytic cells and lung epithelial cells, however HEK BLUE hTLR4 cells do contain all the other IRAKs which are known to be ubiquitously expressed (Balaci et al., 2007; Du et al., 2014; Wesche et al., 1999).

To confirm the successful transfection of our IRAK3-GFP, the confocal microscope was used to qualitatively observe GFP fluorescence (Figure 6.3 A). HEK BLUE hTLR4 cells transfected with IRAK3 significantly reduced NFκB activity post LPS induction compared to the non-transfected LPS-induced HEK BLUE hTLR4 cells (Figure 6.3 B). This confirms what is already known that IRAK3 acts a negative regulator and suppresses NFκB activation (Kobayashi et al., 2002), and also demonstrates the viability of our experimental system.

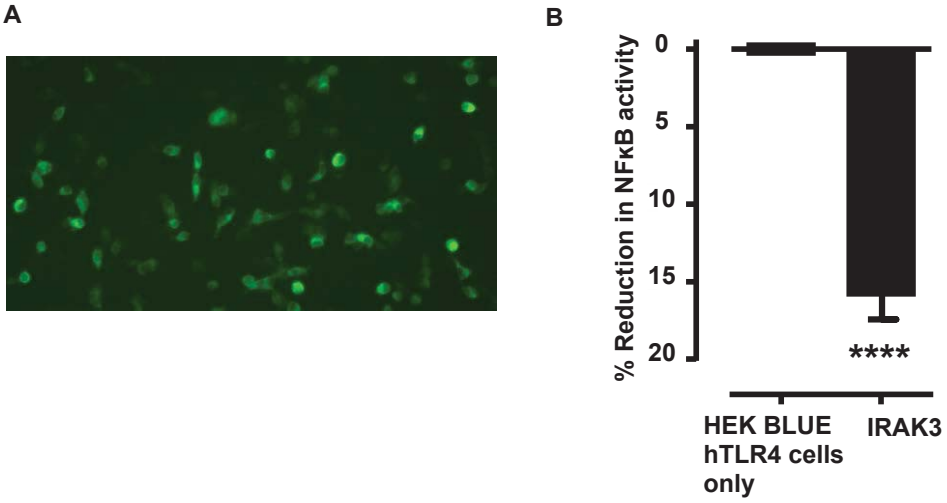

Figure 6.3 Effect of IRAK3 on NFκB activity

(A) Confocal image showing HEK BLUE hTLR4 cells transfected with the IRAK3 gene. (B) IRAK3 transfected HEK BLUE hTLR4 cells significantly reduced NFκB activity when induced with LPS compared to the non-transfected LPS-Induced cells (n= 15, Unpaired t-test P<0.0001).

6.2.4 Effect of IRAK3 mutants expression on HEK BLUE hTLR4 cells

Modelling and recombinant protein studies (Chapter 4 and 5) showed that mutations in the IRAK3 GC centre modified cGMP production. Hence the IRAK3 gene and the IRAK3 mutants S359G361>LL, G361>L and R372>L genes were prepared and expressed in HEK BLUE hTLR4 cells as described (Chapter 2 Section 2.4.2). To confirm expression of our genes of interest after transfection a quantitative reverse transcriptase PCR was done. All the transfected cells expressed IRAK3 RNA at relatively similar levels. (Figure 6.4 A).

HEK BLUE hTLR4 cells transfected with the IRAK3 G361>L mutant produced similar effects to that seen with wildtype IRAK3, therefore signifying that the G361>L mutation may not have an effect on the normal function of IRAK3.

In chapter 5 (Figure 5.5 B, section 5.2.4) it was demonstrated that the G361>L mutation in the GC centre of IRAK3 had no effect on cGMP production. The IRAK3 R372>L mutant however did not behave in the same way (Figure 6.4 B). These cells functioned as though IRAK3 was not present at all and therefore NFκB activity was not reduced. This is also supported by the data in chapter 5 where the IRAK3 R372>L mutant produced significantly less cGMP compared to wildtype IRAK3 (Section 5.2.4, figure 5.5 B). This result may implicate that residue R372 present in the GC centre is perhaps essential for proper IRAK3 function.

The IRAK3 S359G361>LL mutant did not significantly affect NFκB activity, the data produced by this mutant over several separate experiments was quite variable (Figure 6.4 B). Either a reduction in NFκB activity was observed or no overall effect was seen, although the experimental conditions were kept constant. This variability is highlighted by the larger error bar present in the graph (Figure 6.4 B). Therefore, a proper conclusion cannot be made and further investigation in terms of its effect on NFκB activity is necessary for this particular mutant.

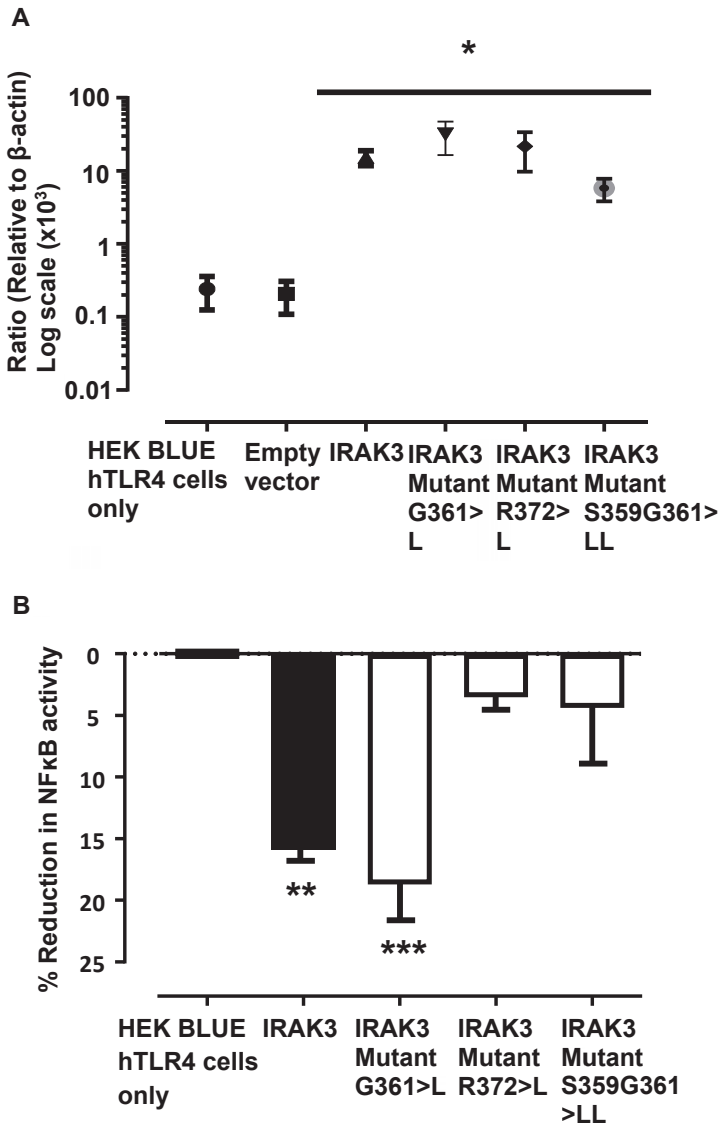

Figure 6.4 Effect of the IRAK3 mutants on NFκB activity

(A) The presence of selected IRAK3 and IRAK3 mutant genes was validated by quantitative RT-PCR after transfection into HEK BLUE hTLR4 cells (n=2-3). (B) Reduction of NFκB activity is measured after induction of the non-transfected and transfected HEK BLUE hTLR4 cells with 10 ng/μl LPS. HEK BLUE hTLR4 cells transfected with the wildtype IRAK3 reduced NFκB activity to the same level as the IRAK3 mutant G361>L when compared to the non-transfected control cells. The IRAK3 R372>L and IRAK3 S359G361>LL mutants transfected cells did not significantly reduce NFκB activity when compared to the non-transfected control cells (n=15-30, from at least 3 separate experiments, P value < 0.0001 One-way ANOVA, Dunnetts multiple comparison test).

6.2.5 Effect of cGMP on IRAK3 transfected HEK BLUE hTLR4 cells

Previous observations (Figure 6.2 A) demonstrated that cGMP alone had no effect on NFκB activity in non-transfected HEK BLUE hTLR4 cells. However when these cells were induced with LPS in the presence of cGMP, a significant suppression of NFκB activity is observed (Figure 6.2 B and Figure 6.5). IRAK3 was shown to generate cGMP (Chapter 5, section 5.2.1), and IRAK3 transfected HEK BLUE hTLR4 cells suppressed LPS-induced NFκB activity (Figure 6.3). We therefore, further explored whether the excess 8-bromo-cGMP enhanced the effect of IRAK3 on the suppression of NFκB activity. HEK BLUE hTLR4 cells transfected with IRAK3 and induced with LPS showed a reduction in NFκB activity (as previously demonstrated) when compared to the non-transfected HEK BLUE hTLR4 cells induced with LPS alone which was set at zero percent (Figure 6.5). However the IRAK3 inhibitory effect on NFκB was not augmented by a subnanomolar concentration of cell permeable 8-bromo-cGMP of 0.1 nM (Figure 6.5). The subnanomolar concentration of 0.1 nM of cell permeable 8-bromo-cGMP was primarily selected to investigate the effect of added cGMP on IRAK3 to suppress NFκB activity, higher concentrations of cell permeable cGMP may mask or overpower the effect of IRAK3 itself on NFκB activity. This subnanomolar concentration also showed a significant decrease in LPS-induced, NFκB activity (Figure 6.2 B). We show that excess cGMP does not have an additional effect on IRAK3 to reduce NFκB activity in this cell type. This effect however needs to be further explored at different cGMP concentrations, as the effect observed may be due to a concentration dependent modulating effect. Also, the HEK BLUE hTLR4 cells SEAP reporter system, may not detect NFκB activity above or below a certain threshold, therefore the system may need further validation. Alternatively, the NFκB activity reduction seen may not be due to the cGMP produced by IRAK3 alone, as other factors, such as the IRAK3 protein structure itself as well as other molecules involved in the signalling pathway may also be involved. Zhou et al. (2016) demonstrated that depending on the concentration of

the inducing agent LPS, different signalling pathways may be activated by IRAK3 to produce its anti-inflammatory response. Therefore, upon a concentration dependent induction of TLR4 with LPS, IRAK3 was shown to either activate the classical pathway to suppress NFκB activity and therefore reduce cytokine production. Or alternatively take the IRAK3 myddosome pathway where it activates NFκB to produce inflammatory inhibitors such as SOCS1 and A20 (Zhou et al., 2016). Therefore further investigation is needed to look at the IRAK3 pathway selectivity and the effect of cGMP on NFκB activity as well as downstream cytokine production.

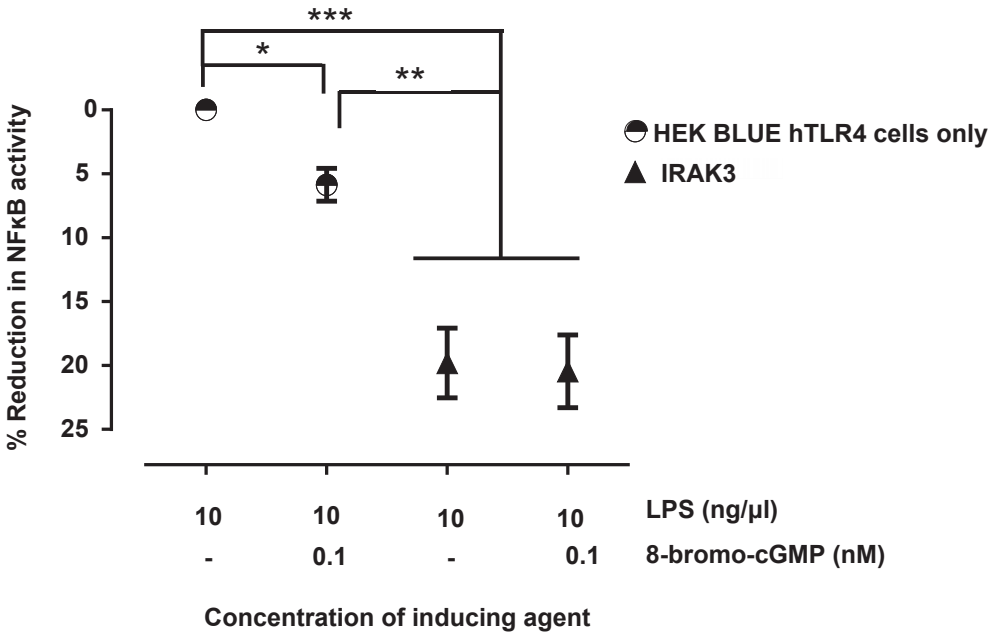

Figure 6.5 Effect of 8-bromo-cGMP on non-transfected and IRAK3 transfected HEK BLUE hTLR4 cells.

Non-transfected and wildtype IRAK3 transfected HEK BLUE hTLR4 cells are induced with 10 ng/µl of LPS, the percent reduction of NFκB activity in the presence or absence of 0.1 nM of 8- bromo-cGMP is measured. (n= 3, P value <0.0002 One-way ANOVA, Dunnetts multiple comparison test).

6.2.6 Effect of cGMP on IRAK3 R372>L mutant transfected HEK BLUE hTLR4 cells

The IRAK3 mutant R372>L does not reduce NFκB activity stimulated by LPS unlike wildtype IRAK3 (Figure 6.4 B). To see if we can reverse the negligible effect of the IRAK3 R372>L mutant on suppression of NFκB activity, the IRAK3 R372>L mutant transfected HEK BLUE hTLR4 cells were induced with increasing concentrations of cGMP after LPS induction. A significant reduction in NFκB activity is observed from 0.0001 to 1 μM cGMP, however this effect is more pronounced at 0.0001, 0.01 and 0.1 μM cGMP, possibly highlighting a concentration dependent modulating effect that may need further investigation (Figure 6.6). This suggests that cGMP has a role in NFκB suppression and may reverse the effect the IRAK3 R372>L mutation has lost, highlighting the importance of the cGMP production of IRAK3 on NFκB suppression.

Previous studies described (Section 6.1) and (Figure 6.2 B) demonstrate that cGMP alone can suppress LPS-induced NFκB activity. The suppression observed in the presence of IRAK3 R372>L and 0.1 nM cGMP however, may be due to the cGMP acting alone, highlighting the importance to undertake further studies. Investigating not only the novel catalytic activity of IRAK3 in terms of cGMP production but also the IRAK3 structure/function effect on the signalling pathway is necessary. This can aid in explaining the modulating effect the cGMP produced by IRAK3 has on the signalling pathway. Interestingly, (Figure 6.5) added cGMP did not enhance the NFκB suppression effect of IRAK3, which may explain or further complicate the effect observed with the IRAK3 R372>L mutant in the presence of cGMP. This can be investigated further through mutagenesis studies, by designing an alternative IRAK3 GC centre mutant that is catalytically inactive/ impaired cGMP production. The effect of added cGMP under similar test conditions as the IRAK3 R372>L mutant can be looked at and compared.

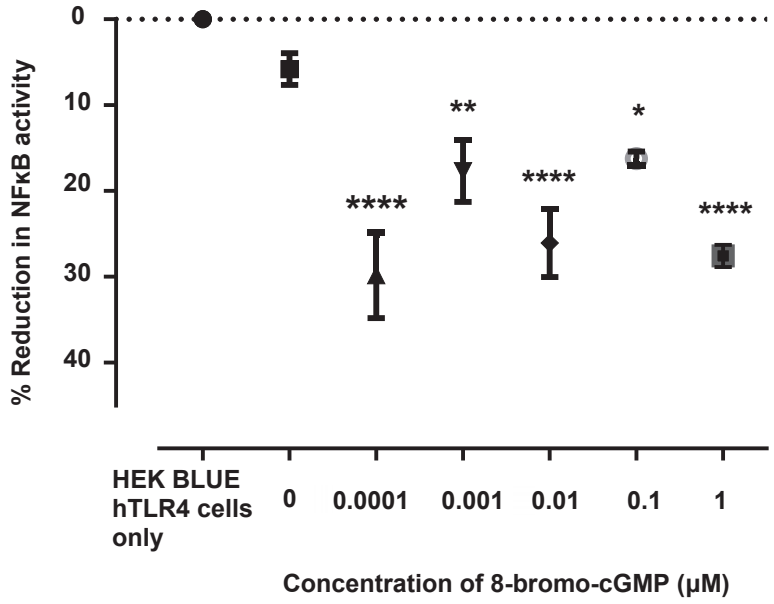

Figure 6.6 IRAK3 Mutant R372>L transfected HEK BLUE hTLR4 cells induced with 8-bromo-cGMP

Effect of increasing concentrations of membrane permeable 8-bromo-cGMP on LPS-induced IRAK3 mutant R372>L transfected cells compared to non-transfected/empty vector transfected cells, cGMP-induced cell values are compared to the cell only control value set at zero% (n= 4-8, P value <0.0001 One-way ANOVA, Dunnetts multiple comparison test).

6.3 CONCLUSION

Using HEK BLUE hTLR4 cells we were able to look at downstream signalling through NFκB activation, using a SEAP reporter. Upon LPS activation of the TLR4, a signal cascade results in activation of NFκB which induces the SEAP reporter. This activation is quantitatively measured. Induction of these cells with membrane permeable cGMP alone had no effect on NFκB activity, therefore NFκB was not effected by cGMP alone. At specific concentrations cGMP was able to significantly decrease LPS-induced NFκB activity, therefore implying that cGMP may have an anti-inflammatory effect. This effect however has previously been reported in numerous studies where increased cGMP showed an anti-inflammatory effect, described in further detail in section 6.1. IRAK3 is known to act as a negative regulator of inflammation, this can be detected through its influence on NFκB activity suppression. IRAK3 transfected HEK BLUE hTLR4 cells showed decreased LPS-induced NFκB activity, confirming its anti-inflammatory function.

IRAK3 cGMP production was abolished by mutating specific residue in the GC centre. The IRAK3 R372>L mutant had reduced cGMP production compared to wildtype IRAK3, however the IRAK3 G361>L mutation in the GC centre did not affect cGMP production. (Chapter 5, section 5.2.4, figure 5.5 B). In addition to the inability of IRAK3 R372>L mutant to produce cGMP, this mutant also did not suppress NFκB activity. This is distinct to wildtype IRAK3 and its G361>L mutant where a significant suppression of LPS-induced NFκB activity is observed. Therefore, the usual IRAK3 function to reduce NFκB activity was only abolished by the R372>L mutation. This effect however was reversed by introducing specific concentrations of cell permeable cGMP to the IRAK3 R372>L mutant transfected cells, therefore suppressing LPS-induced NFκB activity and possibly returning function to this IRAK3 mutant. These studies reinforce the role of IRAK3 to decrease or inhibit NFκB activation. However,

the ability of IRAK3 to generate cGMP appears to contribute to its effect on NFκB signalling.

Further analysis is however necessary to look at the effect specific mutations may have on the protein scaffold of IRAK3. IRAK3 is known to act as a protein scaffold as part of the myddosome complex formed in the innate immune signalling cascade. IRAK3 interacts with the other IRAK and adapter proteins through its death domain, it also interacts with TRAF6 through its C-terminal domain. Myddosome complex formation and function of IRAK3 is supressed by mutating specific residues in either the IRAK3 death domain or the C-terminal domain (Du et al. 2014 and Zhou et al. 2013), discussed in chapter 1 and chapter 4. Therefore how an inactive GC IRAK3 mutant like IRAK3 R372>L mutant or comparatively wildtype IRAK3 may affect the IRAK3 protein scaffold activity needs to be investigated. Downstream signalling can be further looked at perhaps through protein: protein binding and interaction studies, as well as downstream cytokine production. Production of different cytokines can be quantitatively measured by ELISA and PCR studies, to give us an indication of specific pathways activated by the different IRAK3 mutants.

Wildtype IRAK3 did not show further suppression of NFκB activity when membrane permeable cGMP was added. Therefore it would be of particular interest to investigate how IRAK3 precisely exerts its effect and how cGMP may contribute to its function. This can primarily be explored by preparing dose response curves to see if small amounts of added cGMP effect IRAK3-induced NFκB suppression. Further investigation is necessary however beyond that to see if the cGMP generated by IRAK3 may act as a switch between the two separate signalling pathways (Zhou et al., 2013) that IRAK3 may take in the innate immune signalling cascade.

CHAPTER 7

GENERAL DISCUSSION

CHAPTER 7

GENERAL DISCUSSION

7.1 RESEARCH FOCUS

The innate immune response is the first line of defence against invading pathogens. The immune response is initiated when particular pathogen-associated molecular patterns are sensed by TLRs or IL-1 receptors. Activated TLRs (except for TLR3) complex with myeloid differentiation primary response gene 88 (MyD88) and members of the IRAK family to form a myddosome complex (Lin et al., 2010). This causes a signalling cascade that induces the production and secretion of inflammatory mediators essential for the immune response against the invading organism. A severe uncontrolled inflammatory response is damaging, therefore; a balance is necessary. Various cellular mechanisms to suppress the innate response are present, one of these include the upregulation of IRAK3 which suppresses NFκB induction by interfering with the IRAK1, 2 and 4 signalling cascades. IRAK3 knockout mice demonstrated overproduction of pro-inflammatory cytokines, hence; were more susceptible to septic shock (Kobayashi et al., 2002). Overexpression of IRAK3 was shown to mediate and promote cancer progression by allowing a more favoured tumour microenvironment (del Fresno et al., 2005; Jain et al., 2014). The IRAK family kinase activity is considered as a potential drug target in a number of studies and is of continuous and renewed interest for cancer drug development (Rhyasen and Starczynowski, 2015). The IRAK3 expression pattern is known to be relatively tissue-restricted which can allow targeted therapy, potentially reducing the chance of off-target inflammatory related adverse effects (Rhyasen, 2016; Rhyasen and Starczynowski, 2015).

In the innate immune signalling cascade, IRAK3 upon activation can bind to IRAK2 which acts through an IRAK2 dependent pathway, preventing the dissociation of the myddosome complex. This pathway prevents mRNA stabilisation and translational control of cytokines and chemokines, therefore; reducing the inflammatory response. Alternatively, Zhou et al. (2013) showed that mouse IRAK3 can activate NFκB through a unique IRAK4/IRAK3 mediated MEKK3 dependent pathway causing transcription of inflammatory inhibitory molecules such as A20, SOCS1, IκBα and SHIP-1 (Zhou et al., 2013).

The death domain of the IRAK family is essential in the interaction of the proteins in the signalling cascade. Individuals with the single P22L mutation in the death domain of IRAK3 developed early-onset asthma (Balaci et al., 2007). Also, this mutation decreases inflammatory cytokine, IL-6 in macrophages after TLR stimulation (Du et al., 2014). Little is known of how IRAK3 selectively binds to either myddosome complex activating the different signalling pathways.

This study has shown that IRAK3 is a novel GC *in vitro*, and furthermore that it produces cGMP in different systems. The GC activity of IRAK3 was demonstrated to contribute to IRAK3s inhibitory function in the innate immune response.

7.2 DESIGN OF A cGMP DETECTION METHOD

cGMP is an important second messenger in the signalling cascade, therefore it is useful to examine new ways to detect cGMP in signalling pathways. Our work involves the screening of novel guanylate cyclases and the detection of cGMP is important in these studies. Current ELISA cGMP detection kits are relatively expensive in cost and time. Alternatives such as mass spectrometry are of limited use when detecting time course changes occurring in dynamic cell samples. A suitable reporter system is needed for bacterial and mammalian cells that can measure alterations in downstream gene expression following changes in intracellular levels of cyclic nucleotides. To

address this need, we developed a non-invasive cGMP sensitive reporter system screening tool to determine guanylate cyclase activity in cells. This tool can be used to measure changes in GC activity in cells transfected with genes like IRAK3.

We designed a promoter system containing the oligopeptide transporter X (OPTX) promoter fused to a luciferase gene. OPTX is responsive to cGMP in plant cells, and surprisingly the OPTX promoter fragment contains the mammalian cGMP response element. To enhance the promoter response to cGMP, we inserted three additional cGMP response elements into the OPTX promoter. A third construct was designed containing five gibberellic acid response elements (GARE) that we postulated may be upregulated by cGMP since GA treatment raises cGMP levels in plant cells. The constructs were tested for response to cGMP and cAMP in BL21-AI as a representative of bacterial cells and HEK 293T cells representing mammalian cells. Significantly increased luciferase activity occurred in bacterial cells transformed with the OPTX promoter system in response to both cAMP and cGMP. Bacteria may not differentiate between cAMP and cGMP as to date only the α-proteabacteria are known to synthesise cGMP. Since a receptor for cGMP has not been found, a physiological role of cGMP may be improbable in *E. coli* like BL21-AI (Linder, 2010). A drawback of bacterial protein expression is that some proteins cannot be expressed due to instability and inclusion bodies, therefore their use can bring out some constraints in addition to the benefits of bacterial expression.

Bacteria co-transformed with the OPTX promoter system and the soluble cytoplasmic domain of PSKR1 a novel guanylate cyclase had enhanced luciferase activity following induction of PSKR1 expression, highlighting an increase in cGMP production. This system was also used to test the GC activity of another novel GC, neurotrophic receptor tyrosine kinase 1 (NTRK1) which also confirmed a significant increase in luciferase activity, representing an increase in cGMP production. We have shown that the OPTX promoter system presents an effective screening tool that can be used in

bacteria to screen recombinant proteins for guanylate cyclase activity as increases in intracellular cGMP levels result in altered gene transcription and luciferase activity. This system proved to be an effective method for screening GC, however, is limited to proteins that are stable in bacteria and thus was not appropriate for IRAK3 which is quite unstable *in vitro*, however using this system we were able to detect cGMP generated by both PSKR1 and NTRK1.

7.3 MAJOR FINDINGS

7.3.1 IRAK3 structure

A crystal structure of IRAK3 is not yet available, therefore to explain the possible IRAK3 structure and how the GC centre may fit in, an IRAK3 homology model was prepared based on the IRAK4 kinase domain (2NRU) crystal structure. The IRAK family including IRAK4 are serine/threonine kinases. However, the IRAK4 crystal structure showed a phosphate ligand interaction pattern in the activation loop similar to that of tyrosine kinases (Wang et al., 2006). The homology model of IRAK3 gives an insight into the predicted GC centre within the kinase domain. The model was used to dock the expected substrate GTP, using knowledge from experiments on novel GC models, PSKR1 and BRI1. Wong et al., demonstrated through GTP docking that the arginine in position number 14 of the GC centre is predicted to stabilise the transition state from GTP to cGMP (Wong and Gehring, 2013; Wong et al., 2015). Further, the mutation of residue number three in the GC centre of BRI1, and the mutation of residues number one, as well as residue number three in the GC centre of PSKR1, was predicted to interfere with GTP docking, making it unsuitable for catalysis (Wong and Gehring, 2013). The computational method is not indicative of catalytic activity but it can highlight experimental targets for subsequent *in vitro* and *in vivo* experiments, therefore it can serve as a rapid screening approach (Wong et al., 2015). The mutation of residue number 14, arginine 372, in the GC centre of the IRAK3 homology model to

leucine (R372>L) showed reduced GTP interactions upon GTP docking, therefore it is predicted that the R372>L mutation will not allow for the fitting interaction for catalysis and cGMP production.

Alignment of the homology models of the kinase domains of IRAK3 and the kinase domain of the model novel GC, PSKR1; revealed structural similarities between the kinase domains of these two proteins. Also, the surface models of PSKR1 and IRAK3 indicate that the GC centre is associated with a small groove leading into the kinase cleft. However, the groove can change or alter with other possible configurations in the structure, specifically, the KHLW loop was considered, which is adjacent to the GC centre section. This loop was shown to be quite dynamic, as it can adopt one of many conformations all with equal energy (Freihat et al., 2014). Possibly through homodimerization or heterodimerization of the IRAK3 protein, a catalytic or binding site can be developed. IRAK3 interacts through its death domain as part of the myddosome complex with the other IRAKs and adapter proteins. IRAK3 also interacts with TRAF6 through its C-terminal domain (Du et al., 2014). The transient nature of these interactions may be an important regulatory component of the GC response. Therefore the dimerization and interactions of IRAK3 with the signalling components and the anticipated subsequent GC activity needs further investigation.

7.3.2 GC activity of IRAK3

The uniformity in the structural topology of PSKR1 and IRAK3 may explain the observed GC activity of IRAK3 (Freihat et al., 2014). Using the available cGMP detection techniques including ELISA and mass spectrometry, we showed that recombinant IRAK3 protein is capable of producing cGMP. These levels were comparable to those produced by our positive controls PSKR1 and BRI1. Increased concentrations of calcium non-significantly, albeit it, slightly decreased, cGMP production of recombinant IRAK3 protein *in vitro*. This is opposite to what is seen with

PSKR1. Calcium acts as a switch in PSKR1 between kinase and GC activity, where increasing calcium was shown to increase cGMP production (Muleya et al., 2014). Calcium is known to have a negative effect on classical soluble GCs, where it decreases the stimulatory effects of NO, therefore reducing cGMP production (Lucas et al., 2000). The effect of calcium on IRAK3 GC activity needs to be further considered by also investigating the effect calcium may have on IRAK3 in the innate immune signalling cascade.

In separate experiments, HEK 293T cells transfected with IRAK3 produced significantly higher levels of cGMP when compared to control transfected cells confirming cGMP production and GC activity of IRAK3 in cell. Further studies are however needed, where cGMP production and GC activity can be measured *in vivo* upon induction of IRAK3 in the innate immune signalling cascade in separate immune cells.

Particular amino acids were mutated in the IRAK3 GC centre based on the IRAK3 homology model results. Mutation of residue 3 in the GC centre to leucine, produced IRAK3 G361>L mutant. Recombinant IRAK3 G361>L mutant protein produced significant amounts of cGMP *in vitro* comparable to the amount produced by recombinant wildtype IRAK3 protein. Therefore, mutation of residue 3 in the GC centre (Glycine 361 in IRAK3) to leucine had no effect on cGMP production, however, how the mutation may affect the protein otherwise, is still unknown and requires further studies. Mutation of arginine, residue number 14 in the GC centre of IRAK3 to leucine produced the IRAK3 R372>L mutant. Upon GTP docking, predicted GTP interactions were reduced in the IRAK3 homology model, and this finding was emphasised by the experimental *in vitro* cGMP data. The recombinant IRAK3 R372>L mutant protein had significantly reduced GC activity compared to wildtype recombinant IRAK3 protein. This finding highlight the importance of residue number 14 (Arginine 372 in IRAK3) in the GC centre for cGMP production.

7.3.3 Effect of GC activity of IRAK3 on innate immune signalling

The impact of the cGMP produced by IRAK3 in the signalling cascade is still unknown, however, this study has made some insights to guide further investigations. We have shown that by mutating specific residues in the GC centre, namely R372>L, caused alterations in cGMP production as modelled in chapter 4 and experimentally described in chapter 5. Overexpression of IRAK3 and the IRAK3 GC mutants in HEK BLUE hTLR4 cells showed differential effects on NFκB activity. HEK BLUE hTLR4 cells transfected with wildtype IRAK3 constantly shows a significant decrease in NFκB activity as expected and demonstrated in previous studies.

HEK BLUE hTLR4 cells transfected with the IRAK3 R372>L mutant did not suppress NFκB activity upon LPS induction. The mutant has therefore lost its inhibitory function, and cannot suppress NFκB activity, unlike wildtype IRAK3. Interestingly, the recombinant IRAK3 R372>L protein also had reduced cGMP production *in vitro*. This observation may also link in the possible importance of cGMP in the IRAK3 signalling pathway. Surprisingly, in the presence of membrane permeable 8-bromo-cGMP however, cells transfected with the IRAK3 R372>L mutant were able to suppress LPS-induced NFκB activity, therefore returning the function of IRAK3 as an immunosuppressant. It has been demonstrated by several groups that cGMP alone as well as nitric oxide has an anti-inflammatory effect and inhibits activation of IRAK proteins and downstream innate immune signalling. (Rizzo et al., 2010; Tateya et al., 2011; Xiong et al., 2004). We have also demonstrated using the HEK BLUE hTLR4 cells that cGMP alone suppresses LPS-induced NFκB activity. The effect of the membrane permeable 8-bromo-cGMP on the IRAK3 R372>L mutant occurs at subnanomolar concentrations. Further reduction of LPS-induced NFκB activity is observed in the presence of a subnanomolar concentration of 8-bromo-cGMP when combined with IRAK3 R372>L mutant, compared to cGMP alone. However further research is needed to see the contribution of cGMP to the suppression of the LPS-

induced NFκB activity. The cGMP generated by the IRAK3 protein may be involved in its inhibitory function and pathway selectivity. cGMP may modulate the binding and/or activity of nearby interacting proteins involved in the signalling pathway. These findings are providing insight into the hidden functions of IRAK3 and may assist in explaining the selectivity and functionality of IRAK3 in the inflammatory signalling cascade.

7.4 CONCLUDING REMARKS AND FUTURE DIRECTIONS

There are many opportunities for further investigations and potential therapeutic targeting of IRAK3. A lot is still unknown about the selectivity and specificity of IRAK3 and the mechanisms by which the molecule binds to and acts on the TLR-NFκB pathway are still largely unknown. There is great potential for using IRAK3 as a platform for targeted therapy (Rhyasen and Starczynowski, 2015). Downregulation of IRAK3 in tumour-associated immune cells may allow for tumour recognition so it is proposed that IRAK3 is a potential anti-cancer target (Norton et al., 2011). Additionally, further research may focus on IRAK3 as a potential diagnostic and prognostic marker for obesity and associated disorders (Hulsmans et al., 2012). In addition, the fact that IRAK3 is a pseudokinase is very interesting, several studies are now looking at pseudokinases as an unexplored family of therapeutic targets. IRAK3 was shown to be capable of binding the generic kinase inhibitors DAP and VI16832. This indicates the presence of a potentially intact ATP-binding cleft, which can allow for binding of nucleotides at affinities possibly below the sensitivity of the assays used in the studies (Murphy et al., 2014).

Within the innate immune response, the control of IRAK3 function is seen as having an important role in regulating inflammatory responses (Biswas et al., 2011). Studies considering IRAK3 involvement in different disease and inflammatory conditions demonstrated either an upregulation or downregulation of IRAK3 expression to combat disease progression like in some cancers. However, in conditions such as in sepsis,

alternative pathways are also apparent. Sepsis is a severe, life-threatening infection resulting in organ dysfunction, causing major defects in host innate and adaptive immunity. How the immune system responds to sepsis is controversial, some studies pinpoint it to excessive inflammation, other studies, however, have demonstrated it to be due to immunosuppression (Hotchkiss et al., 2013). This is in part due to the initial immune response producing a cytokine storm followed by immunosuppression due to endotoxin tolerance and increased susceptibility to alternative infections. Under sepsis conditions, hypoxia inducible factor-1α (HIF1α) acted as a strategic mediator of monocyte re-programming and was shown to induce IRAK3 expression in an act to reduce excessive inflammation. IRAK3 induction by HIF1α led to the conversion of the functional plasticity of blood monocytes from a pro-inflammatory to an endotoxin-tolerant phenotype (Shalova et al., 2015).

A study using polymicrobial induced sepsis model mice showed that treatment with sildenafil, which functions to accumulate cGMP, reduced inflammation in the earlier stages of sepsis, therefore producing a protective effect against lung and kidney damage (Deng et al., 2015). The immunological and molecular basis of the sepsis stages is under continuous investigation. Human post-mortem analysis showed that secondary microbial infections with opportunistic bacteria and fungi were observed in immunosuppressed states (Hotchkiss et al., 2013; Otto et al., 2011; Zhao et al., 2016).

An earlier study by Xiong et al. (2011) on endotoxin tolerance in THP1 cells and human monocytes, identified an increase in the inhibitory cytokine A20 and a decrease in LPS-mediated receptor recruitment through the classical myddosome complex formation. This study possibly set the scene and supports the later studies by Zhou et al. (2013) that identified an alternative pathway through IRAK3 myddosome complex formation. This pathway is known to cause MEKK3-dependent NFκB activation and the production of inhibitory molecules like A20 and SOCS1 causing immunosuppression (Xiong et al., 2011; Zhou et al., 2013). The effect of IRAK3 on endotoxin tolerance and

its function in the different stages of sepsis tells us that IRAK3 can be mediated to take an alternative pathway depending on the stage of infection, however, the molecular regulation and possible mediator still remains to be investigated. How cGMP causes the anti-inflammatory effect in the early stages of sepsis, although demonstrated using sildenafil in mouse studies is still unclear and human clinical studies are also required.

IRAK3 myddosome formation was shown to depend on the concentration of the inducing agent (LPS), representing the degree of infection. High dose infections activate a separate pathway to low dose infections. Low dose LPS induction was demonstrated to activate IRAK3 myddosome complex formation, therefore inducing a MEKK3-dependent NFκB activation to produce inhibitory molecules (Zhou et al., 2016). This all highlights the importance of IRAK3 as a mediator in the innate immune signalling pathway and how IRAK3 is controlled is essential to guide our understanding of the signalling cascade in the different disease states.

Experimentally we have demonstrated that the GC activity of IRAK3 contributes to its inhibitory function in the innate immune response by looking at its effect on LPS-induced NFκB activity. The exact effect of the GC activity of IRAK3 on the signalling cascade is however still largely unclear and further evaluation is needed. Future directions are aimed at *in vivo* and further in cell studies on the GC function and activity of IRAK3 in the innate immune signalling cascade. By looking at downstream mediators such as TNFα and IL-6 and the inhibitory molecules A20 and SOCS-1 of the alternative MEKK3-dependent pathway we can possibly identify the signalling pathway taken by IRAK3 under variable conditions. Factors such as cGMP production of IRAK3 can be investigated through further mutagenesis studies.

Binding studies are necessary to look at possible dimerization of IRAK3 in the signalling pathways which may be necessary to form a more distinct GC pocket to catalyse the formation of cGMP. However, IRAK3 interacts with several other adapter

proteins as well as the IRAK proteins. Therefore, through binding studies, GC activity needs to be tested throughout the different interactions observed in the immune signalling pathway. Possible interactions need to be explored to demonstrate the essential interaction to induce cGMP production.

How the GC activity may selectively guide the interactions between IRAK3 and the other signalling proteins to take one signalling pathway over the alternate pathways forms a fundamental research question. This can be verified by comparing the non-cGMP producing IRAK3 GC mutant interactions to the known interactions of wildtype IRAK3 previously demonstrated in literature and tested under similar conditions. NFκB activity, as well as downstream cytokine production from the alternative pathways, needs to be considered to further guide our understanding of the specificity of IRAK3 in the signalling cascade and how the GC centre influences or mediates its function through its cGMP production.

The effect of calcium on the GC activity of IRAK3 can also be tested, it is known that calcium modulates classical soluble and transmembrane GC activity. Experimentally we have demonstrated that recombinant IRAK3 proteins had slightly reduced cGMP production in the presence of calcium, however it was not significant. Further investigation into the effect of calcium on IRAK3s GC activity is nevertheless necessary in cells and possibly other systems. This can be achieved by looking for changes in downstream pathway activation in the presence and absence of calcium. Changes in cGMP production also needs to be measured upon calcium induction in the different systems. The effects observed can also be compared with non-cGMP producing IRAK3 GC mutants to demonstrate that the cGMP produced is by IRAK3 itself not the basal levels produced by the other guanylate cyclases present in the cells.

To look at the GC activity of IRAK3 in macrophages, CRISPR can be employed to remove or mutate the GC centre, cGMP production can be measured after

mutagenesis to confirm that GC activity has been abolished when compared to wildtype or non-mutated cells. Incorporating the IRAK3 R372>L mutation through CRISPR can guide future IRAK3 GC centre mutagenesis studies, as the IRAK3 R372>L mutant was demonstrated to produce very little to no cGMP *in vitro*. Therefore the effect the GC activity has on IRAK3 signalling using the GC mutant downstream cytokine signalling data can be explored by comparing it to wildtype IRAK3 signalling in cell and further *in vivo* work. The effect cGMP has on the selectivity and function of IRAK3 can be looked at in a more ideal system using CRISPR, without the need for overexpression of the gene in high expressing cells. Possibly giving us a more detailed look at closer to normal innate immune conditions. The pathways can be looked at using cytokine ELISA assays as well as further quantitative reverse transcriptase PCR analysis to measure and quantitatively identify different cytokines to look at the signalling pathways activated by IRAK3.

Understanding how this novel GC function impacts on the anti-inflammatory effect of IRAK3 is likely to be important when targeting this protein in different disease states. Such knowledge would also add to the limited understanding currently available for IRAK3s structure-function relationship.

REFERENCES

Andric, S.A., Kostic, T.S., Tomić, M., Koshimizu, T.-a., and Stojilkovic, S.S. (2001). Dependence of Soluble Guanylyl Cyclase Activity on Calcium Signaling in Pituitary Cells. The Journal of Biological Chemistry *276*, 844-849.

Arnold, W.P., Mittal, C.K., Katsuki, S., and Murad, F. (1977). Nitric oxide activates guanylate cyclase and increases guanosine 3':5'-cyclic monophosphate levels in various tissue preparations. Proceedings of the National Academy of Sciences of the United States of America *74*, 3203-3207.

Assmann, S.M. (1995). Cyclic AMP as a Second Messenger in Higher Plants (Status and Future Prospects). Plant Physiology *108*, 885-889.

Bachiller, P.R., Cornog, K.H., Kato, R., Buys, E.S., and Roberts, J.D. (2013). Soluble guanylate cyclase modulates alveolarization in the newborn lung. American Journal of Physiology - Lung Cellular and Molecular Physiology *305*, L569-L581.

Balaci, L., Spada, M.C., Olla, N., Sole, G., Loddo, L., Anedda, F., Naitza, S., Zuncheddu, M.A., Maschio, A., Altea, D.*, et al.* (2007). IRAK-M is involved in the pathogenesis of early-onset persistent asthma. Americal Journal of Human Genetics *80*, 1103-1114.

Barnett, C.F., and Machado, R.F. (2006). Sildenafil in the treatment of pulmonary hypertension. Vascular Health and Risk Management *2*, 411-422.

Bastian, R., Dawe, A., Meier, S., Ludidi, N., Bajic, V.B., and Gehring, C. (2010). Gibberellic acid and cGMP-dependent transcriptional regulation in *Arabidopsis thaliana*. Plant Signaling & Behavior *5*, 224-232.

Bender, A.T., and Beavo, J.A. (2006). Cyclic nucleotide phosphodiesterases: molecular regulation to clinical use. Pharmacological Reviews *58*, 488-520.

Bers, D.M., Patton, C.W., and Nuccitelli, R. (2010). A practical guide to the preparation of Ca(2+) buffers. Methods in Cell Biology *99*, 1-26.

Biswas, K., Shenoy, A., Dutta, A., and Visweswariah, S. (2009). The Evolution of Guanylyl Cyclases as Multidomain Proteins: Conserved Features of Kinase-Cyclase Domain Fusions. Journal of Molecular Evolution *68*, 587-602.

Bocanera, L.V., Martinetto, H., Flawia, M.M., and Pisarev, M.A. (1999). Partial characterization of guanylyl cyclase activity in calf thyroid. Endocrine Research *25*, 215-228.

Bojar, D., Martinez, J., Santiago, J., Rybin, V., Bayliss, R., and Hothorn, M. (2014). Crystal structures of the phosphorylated BRI1 kinase domain and implications for brassinosteroid signal initiation. Plant Journal *78*, 31 - 43.

Brubaker, S.W., Bonham, K.S., Zanoni, I., and Kagan, J.C. (2015). Innate immune pattern recognition: a cell biological perspective. Annual Review of Immunology *33*, 257-290.

Calderon-Villalobos, L.I.A., Kuhnle, C., Li, H., Rosso, M., Weisshaar, B., and Schwechheimer, C. (2006). LucTrap vectors are tools to generate luciferase fusions for the quantification of transcript and protein abundance in vivo. Plant Physiology *141*, 3-14.

Cao, Z., Henzel, W.J., and Gao, X. (1996). IRAK: a kinase associated with the interleukin-1 receptor. Science *271*, 1128-1131.

Carlton, V.E., Ireland, J.S., Useche, F., and Faham, M. (2006). Functional single nucleotide polymorphism-based association studies. Human Genomics *2*, 391-402.

Chen, C.N., Watson, G., and Zhao, L. (2013). Cyclic guanosine monophosphate signalling pathway in pulmonary arterial hypertension. Vascular Pharmacology *58*, 211-218.

Chester, M., Seedorf, G., Tourneux, P., Gien, J., Tseng, N., Grover, T., Wright, J., Stasch, J.-P., and Abman, S.H. (2011). Cinaciguat, a soluble guanylate cyclase activator, augments cGMP after oxidative stress and causes pulmonary vasodilation in neonatal pulmonary hypertension. American Journal of Physiology - Lung Cellular and Molecular Physiology *301*, L755-L764.

Chinkers, M., and Garbers, D.L. (1989). The protein kinase domain of the ANP receptor is required for signaling. Science *245*, 1392-1394.

Chinkers, M., and Wilson, E.M. (1992). Ligand-independent oligomerization of natriuretic peptide receptors. Identification of heteromeric receptors and a dominant negative mutant. The Journal of Biological Chemistry *267*, 18589-18597.

Cushing, L., Stochaj, W., Siegel, M., Czerwinski, R., Dower, K., Wright, Q., Hirschfield, M., Casanova, J.L., Picard, C., Puel, A.*, et al.* (2014). Interleukin 1/Toll-like receptor-induced autophosphorylation activates interleukin 1 receptor-associated kinase 4 and controls cytokine induction in a cell type-specific manner. The Journal of Biological Chemistry *289*, 10865-10875.

De Carvalho, D.D., Sharma, S., You, J.S., Su, S.F., Taberlay, P.C., Kelly, T.K., Yang, X., Liang, G., and Jones, P.A. (2012). DNA methylation screening identifies driver epigenetic events of cancer cell survival. Cancer Cell *21*, 655-667.

del Fresno, C., Gomez-Garcia, L., Caveda, L., Escoll, P., Arnalich, F., Zamora, R., and Lopez-Collazo, E. (2004). Nitric oxide activates the expression of IRAK-M via the release of TNF-alpha in human monocytes. Nitric Oxide *10*, 213-220.

del Fresno, C., Otero, K., Gomez-Garcia, L., Gonzalez-Leon, M.C., Soler-Ranger, L., Fuentes-Prior, P., Escoll, P., Baos, R., Caveda, L., Garcia, F.*, et al.* (2005). Tumor cells deactivate human monocytes by up-regulating IL-1 receptor associated kinase-M expression via CD44 and TLR4. The Journal of Immunology *174*, 3032-3040.

Deng, M., Loughran, P.A., Zhang, L., Scott, M.J., and Billiar, T.R. (2015). Shedding of the tumor necrosis factor (TNF) receptor from the surface of hepatocytes during sepsis limits inflammation through cGMP signaling. Science Signaling *8*, ra11-ra11.

Derbyshire, E.R., and Marletta, M.A. (2012). Structure and regulation of soluble guanylate cyclase. Annual Review of Biochemistry *81*, 533-559.

Deshmane, S.P., Parkinson, S.J., Crupper, S.S., Robertson, D.C., Schulz, S., and Waldman, S.A. (1997). Cytoplasmic domains mediate the ligand-induced affinity shift of guanylyl cyclase C. Biochemistry *36*, 12921-12929.

Dossang, A.C.G., Motshwene, P.G., Yang, Y., Symmons, M.F., Bryant, C.E., Borman, S., George, J., Weber, A.N.R., and Gay, N.J. (2016). The N-terminal loop of IRAK-4 death domain regulates ordered assembly of the Myddosome signalling scaffold. Scientific Reports *6*, 37267.

Du, J., Nicolaes, G.A., Kruijswijk, D., Versloot, M., van der Poll, T., and van 't Veer, C. (2014). The structure function of the death domain of human IRAK-M. Cell Communication and Signaling *12*, 1-19.

Duda, T., Pertzev, A., Makino, C.L., and Sharma, R.K. (2016). Bicarbonate and Ca(2+) Sensing Modulators Activate Photoreceptor ROS-GC1 Synergistically. Frontiers in Molecular Neuroscience *9*, 5.

Duda, T., Yadav, P., and Sharma, R.K. (2011). Allosteric Modification, the Primary ATP Activation Mechanism of Atrial Natriuretic Factor Receptor Guanylate Cyclase. Biochemistry *50*, 1213-1225.

Endicott, J.A., Noble, M.E., and Johnson, L.N. (2012). The structural basis for control of eukaryotic protein kinases. Annual Review of Biochemistry *81*, 587-613.

Fimia, G.M., and Sassone-Corsi, P. (2001). Cyclic AMP signalling. Journal of Cell Science *114*, 1971-1972.

Flannery, S., and Bowie, A.G. (2010). The interleukin-1 receptor-associated kinases: critical regulators of innate immune signalling. Biochemical Pharmacology *80*, 1981-1991.

Freihat, L., Muleya, V., Manallack, D.T., Wheeler, J.I., and Irving, H.R. (2014). Comparison of moonlighting guanylate cyclases: roles in signal direction? Biochemical Society Transactions *42*, 1773-1779.

Gasteiger, E., Hoogland, C., Gattiker, A., Duvaud, S.e., Wilkins, M.R., Appel, R.D., and Bairoch, A. (2005). Protein Identification and Analysis Tools on the ExPASy Server. In The Proteomics Protocols Handbook, J.M. Walker, ed. (Totowa, NJ: Humana Press), pp. 571-607.

Gay, N.J., Symmons, M.F., Gangloff, M., and Bryant, C.E. (2014). Assembly and localization of Toll-like receptor signalling complexes. Nature Reviews Immunolgy *14*, 546-558.

Gehring, C. (2010). Adenyl cyclases and cAMP in plant signaling - past and present. Cell Communication and Signaling *8*, 15.

Gerzer, R., Bohme, E., Hofmann, F., and Schultz, G. (1981). Soluble guanylate cyclase purified from bovine lung contains heme and copper. FEBS Letters *132*, 71-74.

Gerzer, R., Hamet, P., Ross, A.H., Lawson, J.A., and Hardman, J.G. (1983). Calcium-induced release from platelet membranes of fatty acids that modulate soluble guanylate cyclase. The Journal of Pharmacology and Experimental Therapeutics *226*, 180-186.

Gheorghiade, M., Marti, C.N., Sabbah, H.N., Roessig, L., Greene, S.J., Bohm, M., Burnett, J.C., Campia, U., Cleland, J.G., Collins, S.P.*, et al.* (2013). Soluble guanylate cyclase: a potential therapeutic target for heart failure. Heart Failure Reviews *18*, 123-134.

Gomelsky, M. (2011). cAMP, c-di-GMP, c-di-AMP and now cGMP: bacteria use them all! Molecular Microbiology *79*, 562-565.

Gosu, V., Basith, S., Durai, P., and Choi, S. (2012). Molecular evolution and structural features of IRAK family members. PLoS One *7*, e49771.

Gross, I., and Durner, J. (2016). In Search of Enzymes with a Role in 3′, 5′-Cyclic Guanosine Monophosphate Metabolism in Plants. Frontiers in Plant Science *7*.

Gukovskaya, A.S., Gukovsky, S., and Pandol, S.J. (2000). Endoplasmic reticulum Ca^{2+}-ATPase inhibitors stimulate membrane guanylate cyclase in pancreatic acinar cells. American Journal of Physiology - Cell Physiology *278*, C363-C371.

Gustafsson, Å.B., and Brunton, L.L. (2002). Attenuation of cAMP accumulation in adult rat cardiac fibroblasts by IL-1β and NO: role of cGMP-stimulated PDE2. American Journal of Physiology - Cell Physiology *283*, C463-C471.

Hammarén, H.M., Virtanen, A.T., and Silvennoinen, O. (2016). Nucleotide-binding mechanisms in pseudokinases. Bioscience Reports *36*.

Hanna, M.H., Nowicki, J.J., and Fatone, M.A. (1984). Extracellular cyclic AMP during development of the cellular slime mold Polysphondylium violaceum: comparison of accumulation in the wild type and an aggregation-defective mutant. Journal of Bacteriology *157*, 345-349.

Harbrecht, B.G., Wang, S.C., Simmons, R.L., and Billiar, T.R. (1995). Cyclic GMP and guanylate cyclase mediate lipopolysaccharide-induced Kupffer cell tumor necrosis factor-alpha synthesis. Journal of Leukocyte Biology *57*, 297-302.

Hardison, R.C. (2003). Comparative Genomics. PLoS Biology *1*, e58.

Hardman, J.G., and Sutherland, E.W. (1969). Guanyl Cyclase, an Enzyme Catalyzing the Formation of Guanosine 3',5'-Monophosphate from Guanosine Triphosphate. The Journal of Biological Chemistry *244*, 6363-6370.

Hotchkiss, R.S., Monneret, G., and Payen, D. (2013). Sepsis-induced immunosuppression: from cellular dysfunctions to immunotherapy. Nature Reviews, Immunology *13*, 862-874.

Hubbard, L.L., and Moore, B.B. (2010). IRAK-M regulation and function in host defense and immune homeostasis. Infectious Disease Reports *2*.

Hulsmans, M., Geeraert, B., De Keyzer, D., Mertens, A., Lannoo, M., Vanaudenaerde, B., Hoylaerts, M., Benhabiles, N., Tsatsanis, C., Mathieu, C*., et al.* (2012). Interleukin-1 receptor-associated kinase-3 is a key inhibitor of inflammation in obesity and metabolic syndrome. PLoS One *7*, e30414.

Hum, D., Besnard, S., Sanchez, R., Devost, D., Gossard, F., Hamet, P., and Tremblay, J. (2004). Characterization of a cGMP-response element in the guanylyl cyclase/natriuretic peptide receptor A gene promoter. Hypertension *43*, 1270-1278.

Humbert, P., Niroomand, F., Fischer, G., Mayer, B., Koesling, D., Hinsch, K.D., Gausepohl, H., Frank, R., Schultz, G., and Bohme, E. (1990). Purification of soluble guanylyl cyclase from bovine lung by a new immunoaffinity chromatographic method. European Journal of Biochemistry *190*, 273-278.

Indo, Y. (2012). Nerve growth factor and the physiology of pain: lessons from congenital insensitivity to pain with anhidrosis. Clinical Genetics *82*, 341-350.

Irving, H.R., Kwezi, L., Wheeler, J., and Gehring, C. (2012). Moonlighting kinases with guanylate cyclase activity can tune regulatory signal networks. Plant Signaling & Behavior *7*, 201-204.

Isner, J.-C., and Maathius, F.J.M. (2011). Measurement of cellular cGMP in plant cells and tissues using the endogenous fluorescent reporter FlincG. Plant Journal *65*, 329-334.

Isner, J.-C., Nühse, T., and Maathius, F.J.M. (2012). The cyclic nucleotide cGMP is involved in plant hormone signalling and alters phosphorylaton of Arabidopsis thaliana root proteins. Journal of Experimental Botany *63*, 3199-3205

Iyer, L.M., Anantharaman, V., and Aravind, L. (2003). Ancient conserved domains shared by animal soluble guanylyl cyclases and bacterial signaling proteins. BMC Genomics *4*, 5.

Jain, A., Kaczanowska, S., and Davila, E. (2014). IL-1 Receptor-Associated Kinase Signaling and Its Role in Inflammation, Cancer Progression, and Therapy Resistance. Frontiers in Immunology *5*, 553.

Johannessen, C.M., Boehm, J.S., Kim, S.Y., Thomas, S.R., Wardwell, L., Johnson, L.A., Emery, C.M., Stransky, N., Cogdill, A.P., Barretina, J*., et al.* (2010). COT drives resistance to RAF inhibition through MAP kinase pathway reactivation. Nature *468*, 968-972.

Kawagoe, T., Sato, S., Matsushita, K., Kato, H., Matsui, K., Kumagai, Y., Saitoh, T., Kawai, T., Takeuchi, O., and Akira, S. (2008). Sequential control of Toll-like receptor-dependent responses by IRAK1 and IRAK2. Nature Immunology *9*, 684-691.

Kesselring, R., Glaesner, J., Hiergeist, A., Naschberger, E., Neumann, H., Brunner, S.M., Wege, A.K., Seebauer, C., Kohl, G., Merkl, S.*, et al.* (2016). IRAK-M Expression in Tumor Cells Supports Colorectal Cancer Progression through Reduction of Antimicrobial Defense and Stabilization of STAT3. Cancer Cell *29*, 684-696.

Kim, M.-Y., Park, J.-H., Mo, J.-S., Ann, E.-J., Han, S.-O., Baek, S.-H., Kim, K.-J., Im, S.-Y., Park, J.-W., Choi, E.-J.*, et al.* (2008). Downregulation by lipopolysaccharide of Notch signaling, via nitric oxide. Journal of Cell Science *121*, 1466-1476.

Klaiber, M., Dankworth, B., Kruse, M., Hartmann, M., Nikolaev, V.O., Yang, R.-B., Völker, K., Gaßner, B., Oberwinkler, H., Feil, R.*, et al.* (2011). A cardiac pathway of cyclic GMP-independent signaling of guanylyl cyclase A, the receptor for atrial natriuretic peptide. Proceedings of the National Academy of Sciences of the United States of America *108*, 18500-18505.

Kobayashi, K., Hernandez, L.D., Galan, J.E., Janeway, C.A., Medzhitov, R., and Flavell, R.A. (2002). IRAK-M is a negative regulator of toll-like receptor signaling. Cell *110*, 191-202.

Koller, K.J., de Sauvage, F.J., Lowe, D.G., and Goeddel, D.V. (1992). Conservation of the kinaselike regulatory domain is essential for activation of the natriuretic peptide receptor guanylyl cyclases. Molecular and Cellular Biology *12*, 2581-2590.

Kuglstatter, A., Villasenor, A.G., Shaw, D., Lee, S.W., Tsing, S., Niu, L., Song, K.W., Barnett, J.W., and Browner, M.F. (2007). Cutting Edge: IL-1 receptor-associated kinase 4 structures reveal novel features and multiple conformations. The Journal of Immunology *178*, 2641-2645.

Kwezi, L., Meier, S., Mungur, L., Ruzvidzo, O., Irving, H., and Gehring, C. (2007). The Arabidopsis thaliana Brassinosteroid Receptor (AtBRI1) Contains a Domain that Functions as a Guanylyl Cyclase In Vitro. PLoS One *2*, e449.

Kwezi, L., Ruzvidzo, O., Wheeler, J.I., Govender, K., Iacuone, S., Thompson, P.E., Gehring, C., and Irving, H.R. (2011). The phytosulfokine (PSK) receptor is capable of guanylate cyclase activity and enabling cyclic GMP-dependant signaling in plants. The Journal of Biological Chemistry *286*, 22580-22588.

Lech, M., Kantner, C., Kulkarni, O.P., Ryu, M., Vlasova, E., Heesemann, J., Anz, D., Endres, S., Kobayashi, K.S., Flavell, R.A.*, et al.* (2011). Interleukin-1 receptor-associated kinase-M suppresses systemic lupus erythematosus. Annals of the Rheumatic Diseases *70*, 2207-2217.

Lek, M., Karczewski, K., Minikel, E., Samocha, K., Banks, E., Fennell, T., O'Donnell-Luria, A., Ware, J., Hill, A., Cummings, B.*, et al.* (2015). Analysis of protein-coding genetic variation in 60,706 humans. BioRxiv.

Lemtiri-Chlieh, F., Thomas, L., Marondedze, C., Irving, H., and Gehring, C. (2011). Cyclic nucleotides and nucleotide cyclases in plant stress responses. In Abiotic Stress Response in Plants - Physiological, Biochemical and Genetic Perspectives, A. Shanker, and B. Venkateswarlu, eds. (http://www.intechopen.com/articles/show/title/cyclic-nucleotides-and-nucleotide-cyclases-in-plant-stress-responses: InTech - Open Access Publisher), pp. 137-182.

Levine, S.N., Steiner, A.L., Earp, H.S., and Meissner, G. (1979). Particulate guanylate cyclase of skeletal muscle: effects of Ca2+ and other divalent cations on enzyme activity. Biochimica et Biophysica acta *566*, 171-182.

Li, S., Strelow, A., Fontana, E.J., and Wesche, H. (2002). IRAK-4: a novel member of the IRAK family with the properties of an IRAK-kinase. Proceedings of the National Academy of Sciences of the United States of America *99*, 5567-5572.

Li, S., Wang, L., Berman, M., Kong, Y.Y., and Dorf, M.E. (2011). Mapping a dynamic innate immunity protein interaction network regulating type I interferon production. Immunity *35*, 426-440.

Lin, S.C., Lo, Y.C., and Wu, H. (2010). Helical assembly in the MyD88-IRAK4-IRAK2 complex in TLR/IL-1R signalling. Nature *465*, 885-U882.

Linder, J.U. (2010). cGMP production in bacteria. Molecular Cell Biochemistry *334*, 215-219.

Lucas, K.A., Pitari, G.M., Kazerounian, S., Ruiz-Stewart, I., Park, J., Schulz, S., Chepenik, K.P., and Waldman, S.A. (2000). Guanylyl cyclases and signaling by cyclic GMP. Pharmacological Reviews *52*, 375-414.

Ludidi, N., and Gehring, C. (2003). Identification of a novel protein with guanylyl cyclase activity in Arabidopsis thaliana. The Journal of Biological Chemistry *278*, 6490-6494.

Lye, E., Mirtsos, C., Suzuki, N., Suzuki, S., and Yeh, W.C. (2004). The role of interleukin 1 receptor-associated kinase-4 (IRAK-4) kinase activity in IRAK-4-mediated signaling. The Journal of Biological Chemistry *279*, 40653-40658.

Lyn-Kew, K., Rich, E., Zeng, X., Wen, H., Kunkel, S.L., Newstead, M.W., Bhan, U., and Standiford, T.J. (2010). IRAK-M regulates chromatin remodeling in lung macrophages during experimental sepsis. PLoS One *5*, e11145.

Maathius, F.J.M. (2006). cGMP modulates gene transcription and cation transport in Arabidopsis roots. Plant Journal *45*, 700-711.

Marden, J.N., Dong, Q., Roychowdhury, S., Berleman, J.E., and Bauer, C.E. (2011). Cyclic GMP controls Rhodospirillum centenum cyst development. Molecular Microbiology *79*, 600-615.

Marondedze, C., Wong, A., Groen, A., Serrano, N., Jankovic, B., Lilley, K., Gehring, C., and Thomas, L. (2015). Exploring the Arabidopsis Proteome: Influence of Protein Solubilization Buffers on Proteome Coverage. International Journal of Molecular Sciences *16*, 857-870.

Martel, G., Hamet, P., and Tremblay, J. (2010). GREBP, a cGMP-response element-binding protein repressing the transcription of natriuretic peptide receptor 1 (NPR1/GCA). The Journal of Biological Chemistry *285*, 20926-20939.

Medzhitov, R., Preston-Hurlburt, P., and Janeway, C.A. (1997). A human homologue of the Drosophila Toll protein signals activation of adaptive immunity. Nature *388*, 394-397.

Meier, S., Ruzvidzo, O., Morse, M., Donaldson, L., Kwezi, L., and Gehring, C. (2010). The Arabidopsis Wall Associated Kinase-Like 10 Gene Encodes a Functional Guanylyl Cyclase and Is Co-Expressed with Pathogen Defense Related Genes. PLoS One *5*, e8904.

Misono, K.S. (2011). Natriuretic peptides and their receptors. FEBS Journal *278*, 1791-1791.

Miyata, M., Lee, J.-Y., Susuki-Miyata, S., Wang, W.Y., Xu, H., Kai, H., Kobayashi, K.S., Flavell, R.A., and Li, J.-D. (2015). Glucocorticoids suppress inflammation via the upregulation of negative regulator IRAK-M. Nature Communications *6*, 6062.

Muleya, V., Marondedze, C., Wheeler, J.I., Thomas, L., Mok, Y.F., Griffin, M.D., Manallack, D.T., Kwezi, L., Lilley, K.S., Gehring, C.*, et al.* (2016). Phosphorylation of the dimeric cytoplasmic domain of the phytosulfokine receptor, PSKR1. The Biochemical Journal.

Muleya, V., Wheeler, J., Ruzvidzo, O., Freihat, L., Manallack, D., Gehring, C., and Irving, H. (2014). Calcium is the switch in the moonlighting dual function of the ligand-activated receptor kinase phytosulfokine receptor 1. Cell Communication and Signaling *12*, 60.

Murphy, James M., Zhang, Q., Young, Samuel N., Reese, Michael L., Bailey, Fiona P., Eyers, Patrick A., Ungureanu, D., Hammaren, H., Silvennoinen, O., Varghese, Leila N*., et al.* (2014). A robust methodology to subclassify pseudokinases based on their nucleotide-binding properties. The Biochemical Journal *457*, 323-334.

Murthy, K.S. (2008). Inhibitory Phosphorylation of Soluble Guanylyl Cyclase by Muscarinic m2 Receptors via Gβγ-Dependent Activation of c-Src Kinase. Journal of Pharmacology and Experimental Therapeutics *325*, 183-189.

Nausch, L.W., Ledoux, J., Bonev, A.D., Nelson, M.T., and Dostmann, W.R. (2009). Differential patterning of cGMP in vascular smooth muscle cells revealed by single GFP-linked biosensors. Proceedings of the National Academy of Sciences of the United States of America *105*, 365-370.

Newton, R.P., and Smith, C.J. (2004). Cyclic nucleotides. Phytochemistry *65*, 2423-2437.

Niino, Y., Hotta, K., and Oka, K. (2010). Blue fluorescent cGMP sensor for multiparameter fluorescence imaging. PLoS One *5*, e9164.

Nolen, B., Taylor, S., and Ghosh, G. (2004). Regulation of Protein Kinases. Molecular Cell *15*, 661-675.

Norton, J.T., Hayashi, T., Crain, B., Corr, M., and Carson, D.A. (2011). Role of IL-1 receptor-associated kinase-M (IRAK-M) in priming of immune and inflammatory responses by nitrogen bisphosphonates. Proceedings of the National Academy of Sciences of the United States of America *108*, 11163-11168.

Nunes, A.K., Raposo, C., Rocha, S.W., Barbosa, K.P., Luna, R.L., da Cruz-Hofling, M.A., and Peixoto, C.A. (2015). Involvement of AMPK, IKbetaalpha-NFkappaB and eNOS in the sildenafil anti-inflammatory mechanism in a demyelination model. Brain Research *1627*, 119-133.

Okano, I., miyazato, M., and Kangawa, K. (2011). A guanosine 3',5'-cyclic monophosphate (cGMP) reporter system based on the G-kinase/CREB/CRE signal transduction pathway. Biochemical and Biophysical Research Communications *407*, 236-241.

Otto, G.P., Sossdorf, M., Claus, R.A., Rodel, J., Menge, K., Reinhart, K., Bauer, M., and Riedemann, N.C. (2011). The late phase of sepsis is characterized by an increased microbiological burden and death rate. Critical Care *15*, R183.

Padh, H., and Brenner, M. (1984). Studies of the guanylate cyclase of the social amoeba Dictyostelium discoideum. Archives of Biochemistry and Biophysics *229*, 73-80.

Pålsson-McDermott, E.M., and O'Neill, L.A.J. (2004). Signal transduction by the lipopolysaccharide receptor, Toll-like receptor-4. Immunology *113*, 153-162.

Pauls, E., Nanda, S.K., Smith, H., Toth, R., Arthur, J.S.C., and Cohen, P. (2013). Two Phases of Inflammatory Mediator Production Defined by the Study of IRAK2 and IRAK1 Knock-in Mice. The Journal of Immunology *191*, 2717-2730.

Peng, H.B., Libby, P., and Liao, J.K. (1995). Induction and stabilization of I kappa B alpha by nitric oxide mediates inhibition of NF-kappa B. The Journal of Biological Chemistry *270*, 14214-14219.

Penson, S.P., Schuurink, R.C., Fath, A., Gubler, F., Jacobsen, J.V., and Jones, R.L. (1996). cGMP is required for gibberellic acid-induced gene expression in barley aleurone layer. Plant Cell *8*, 2325-2333.

Pino-Yanes, M., Ma, S.F., Sun, X., Tejera, P., Corrales, A., Blanco, J., Perez-Mendez, L., Espinosa, E., Muriel, A., Blanch, L*., et al.* (2011). Interleukin-1 receptor-associated kinase 3

gene associates with susceptibility to acute lung injury. American Journal of Respiratory Cell and Molecular Biology *45*, 740-745.

Potter, L.R. (2011a). Guanylyl cyclase structure, function and regulation. Cellular Signalling *23*, 1921-1926.

Potter, L.R. (2011b). Regulation and therapeutic targeting of peptide-activated receptor guanylyl cyclases. Pharmacology and Therapeutics *130*, 71-82.

Potter, L.R., Abbey-Hosch, S., and Dickey, D.M. (2006). Natriuretic peptides, their receptors, and cyclic guanosine monophosphate-dependent signaling functions. Endocrine Reviews *27*, 47-72.

Potter, L.R., and Hunter, T. (2001). Guanylyl cyclase-linked natriuretic peptide receptors: structure and regulation. The Journal of Biological Chemistry *276*, 6057-6060.

Qi, Z., Verma, R., Gehring, C., Yamaguchi, Y., Zhao, Y., Ryan, C.A., and Berkowitz, G.A. (2010). Ca2+ signaling by plant Arabidopsis thaliana Pep peptides depends on AtPepR1, a receptor with guanylyl cyclase activity, and cGMP-activated Ca2+ channels. Proceedings of the National Academy of Sciences of the United States of America *107*, 21193-21198.

Qiu, Y., Ogawa, H., Miyagi, M., and Misono, K.S. (2004). Constitutive Activation and Uncoupling of the Atrial Natriuretic Peptide Receptor by Mutations at the Dimer Interface. The Journal of Biological Chemistry *279*, 6115-6123.

Raposo, C., Luna, R.L., Nunes, A.K., Thome, R., and Peixoto, C.A. (2014). Role of iNOS-NO-cGMP signaling in modulation of inflammatory and myelination processes. Brain Research Bulletin *104*, 60-73.

Rauch, A., Leipelt, M., Russwurm, M., and Steegborn, C. (2008). Crystal structure of guanylyl cyclase Cya2. Proceedings of the National Academy of Sciences of the United States of America *105*, 15720-15725.

Rhyasen, G. (2016). An Immuno-Oncology Target You've (Probably) Never Heard of – Releasing the Brakes on the Innate Immune System. BLOG: ONCOLOGY DISCOVERY *https://oncologydiscovery.com/2016/08/22/an-immuno-oncology-target-youve-probably-never-heard-of-releasing-the-brakes-on-the-innate-immune-system/*.

Rhyasen, G.W., and Starczynowski, D.T. (2015). IRAK signalling in cancer. British Journal of Cancer *112*, 232-237.

Rizzo, N.O., Maloney, E., Pham, M., Luttrell, I., Wessells, H., Tateya, S., Daum, G., Handa, P., Schwartz, M.W., and Kim, F. (2010). Reduced NO-cGMP Signaling Contributes to Vascular Inflammation and Insulin Resistance Induced by High-Fat Feeding. Arteriosclerosis, Thrombosis, and Vascular Biology *30*, 758-765.

Rosati, O., and Martin, M.U. (2002). Identification and characterization of murine IRAK-M. Biochemical and Biophysical Research Communications *293*, 1472-1477.

Saha, S., Biswas, K.H., Kondapalli, C., Isloor, N., and Visweswariah, S.S. (2009). The linker region in receptor guanylyl cyclases is a key regulatory module: mutational analysis of guanylyl cyclase C. The Journal of Biological Chemistry *284*, 27135-27145.

Schaap, P. (2005). Guanylyl cyclases across the tree of life. Frontiers in Biosciences *10*, 1485-1489.

Schlossmann, J., and Schinner, E. (2012). cGMP becomes a drug target. Naunyn-Schmiedeberg's Archives of Pharmacology.

Schultz, G., Böhme, E., and Munske, K. (1969). Guanyl cyclase. Determination of enzyme activity. Life Sciences *8*, 1323-1332.

Shalova, Irina N., Lim, Jyue Y., Chittezhath, M., Zinkernagel, Annelies S., Beasley, F., Hernández-Jiménez, E., Toledano, V., Cubillos-Zapata, C., Rapisarda, A., Chen, J.*, et al.* (2015). Human Monocytes Undergo Functional Re-programming during Sepsis Mediated by Hypoxia-Inducible Factor-1α. Immunity *42*, 484-498.

Shimazu, R., Akashi, S., Ogata, H., Nagai, Y., Fukudome, K., Miyake, K., and Kimoto, M. (1999). MD-2, a Molecule that Confers Lipopolysaccharide Responsiveness on Toll-like Receptor 4. The Journal of Experimental Medicine *189*, 1777-1782.

Singh, T.P. (2010). Clinical use of sildenafil in pulmonary artery hypertension. Expert Review of Respiratory Medicine *4*, 13-19.

Spangler, C.M., Wilhelm, B., Burhenne, H., Rauch, K., Seifert, R., and Kaever, V. (2009). Sensitive assay for the detection of cyclic nucleotides by mass spectrometry. BioMed Central Pharmacology *9*, P66-P66.

Standiford, T.J., Kuick, R., Bhan, U., Chen, J., Newstead, M., and Keshamouni, V.G. (2011). TGF-beta-induced IRAK-M expression in tumor-associated macrophages regulates lung tumor growth. Oncogene *30*, 2475-2484.

Sun, J., Li, N., Oh, K.S., Dutta, B., Vayttaden, S.J., Lin, B., Ebert, T.S., De Nardo, D., Davis, J., Bagirzadeh, R.*, et al.* (2016). Comprehensive RNAi-based screening of human and mouse TLR pathways identifies species-specific preferences in signaling protein use. Science Signaling *9*, ra3.

Szmidt-Jaworska, A., Jaworski, K., Pawelek, A., and Kocewicz, J. (2009). Molecular cloning and characterization of a guanylyl cyclase, PNGC-1, involved in light signaling in Pharbitis nil. Journal of Plant Growth Regulation *28*, 367-380.

Takeuchi, O., and Akira, S. (2010). Pattern recognition receptors and inflammation. Cell *140*, 805-820.

Tan, Q., Majewska-Szczepanik, M., Zhang, X., Szczepanik, M., Zhou, Z., Wong, F.S., and Wen, L. (2014). IRAK-M deficiency promotes the development of type 1 diabetes in NOD mice. Diabetes *63*, 2761-2775.

Tateya, S., Rizzo, N.O., Handa, P., Cheng, A.M., Morgan-Stevenson, V., Daum, G., Clowes, A.W., Morton, G.J., Schwartz, M.W., and Kim, F. (2011). Endothelial NO/cGMP/VASP Signaling Attenuates Kupffer Cell Activation and Hepatic Insulin Resistance Induced by High-Fat Feeding. Diabetes *60*, 2792-2801.

Taylor, S.S., Keshwani, M.M., Steichen, J.M., and Kornev, A.P. (2012). Evolution of the eukaryotic protein kinases as dynamic molecular switches. Philosophical Transactions of the Royal Society of London Series B, Biological sciences *367*, 2517-2528.

van der Windt, G.J., Blok, D.C., Hoogerwerf, J.J., Lammers, A.J., de Vos, A.F., Van't Veer, C., Florquin, S., Kobayashi, K.S., Flavell, R.A., and van der Poll, T. (2012). Interleukin 1 receptor-associated kinase m impairs host defense during pneumococcal pneumonia. The Journal of Infectious Diseases *205*, 1849-1857.

Veltman, D.M., Roelofs, J., Engel, R., Visser, A.J.W.G., and Van Haastert, P.J.M. (2005). Activation of Soluble Guanylyl Cyclase at the Leading Edge during Dictyostelium Chemotaxis. Molecular Biology of the Cell *16*, 976-983.

Villar, J., Cabrera, N.E., Casula, M., Flores, C., Valladares, F., Diaz-Flores, L., Muros, M., Slutsky, A.S., and Kacmarek, R.M. (2010). Mechanical ventilation modulates TLR4 and IRAK-3 in a non-infectious, ventilator-induced lung injury model. Respiratory Research *11*, 27.

Waldman, S.A., and Murad, F. (1988). Biochemical mechanisms underlying vascular smooth muscle relaxation: the guanylate cyclase-cyclic GMP system. Journal of Cardiovascular Pharmacology *12 Suppl 5*, S115-118.

Wan, Y., Xiao, H., Affolter, J., Kim, T.W., Bulek, K., Chaudhuri, S., Carlson, D., Hamilton, T., Mazumder, B., Stark, G.R.*, et al.* (2009). Interleukin-1 receptor-associated kinase 2 is critical for lipopolysaccharide-mediated post-transcriptional control. The Journal of Biological Chemistry *284*.

Wang, Z., Liu, J., Sudom, A., Ayres, M., Li, S., Wesche, H., Powers, J.P., and Walker, N.P.C. (2006). Crystal Structures of IRAK-4 Kinase in Complex with Inhibitors: A Serine/Threonine Kinase with Tyrosine as a Gatekeeper. Structure *14*, 1835-1844.

Wesche, H., Gao, X., Li, X.X., Kirschning, C.J., Stark, G.R., and Cao, Z.D. (1999). IRAK-M is a novel member of the pelle/interleukin-1 receptor-associated kinase (IRAK) family. The Journal of Biological Chemistry *274*, 19403-19410.

Wesche, H., Henzel, W.J., Shillinglaw, W., Li, S., and Cao, Z. (1997). MyD88: An Adapter That Recruits IRAK to the IL-1 Receptor Complex. Immunity *7*, 837-847.

Wheeler, J.I., Freihat, L., and Irving, H.R. (2013). A cyclic nucleotide sensitive promoter reporter system suitable for bacteria and plant cells. BMC Biotechnology *13*, 97.

Wheeler, J.I., Wong, A., Marondedze, C., Groen, A.J., Kwezi, L., Freihat, L., Vyas, J., Raji, M.A., Irving, H.R., and Gehring, C. (2017). The brassinosteroid receptor BRI1 can generate cGMP enabling cGMP-dependent

downstream signaling. The Plant Journal.

White, A.A., and Aurbach, G.D. (1969). Detection of guanyl cyclase in mammalian tissues. Biochimica et Biophysica Acta *191*, 686-697.

Wiersinga, W.J., van't Veer, C., van den Pangaart, P.S., Dondorp, A.M., Day, N.P., Peacock, S.J., and van der Poll, T. (2009). Immunosuppression associated with interleukin-1R-associated-kinase-M upregulation predicts mortality in Gram-negative sepsis (melioidosis). Critical Care Medicine *37*, 569-576.

Winger, J.A., Derbyshire, E.R., H, L.M., Marletta, M.A., and Kuriyan, J. (2008). The crystal structure of the catalytic domain of a eukaryotic guanylate cyclase. BMC Structural Biology *8*, 42.

Wong, A., and Gehring, C. (2013). The Arabidopsis thaliana proteome harbors undiscovered multi-domain molecules with functional guanylyl cyclase catalytic centers. Cell Communication and Signaling *11*, 48.

Wong, A., Gehring, C., and Irving, H.R. (2015). Conserved functional motifs and homology modelling to predict hidden moonlighting functional sites. Frontiers in Bioengineering and Biotechnology *3*.

Wu, Q., Jiang, D., Smith, S., Thaikoottathil, J., Martin, R.J., Bowler, R.P., and Chu, H.W. (2012). IL-13 dampens human airway epithelial innate immunity through induction of IL-1 receptor-associated kinase M. The Journal of Allergy and Clinical Immunology *129*, 825-833 e822.

Xie, Q., Gan, L., Wang, J., Wilson, I., and Li, L. (2007). Loss of the innate immunity negative regulator IRAK-M leads to enhanced host immune defense against tumor growth. Molecular Immunology *44*, 3453-3461.

Xiong, H., Zhu, C., Li, F., Hegazi, R., He, K., Babyatsky, M., Bauer, A.J., and Plevy, S.E. (2004). Inhibition of Interleukin-12 p40 Transcription and NF-κB Activation by Nitric Oxide in Murine Macrophages and Dendritic Cells. The Journal of Biological Chemistry *279*, 10776-10783.

Xiong, Y., Qiu, F., Piao, W., Song, C., Wahl, L.M., and Medvedev, A.E. (2011). Endotoxin Tolerance Impairs IL-1 Receptor-Associated Kinase (IRAK) 4 and TGF-β-activated Kinase 1 Activation, K63-linked Polyubiquitination and Assembly of IRAK1, TNF Receptor-associated Factor 6, and IκB Kinase γ and Increases A20 Expression. The Journal of Biological Chemistry *286*, 7905-7916.

Zacharioudaki, V., Androulidaki, A., Arranz, A., Vrentzos, G., Margioris, A.N., and Tsatsanis, C. (2009). Adiponectin promotes endotoxin tolerance in macrophages by inducing IRAK-M expression. The Journal of Immunology *182*, 6444-6451.

Zanoni, I., Ostuni, R., Marek, L.R., Barresi, S., Barbalat, R., Barton, G.M., Granucci, F., and Kagan, J.C. (2011). CD14 controls the LPS-induced endocytosis of Toll-like Receptor 4. Cell *147*, 868-880.

Zhao, G.-j., Li, D., Zhao, Q., Song, J.-x., Chen, X.-r., Hong, G.-l., Li, M.-f., Wu, B., and Lu, Z.-q. (2016). Incidence, risk factors and impact on outcomes of secondary infection in patients with septic shock: an 8-year retrospective study. Scientific Reports *6*, 38361.

Zhou, H., Yu, M., Fukuda, K., Im, J., Yao, P., Cui, W., Bulek, K., Zepp, J., Wan, Y., Kim, T.W.*, et al.* (2013). IRAK-M mediates Toll-like receptor/IL-1R-induced NFkappaB activation and cytokine production. The EMBO Journal *32*, 583-596.

Zhou, H., Yu, M., Zhao, J., Martin, B.N., Roychowdhury, S., McMullen, M.R., Wang, E., Fox, P.L., Yamasaki, S., Nagy, L.E.*, et al.* (2016). IRAKM-Mincle axis links cell death to inflammation: Pathophysiological implications for chronic alcoholic liver disease. Hepatology *64*, 1978-1993.